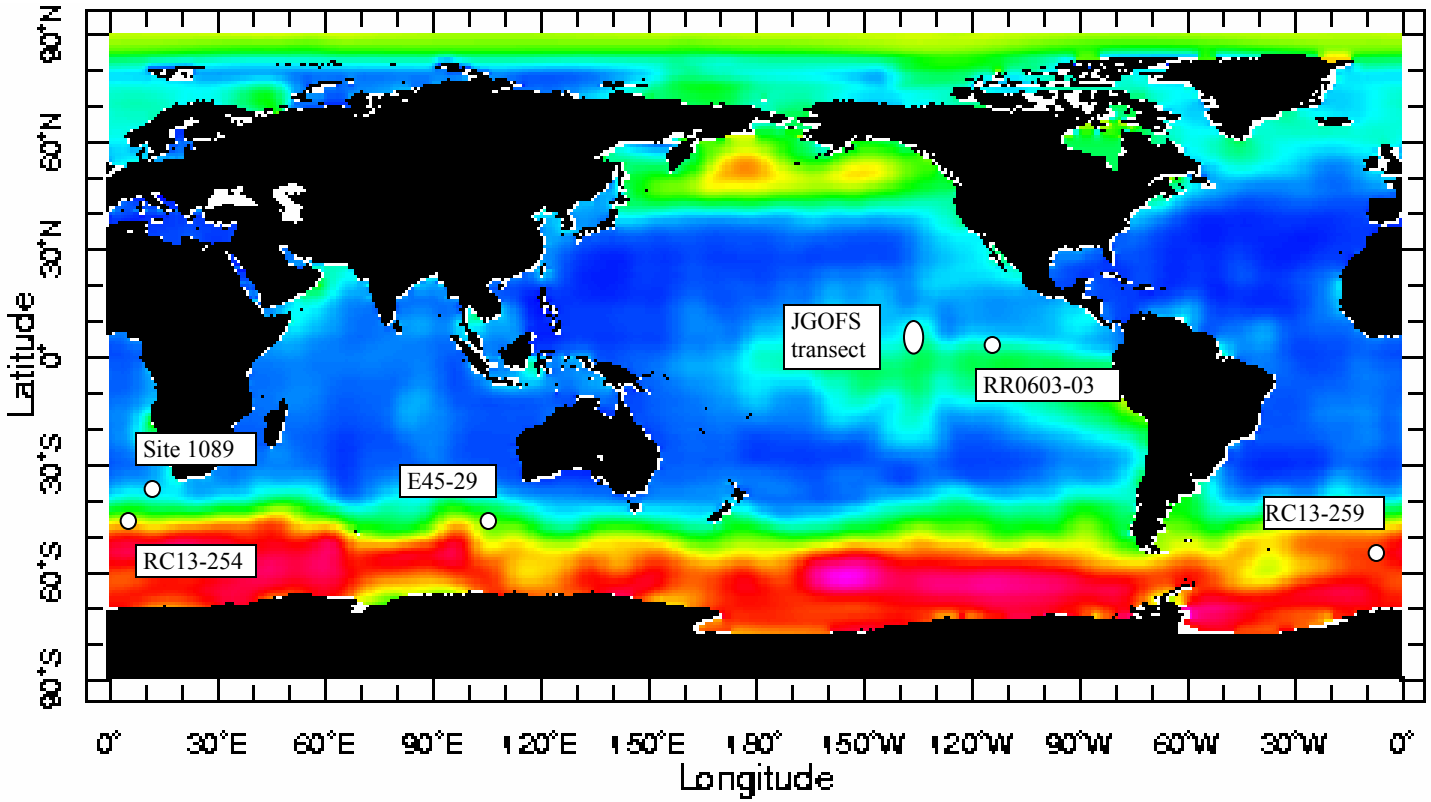

Figure 1. Study site locations plotted on an ocean productivity map. Warm colors indicate high productivity and cool colors represent low areas of productivity.

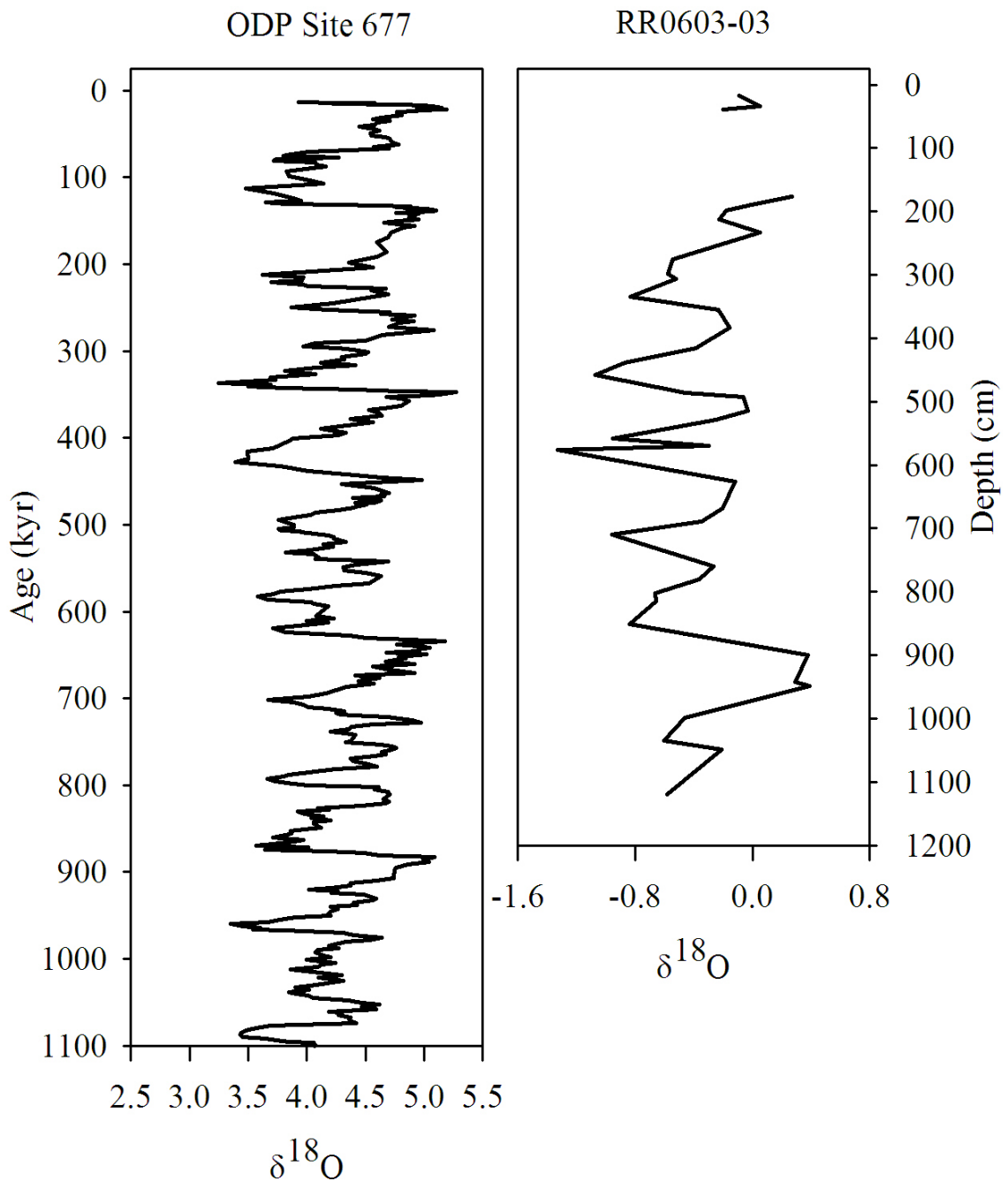

Figure 2. Isotopic $\delta^{18}O$ analysis of benthic foraminifera *Uvigerina* versus age for ODP Site 677 and isotopic $\delta^{18}O$ analysis of planktonic foraminifera *Globigerinoides sacculifer* with depth for RR0603-03.

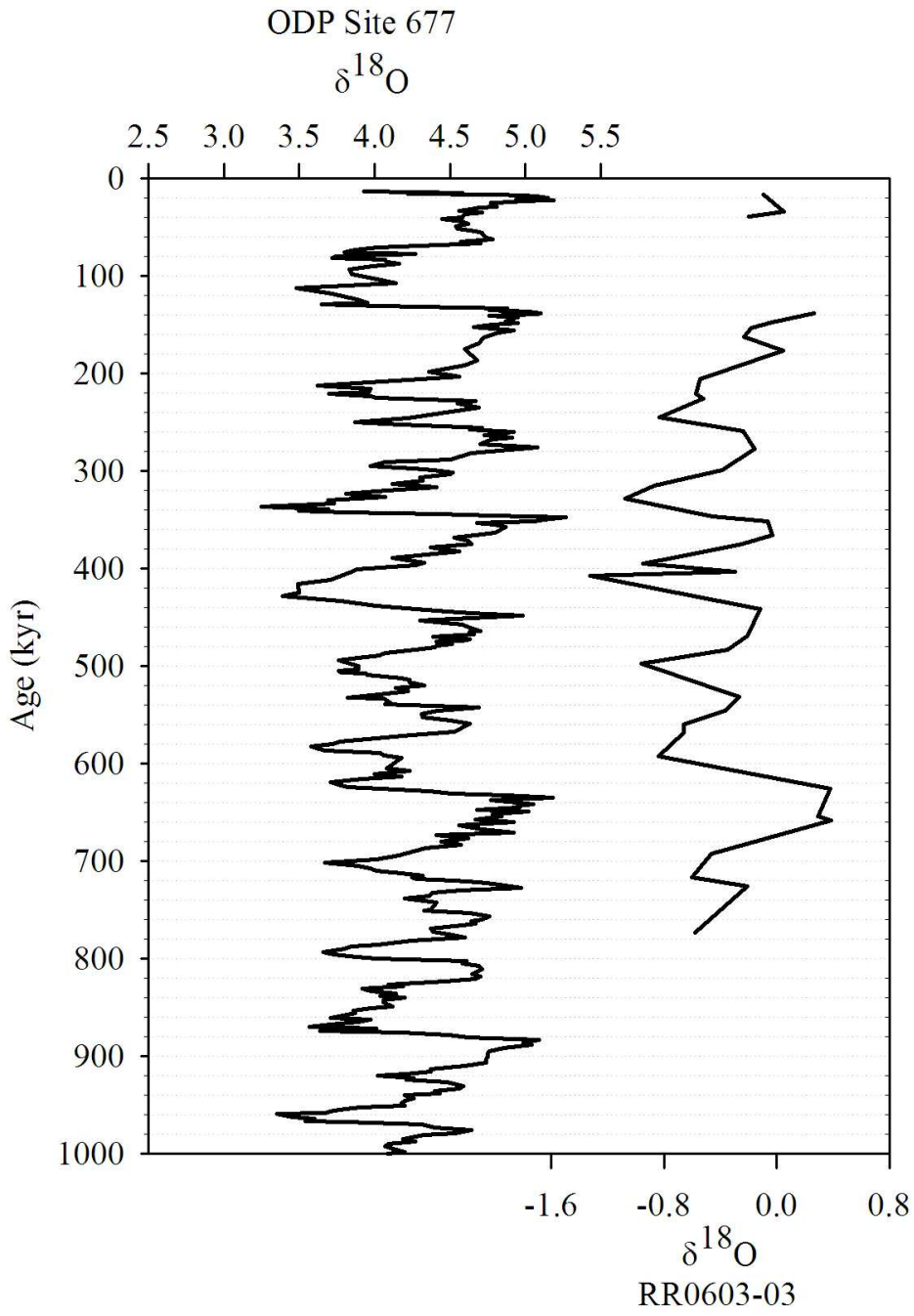

Figure 3. Isotopic $\delta^{18}O$ analysis of benthic foraminifera *Uvigerina* versus age for ODP Site 677 and isotopic $\delta^{18}O$ analysis planktonic foraminifera *Globigerinoides sacculifer* versus age for RR0603-03. Data for RR0603-03 has undergone "wiggle-matching" and has been stretched and compressed to fit the Site 677 age model.

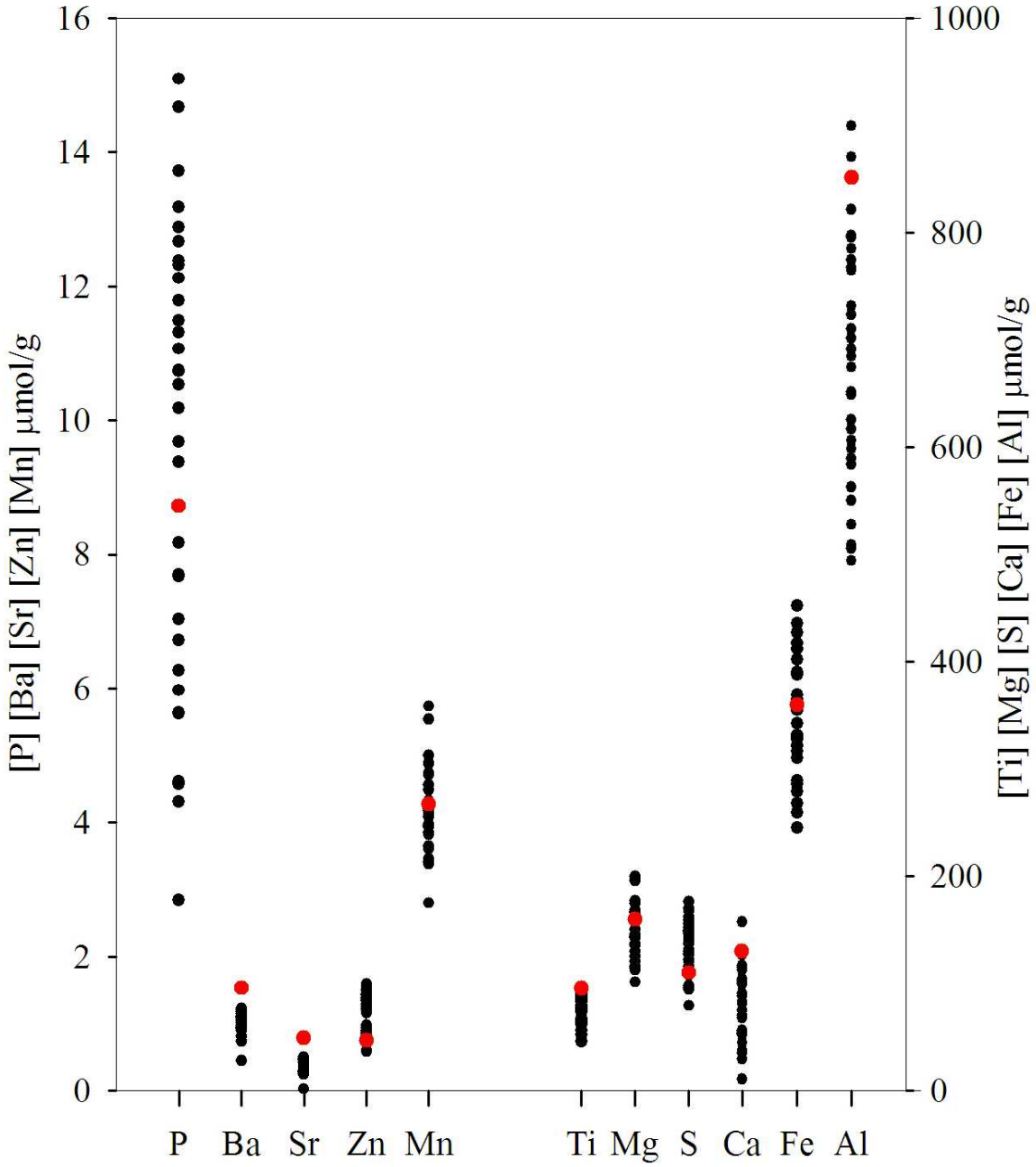

Figure 4. SRM 1646a range of values. Obtained ICP values (black) and certified values (red) for estuarine sediment Standard Reference Material (SRM) 1646a. The certified value, average value and standard deviation for each element are presented in Tables 4 and 5.

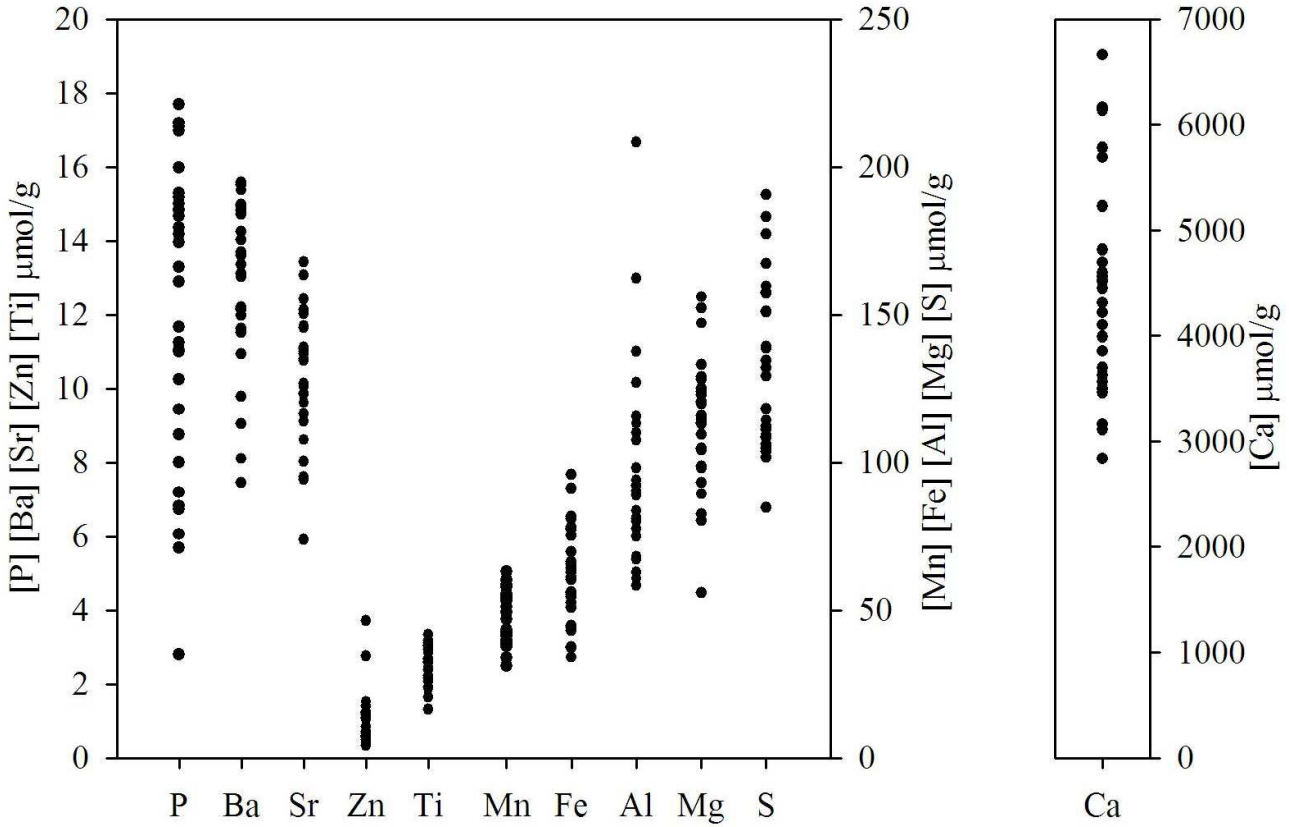

Figure 5. Range of elemental concentration values obtained for the RR0603-03 consistency standard. Averages are listed in Tables 6 and 7.

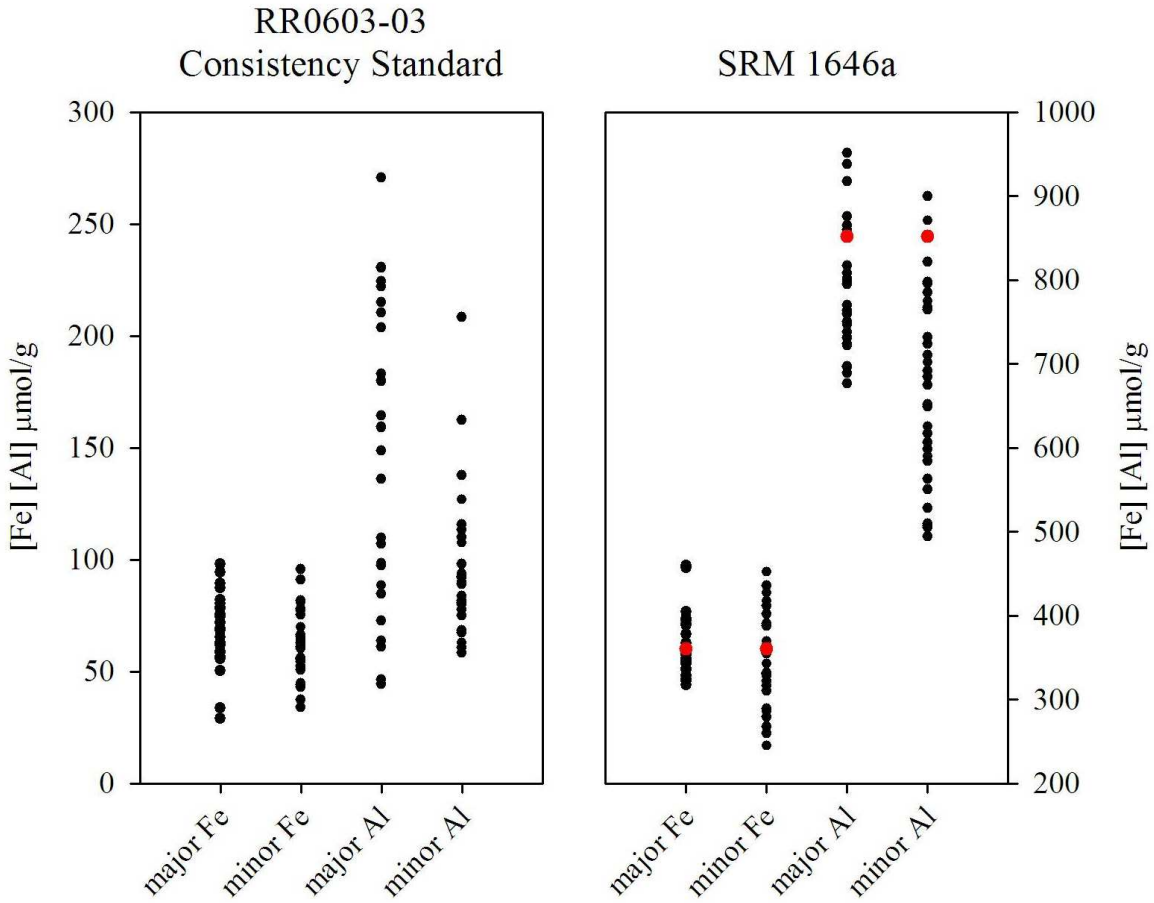

Figure 6. Fe and Al concentrations in both major (1:10) and minor (1:60) dilutions for the RR0603-03 consistency standard and Standard Reference Material (SRM) 1646a. Obtained values (black) and certified values (red) are both presented for the SRM 1646a data. Average values and standard deviations for RR0603-03 consistency standard are listed in Tables 6 and 7. The certified value, average value and standard deviation for SRM 1646a are listed in Tables 4

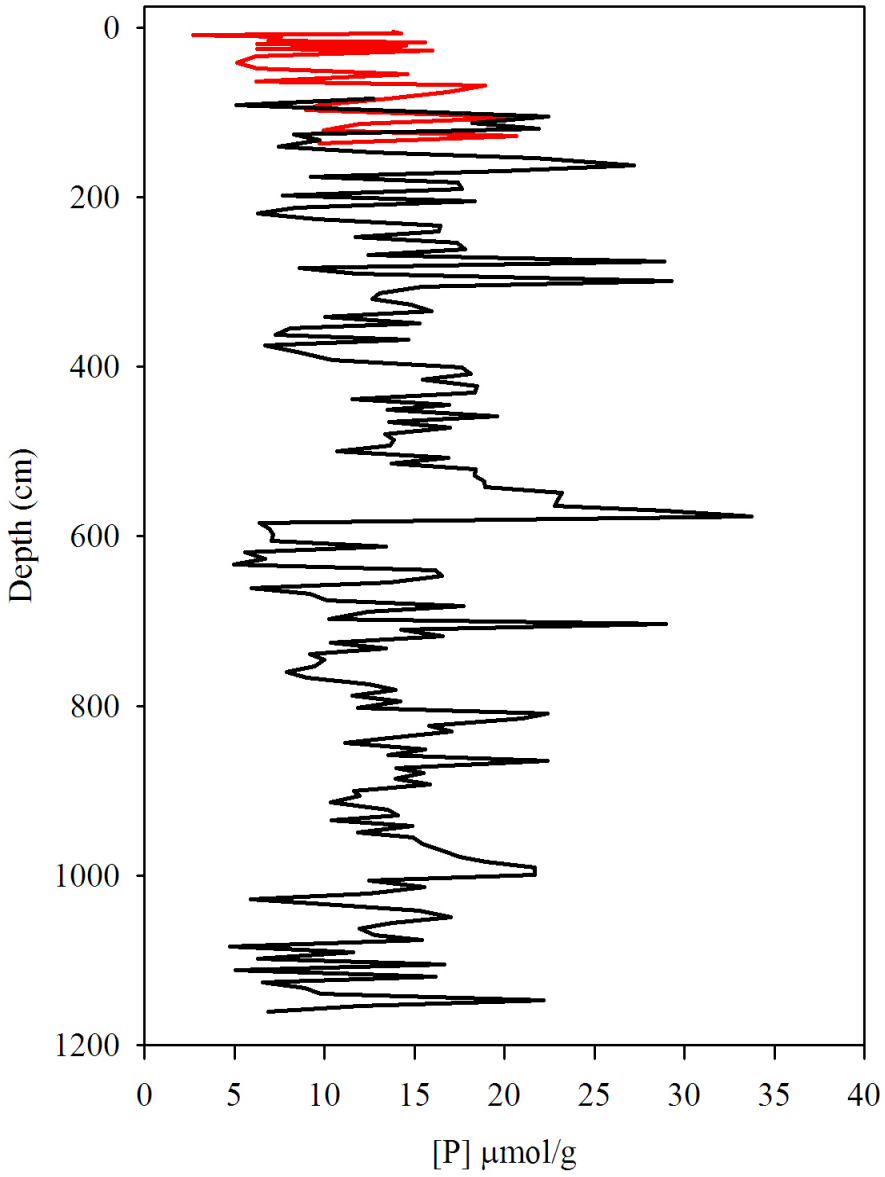

Figure 7. P concentration with depth for RR0603-03. Trigger core data is shown in red.

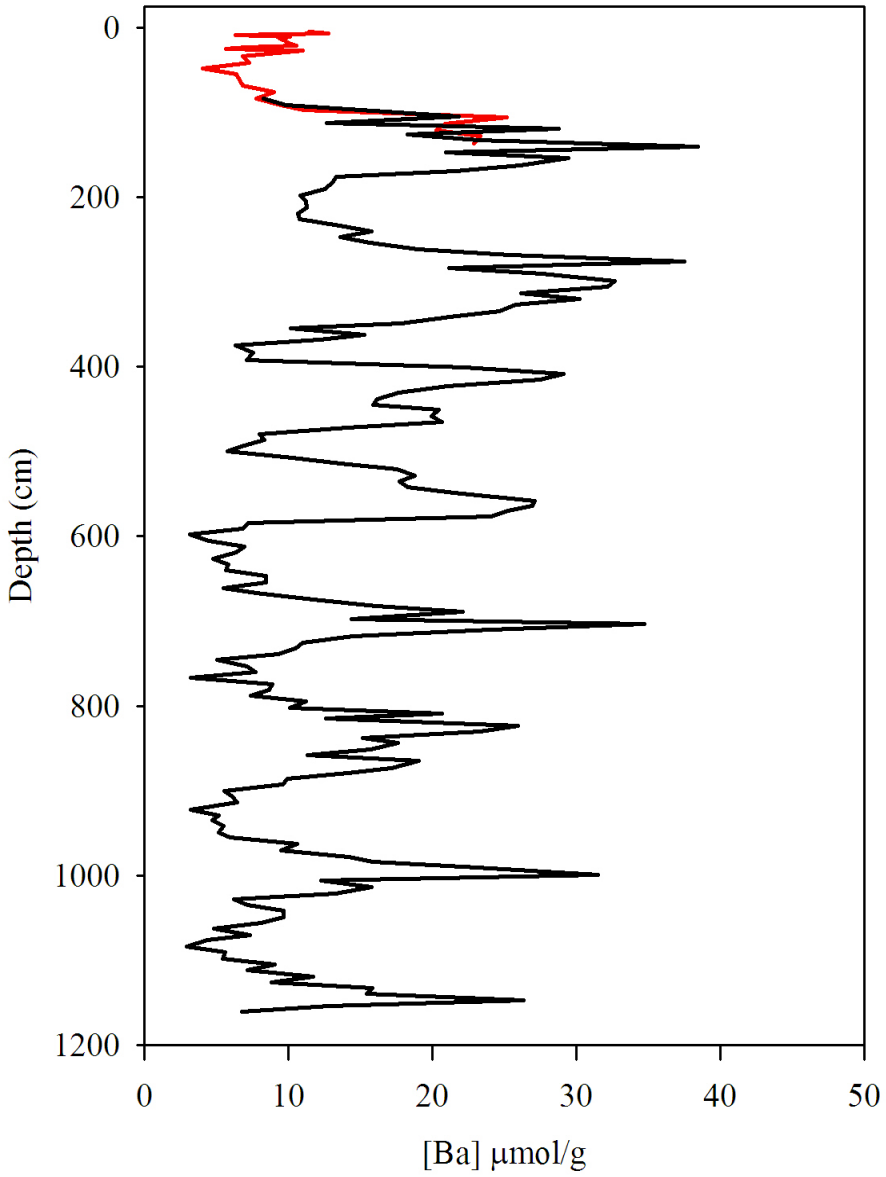

Figure 8. Ba concentration with depth for RR0603-03. Trigger core data is shown in red.

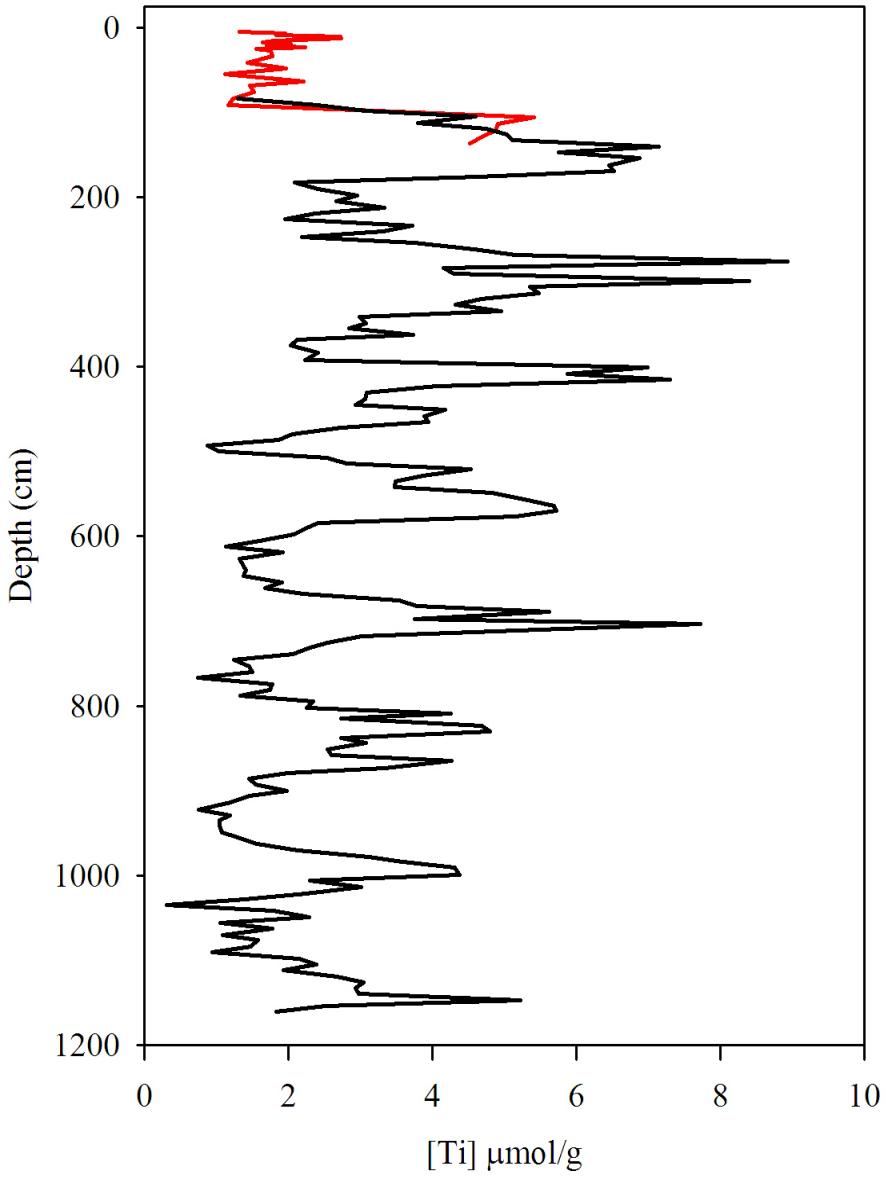

Figure 9. Ti concentration with depth for RR0603-03. Trigger core data is shown in red.

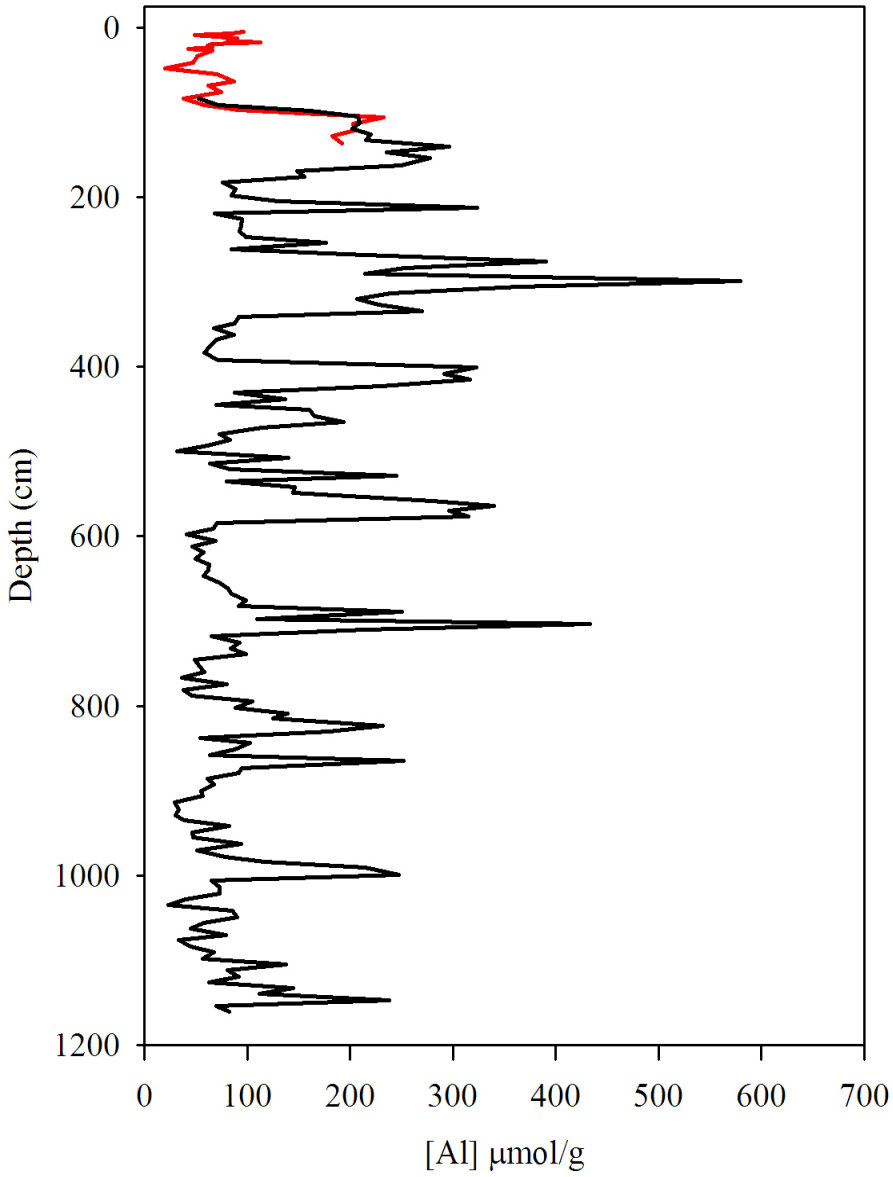

Figure 10. Al concentration with depth for RR0603-03. Trigger core data is shown in red.

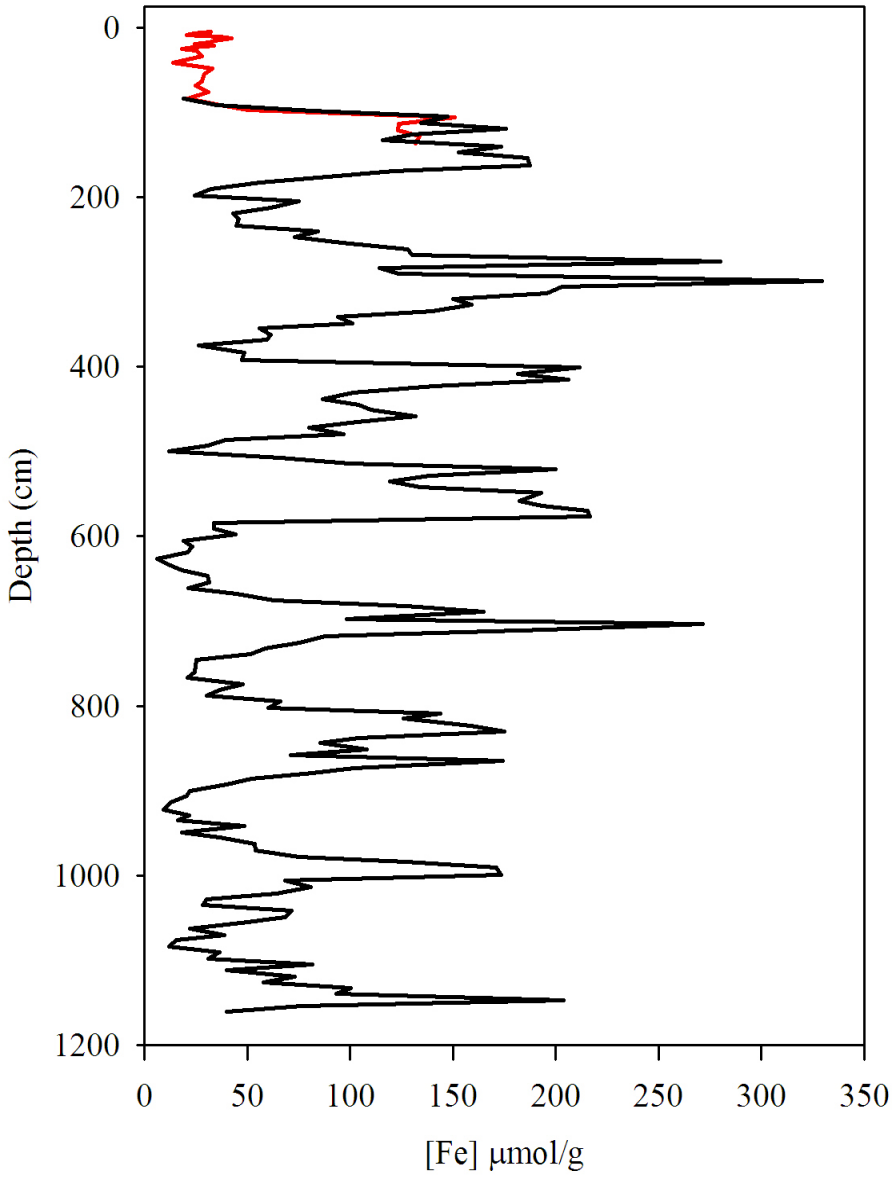

Figure 11. Fe concentration with depth for RR0603-03. Trigger core data is shown in red.

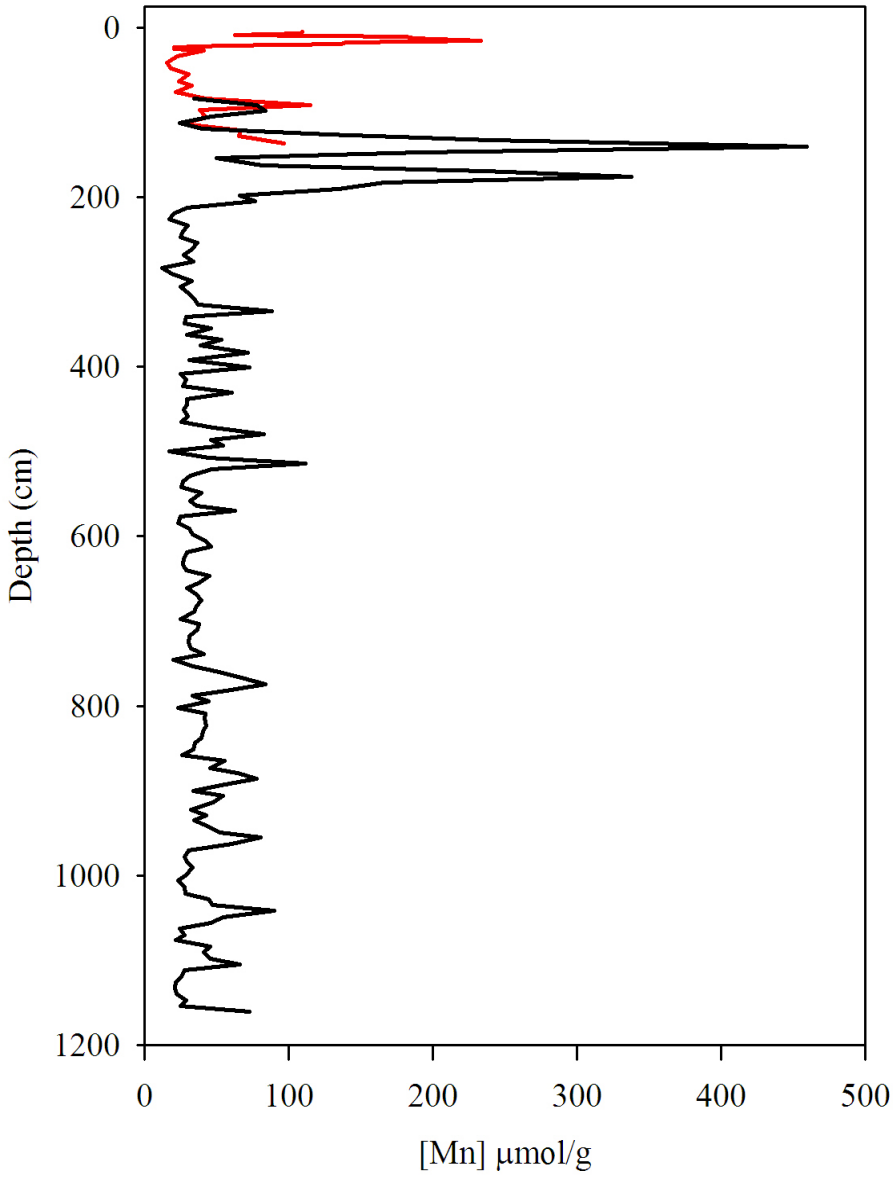

Figure 12. Mn concentration with depth for RR0603-03. Trigger core data is shown in red.

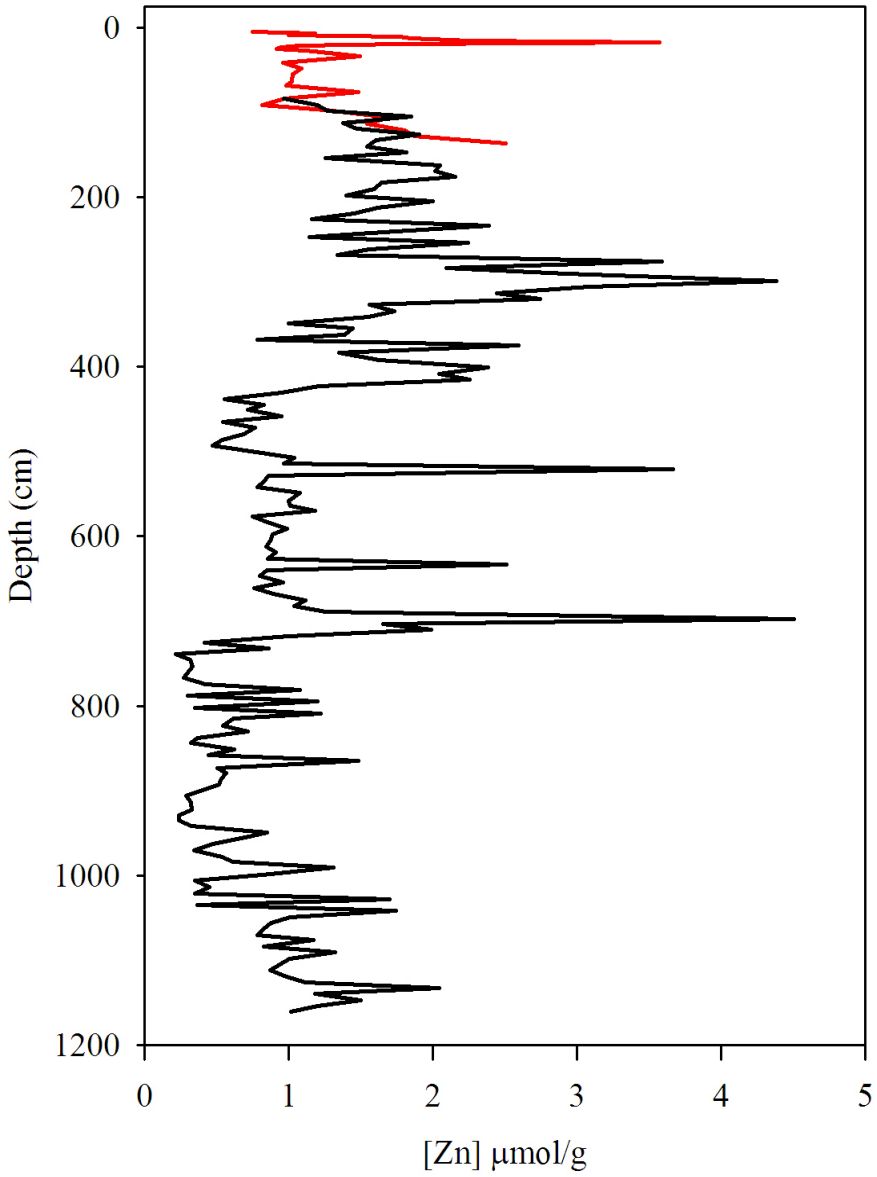

Figure 13. Zn concentration with depth for RR0603-03. Trigger core data is shown in red.

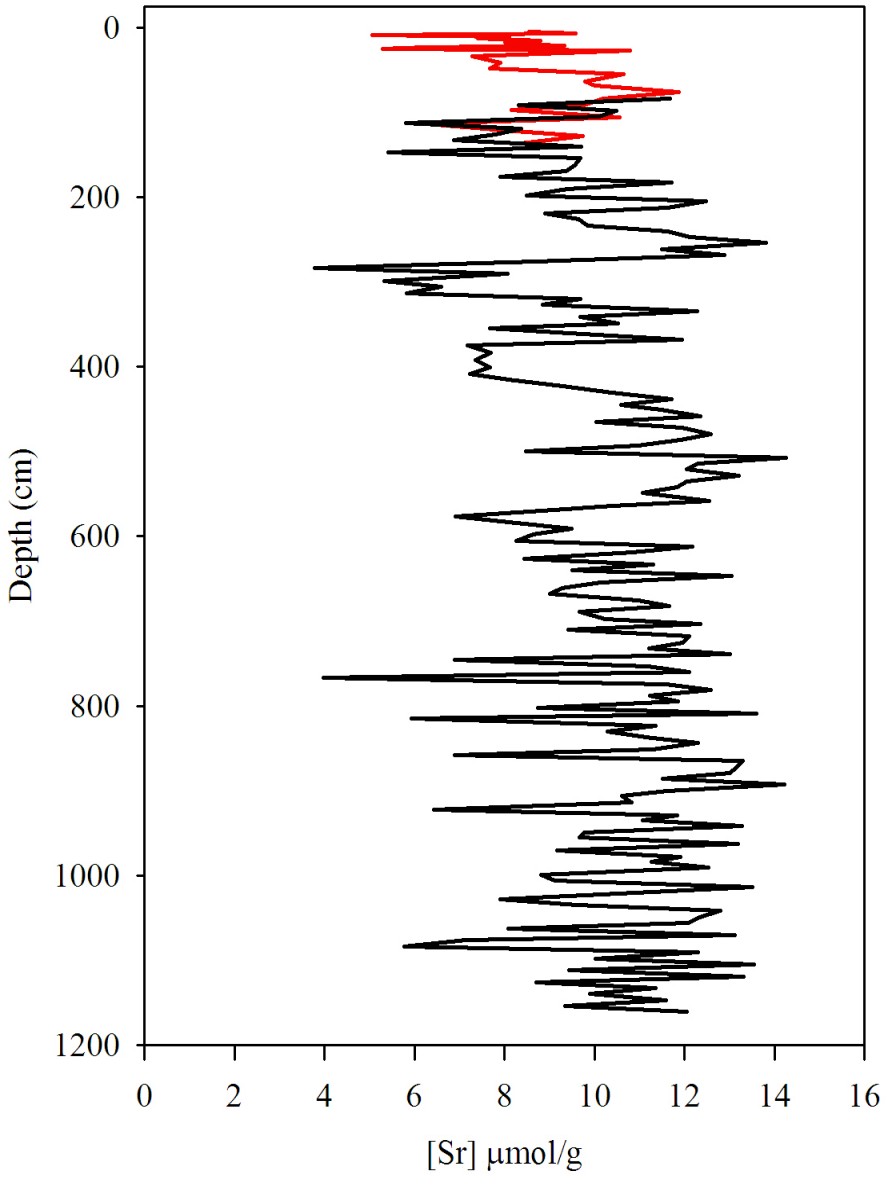

Figure 14. Sr concentration with depth for RR0603-03. Trigger core data is shown in red.

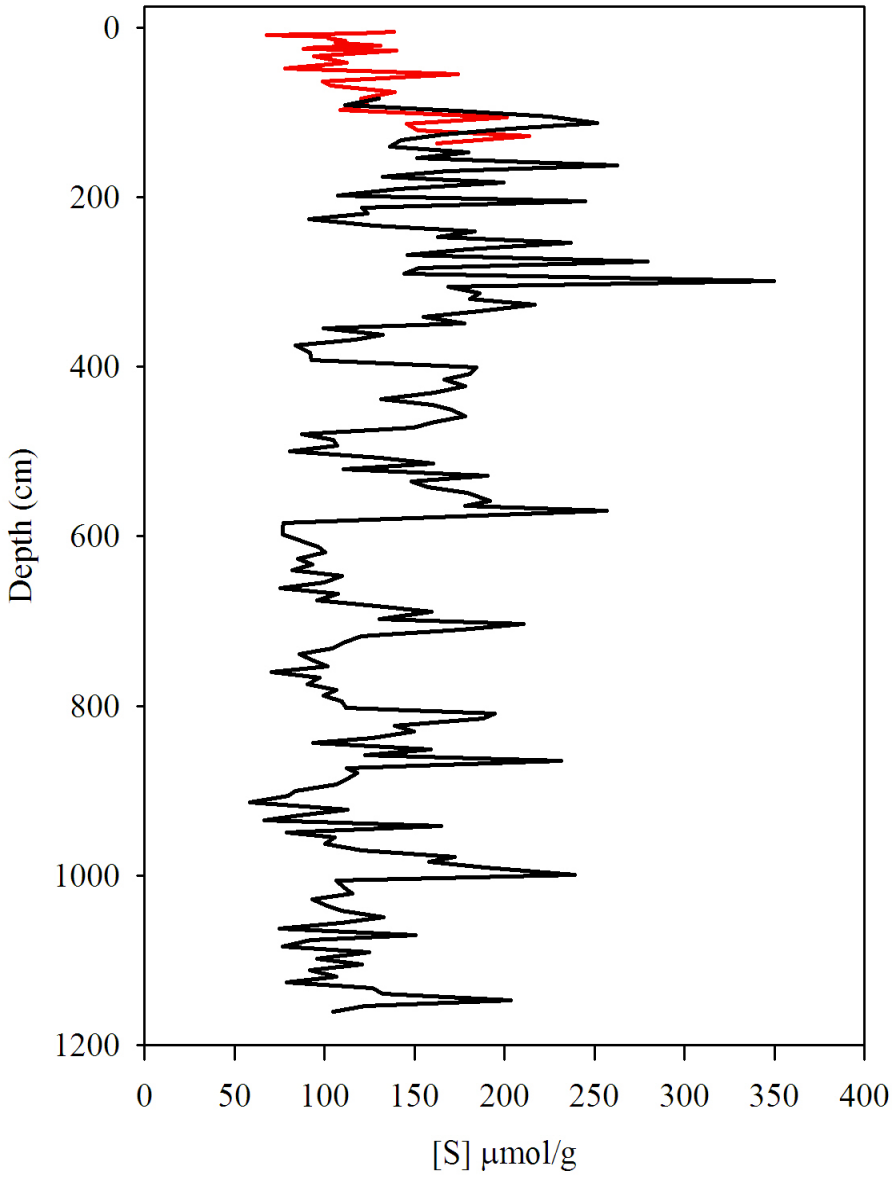

Figure 15. S concentration with depth for RR0603-03. Trigger core data is shown in red.

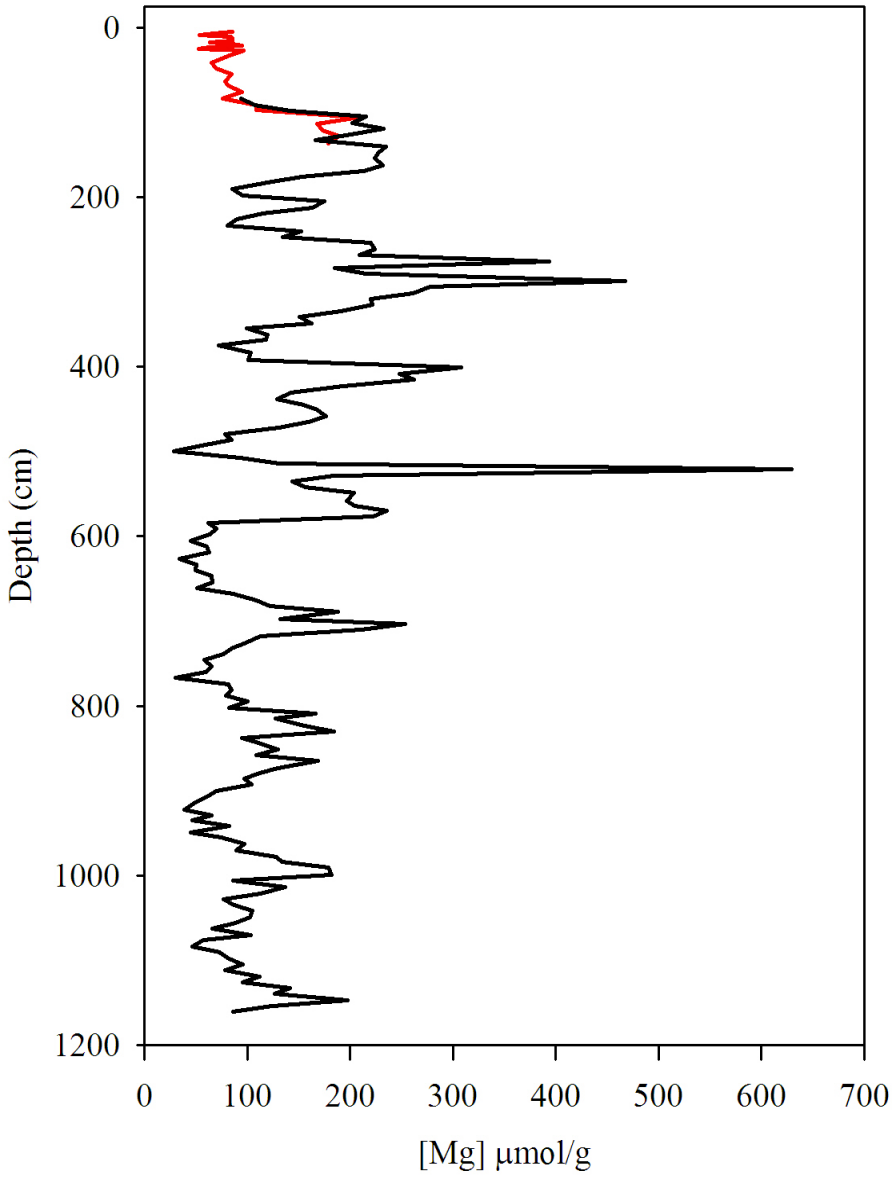

Figure 16. Mg concentration with depth for RR0603-03. Trigger core data is shown in red.

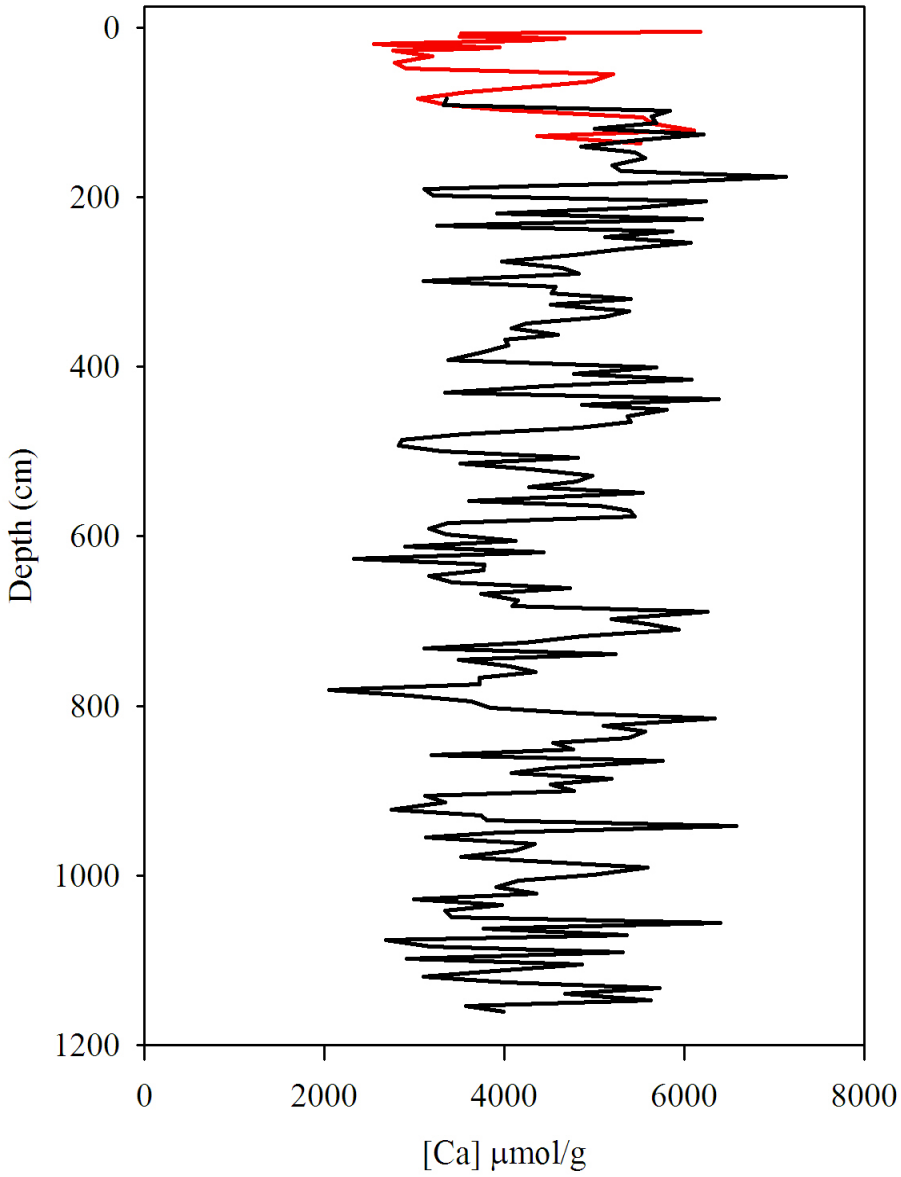

Figure 17. Ca concentration with depth for RR0603-03. Trigger core data is shown in red.

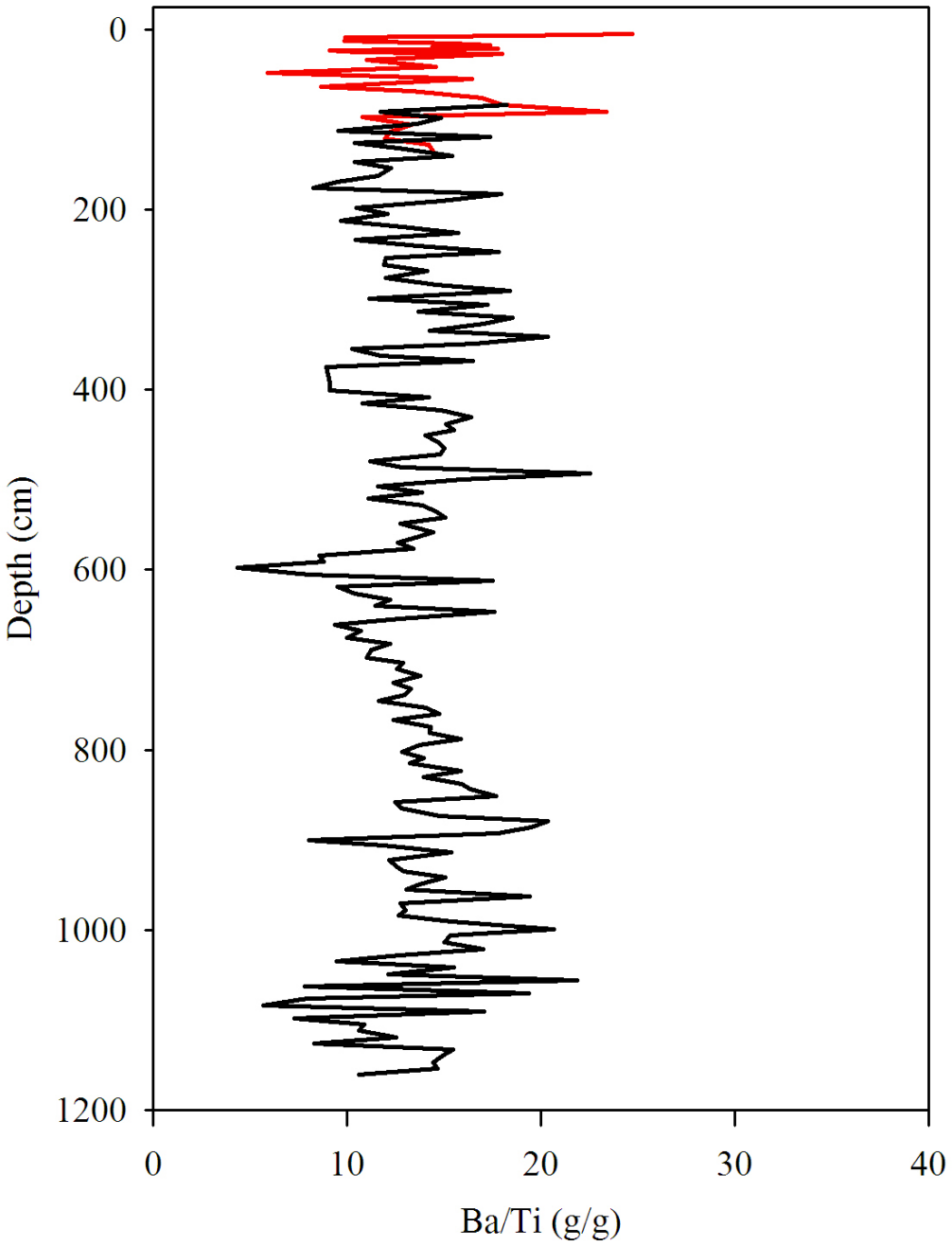

Figure 18. Ba/Ti ratio with depth for RR0603-03. Trigger core data is shown in red.

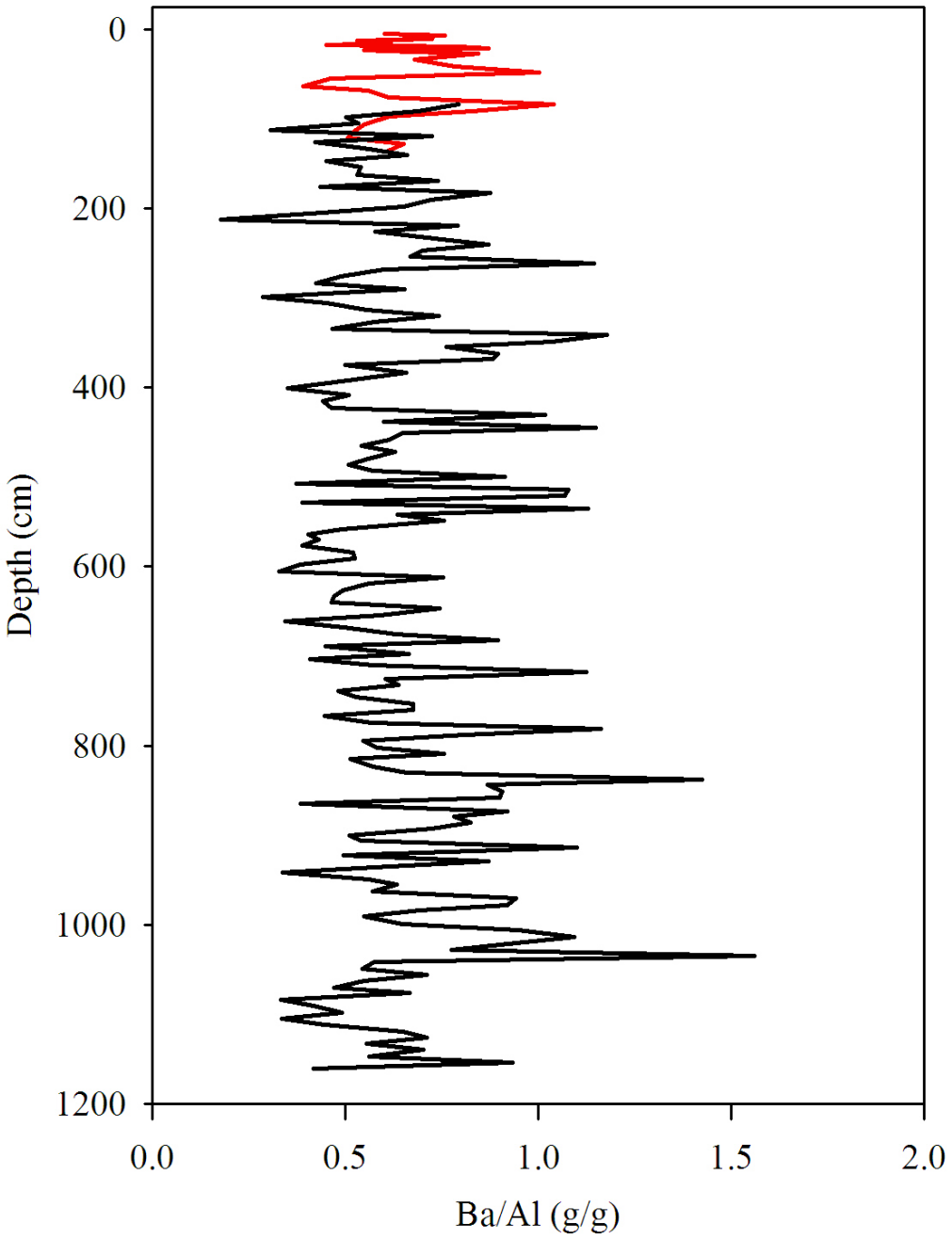

Figure 19. Ba/Al ratio with depth for RR0603-03. Trigger core data is shown in red.

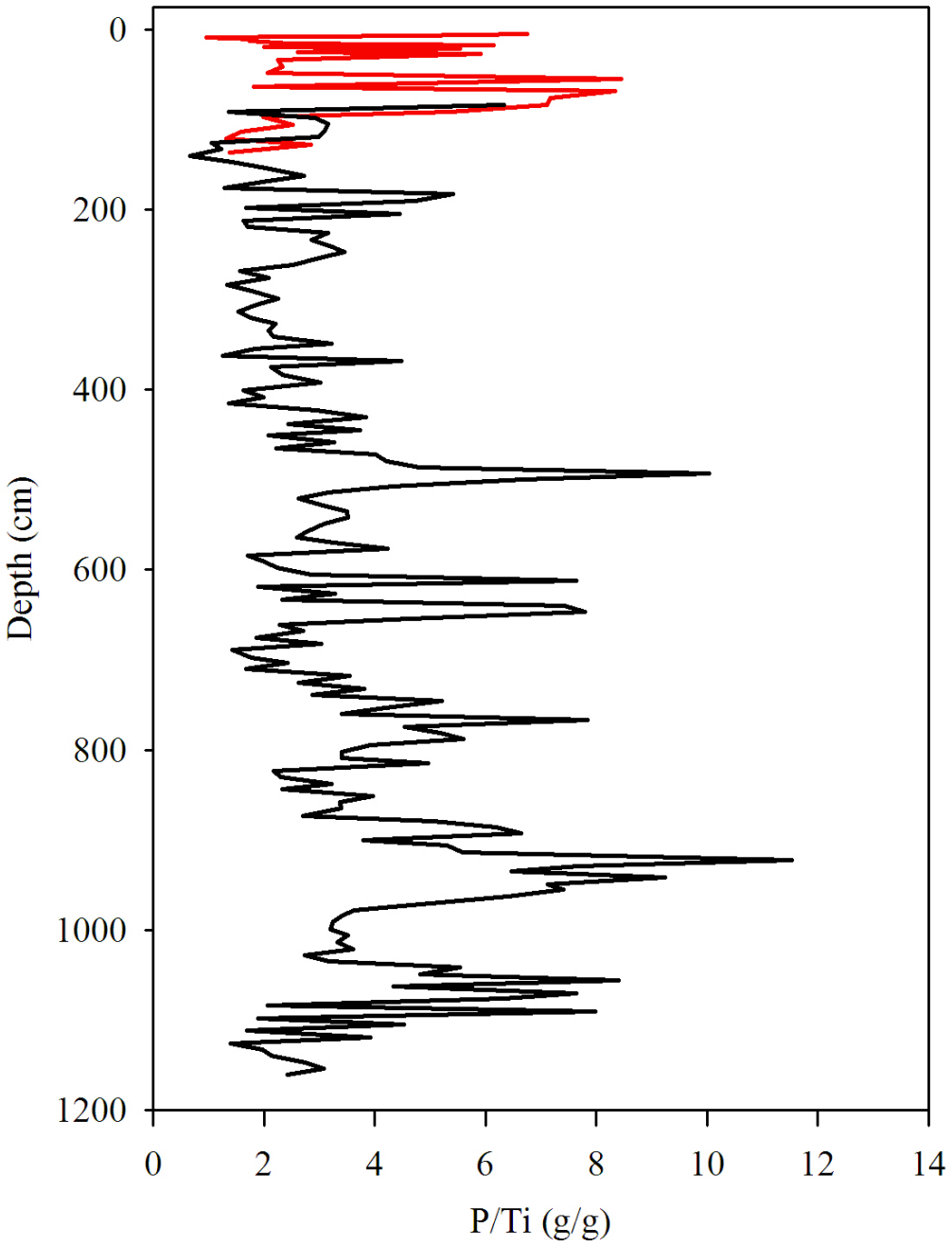

Figure 20. P/Ti ratio with depth for RR0603-03. Trigger core data is shown in red.

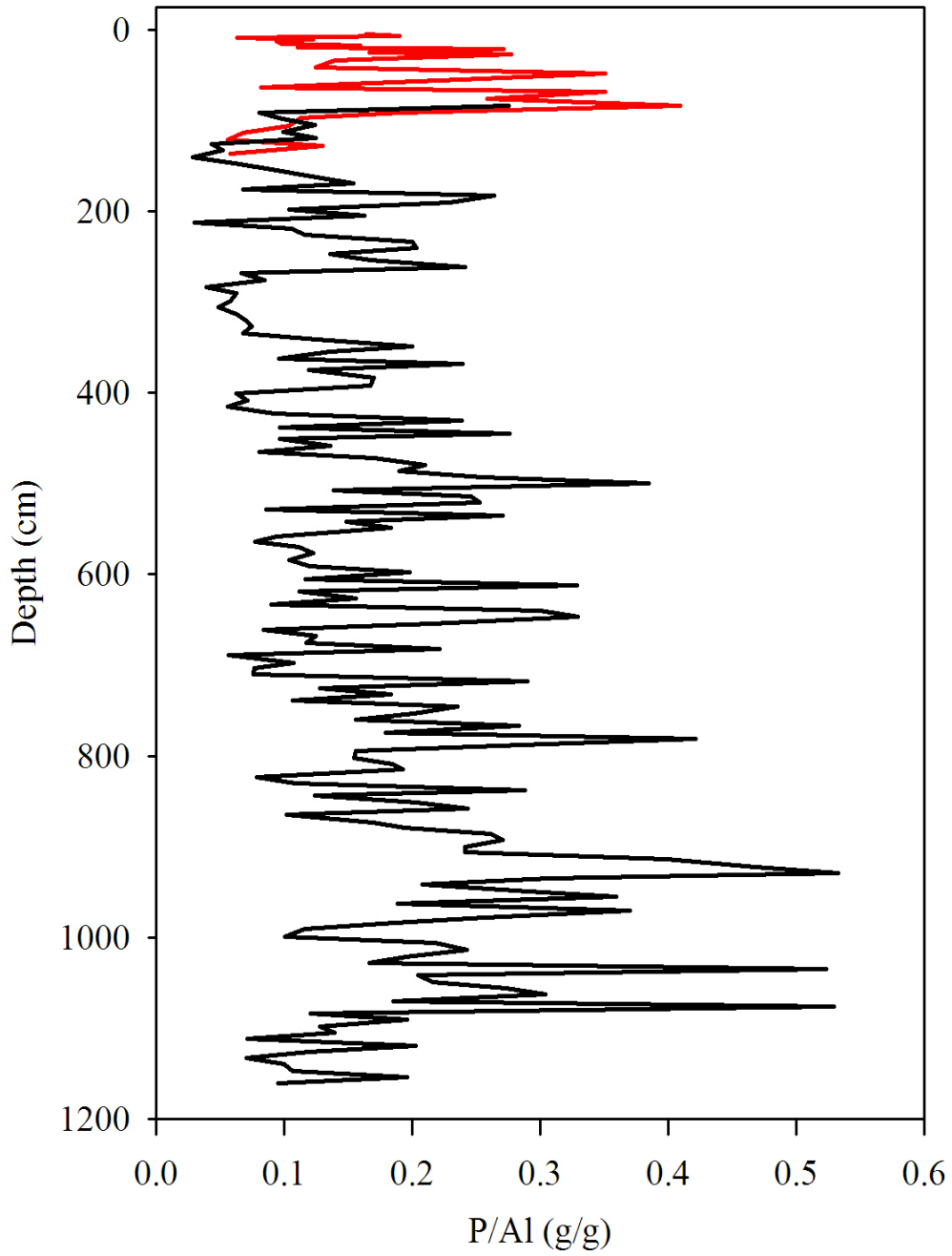

Figure 21. P/Al ratio with depth for RR0603-03. Trigger core data is shown in red.

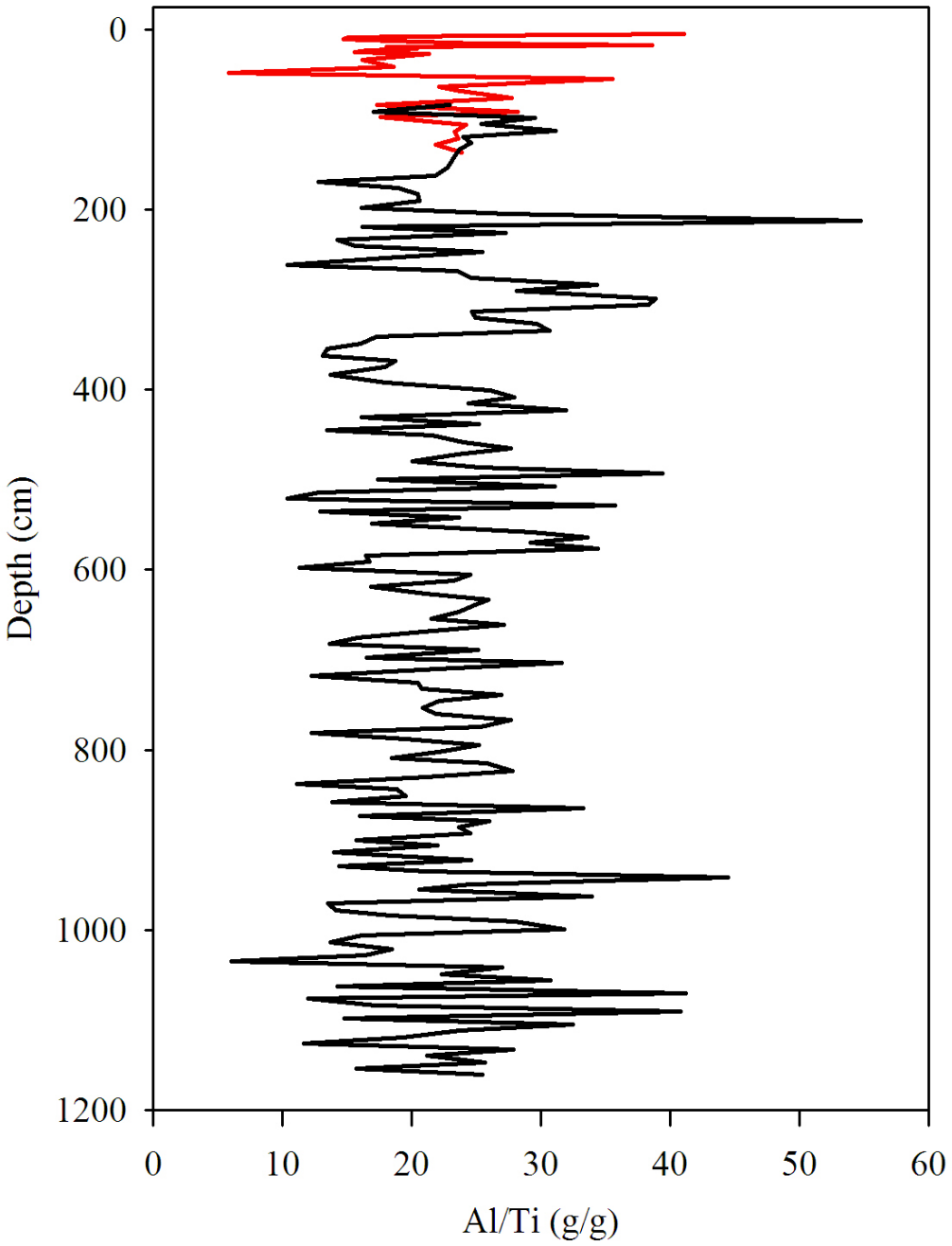

Figure 22. Al/Ti ratio with depth for RR0603-03. Trigger core data is shown in red.

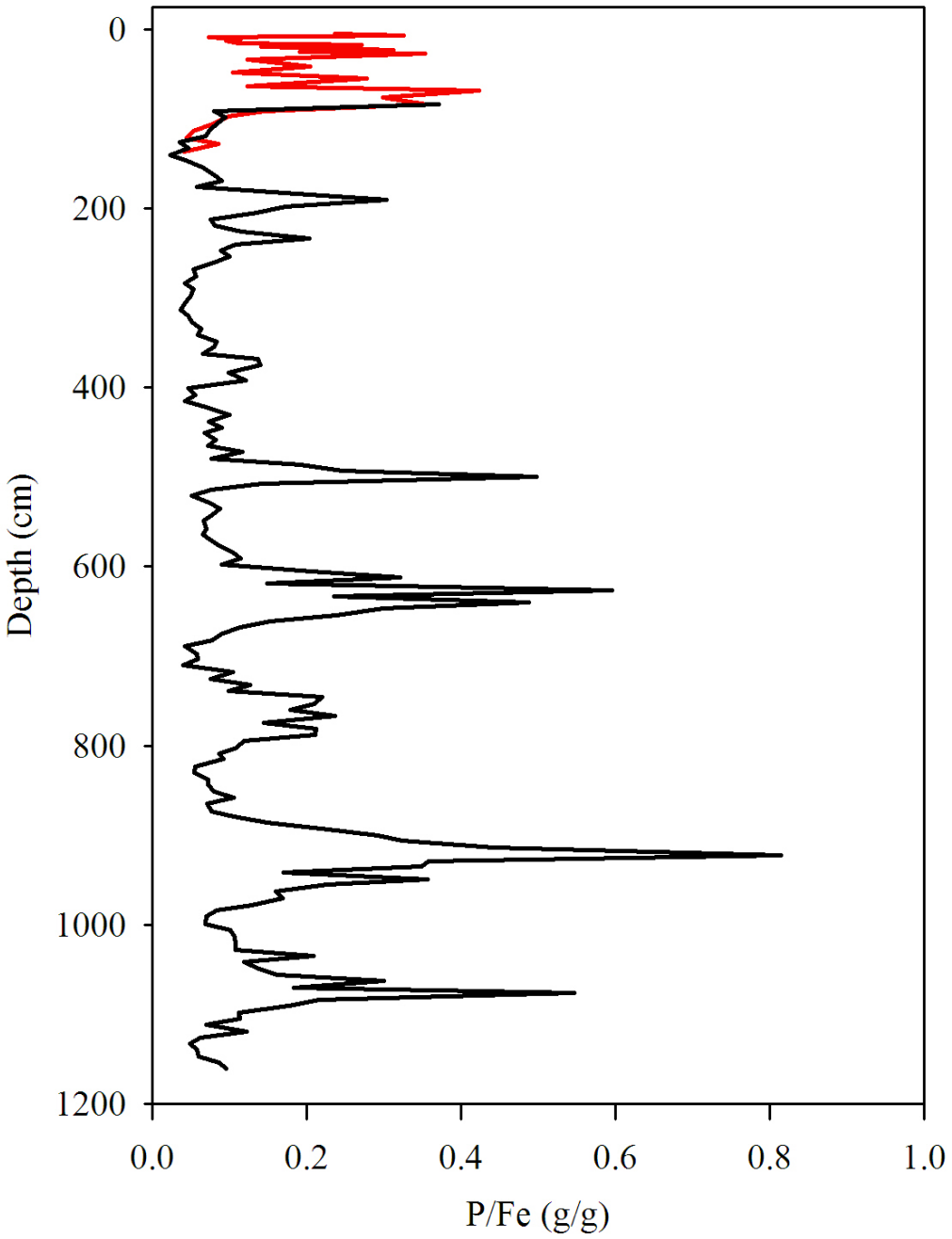

Figure 23. P/Fe ratio with depth for RR0603-03. Trigger core data is shown in red.

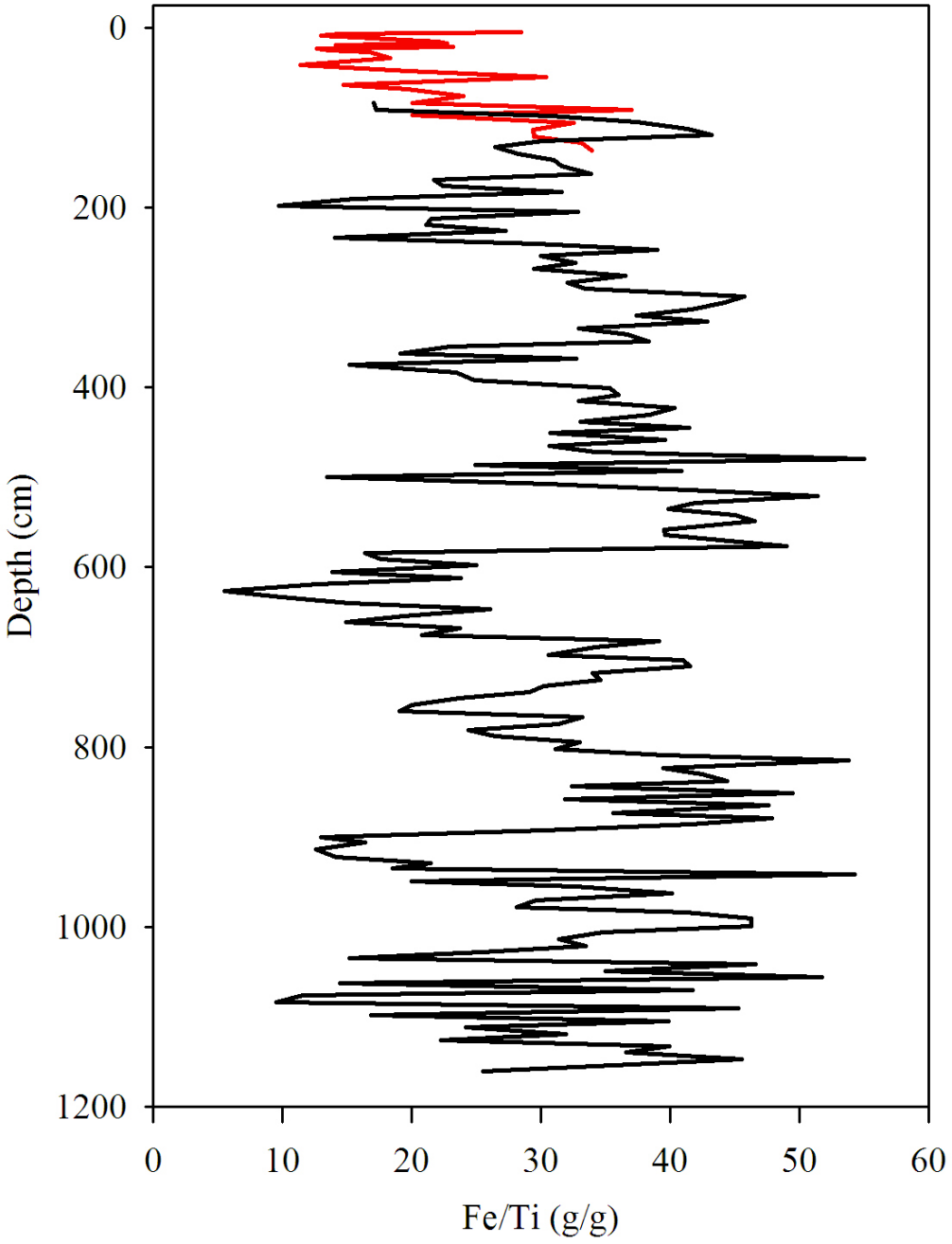

Figure 24. Fe/Ti ratio with depth for RR0603-03. Trigger core data is shown in red.

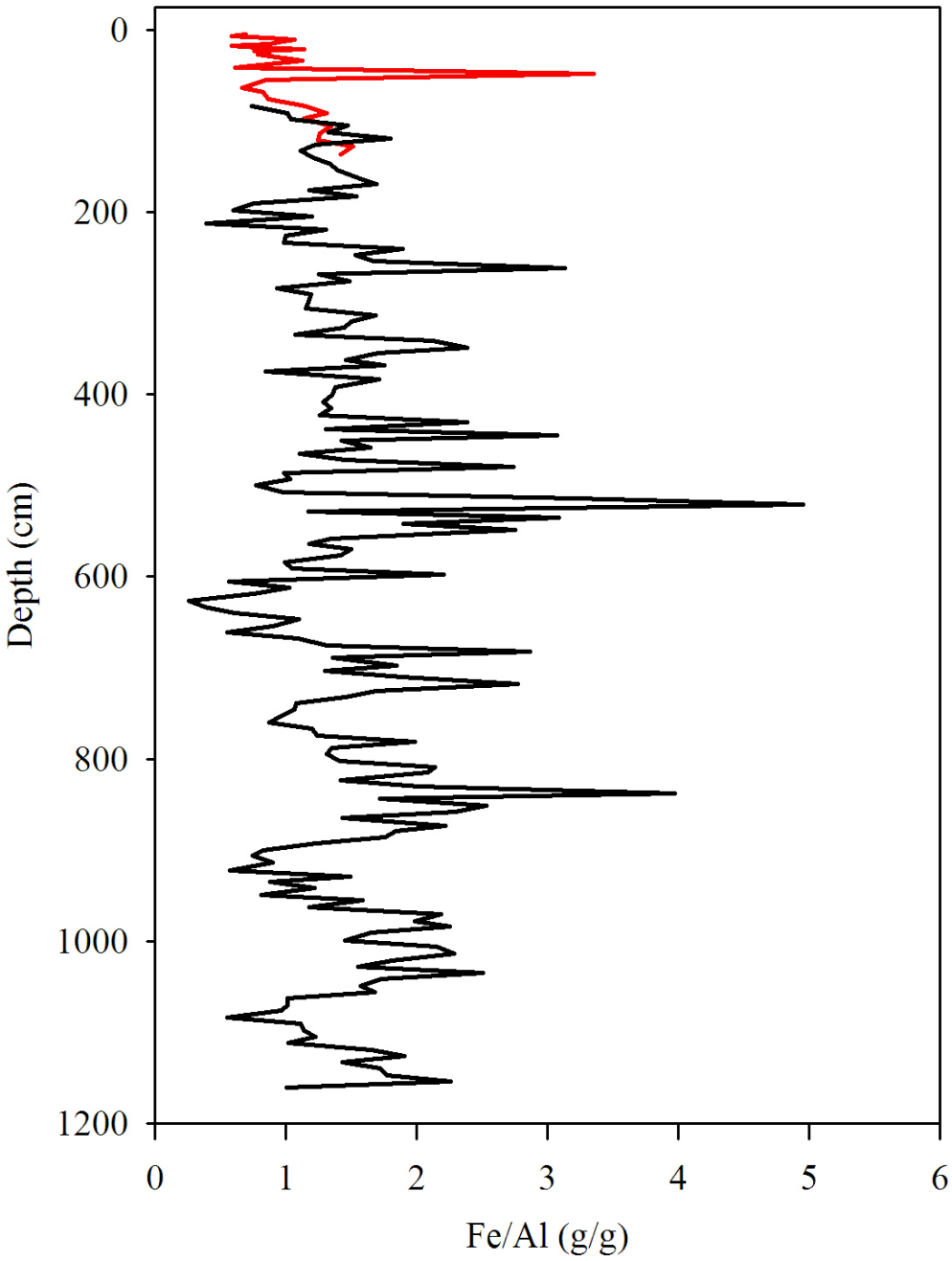

Figure 25. Fe/Al ratio with depth for RR0603-03. Trigger core data is shown in red.

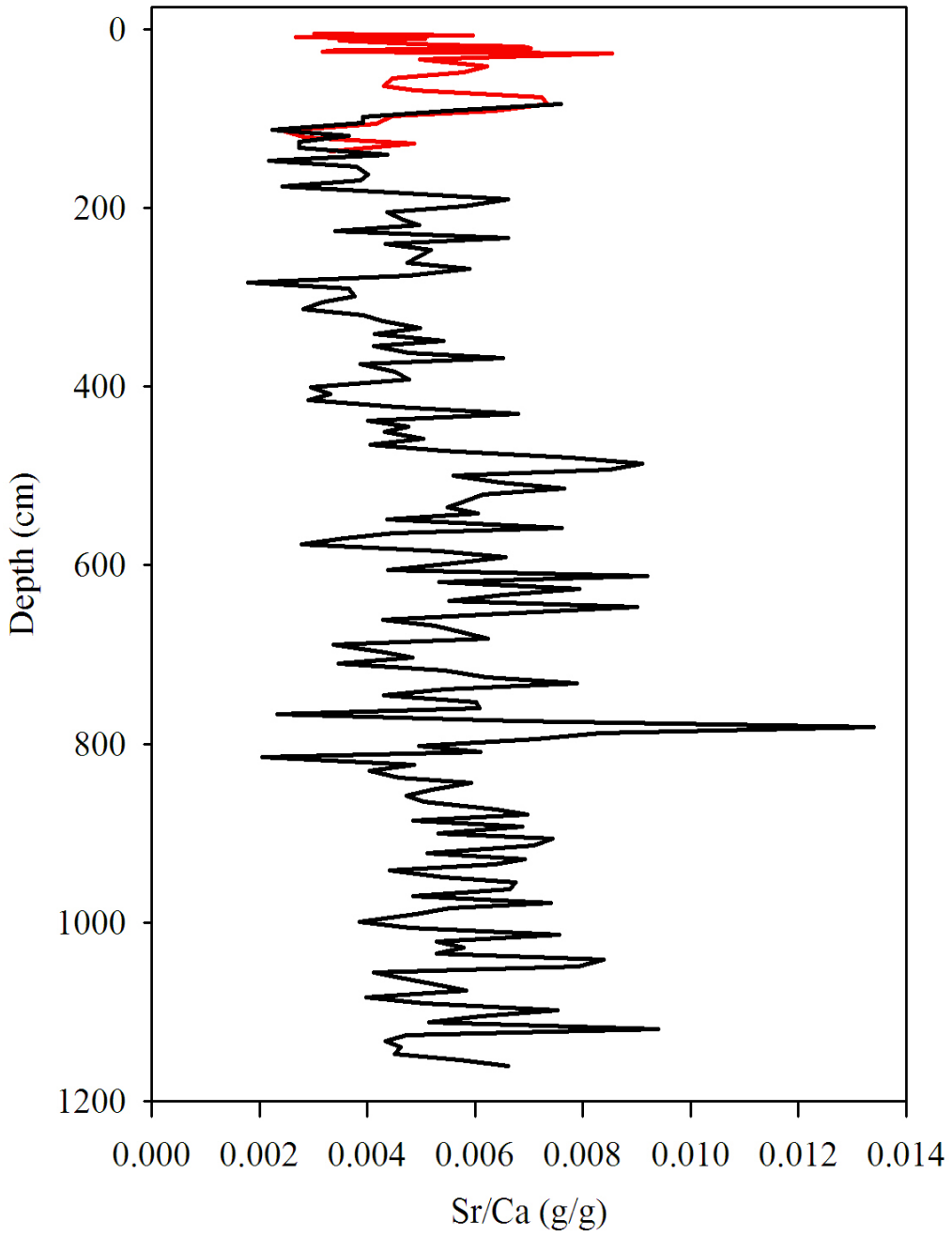

Figure 26. Sr/Ca ratio with depth for RR0603-03. Trigger core data is shown in red.

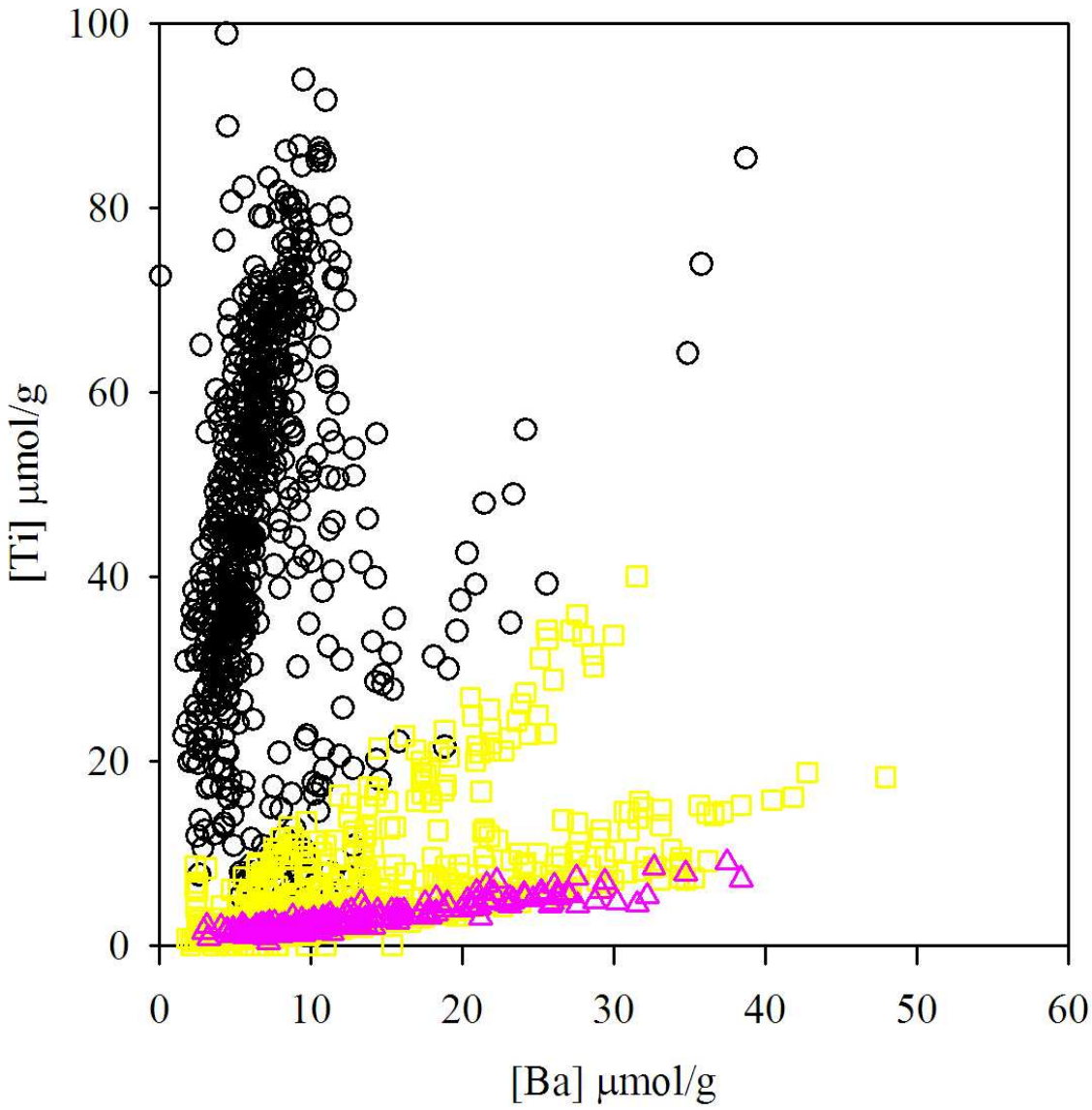

Figure 27. Ti concentration versus Ba concentration comparison plot for RR0603-03 (pink triangles), the JGOFS transect (yellow squares) and the Southern Ocean sites (black circles).

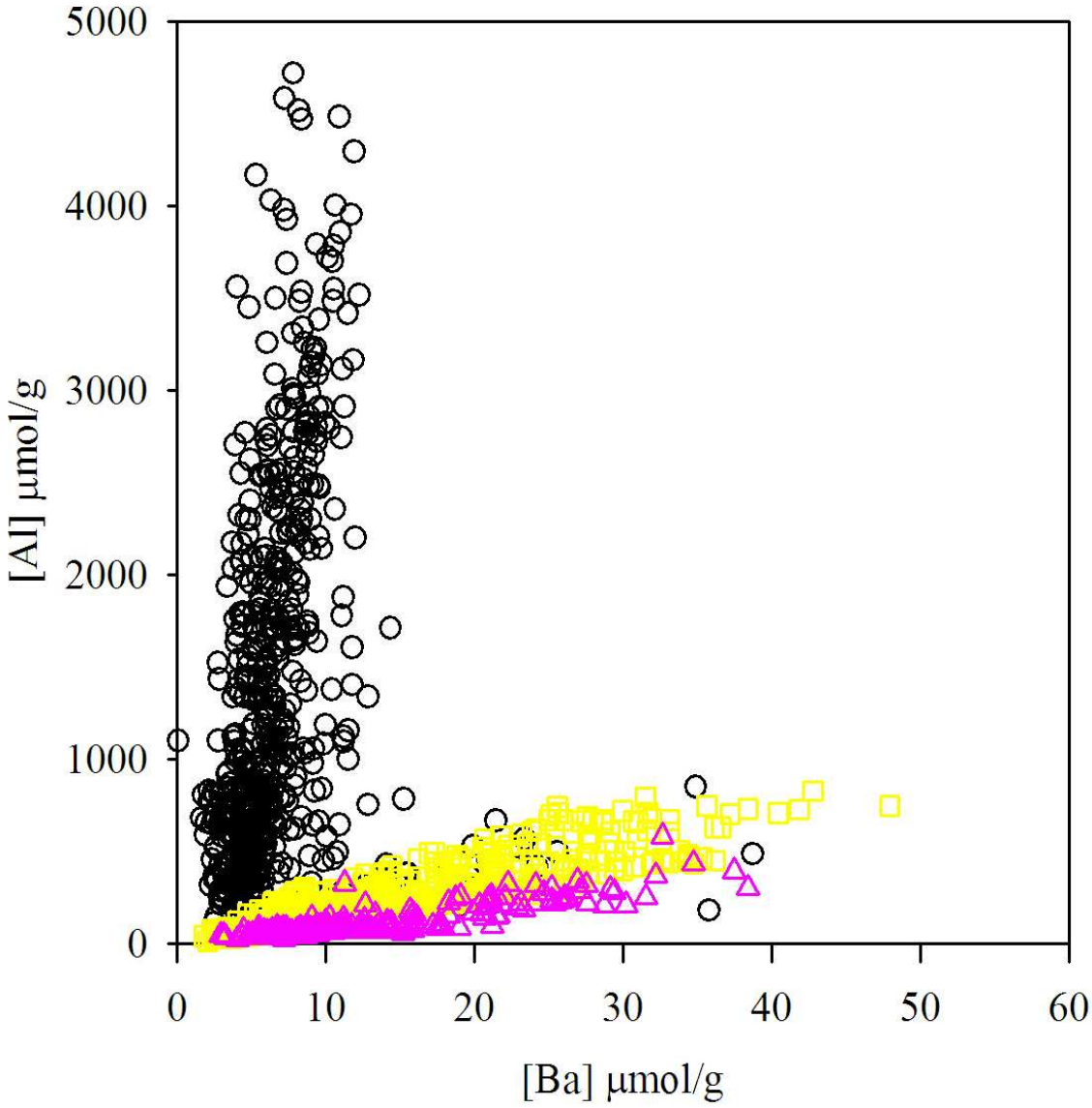

Figure 28. Al concentration versus Ba concentration comparison plot for RR0603-03 (pink triangles), the JGOFS transect (yellow squares) and the Southern Ocean sites (black circles).

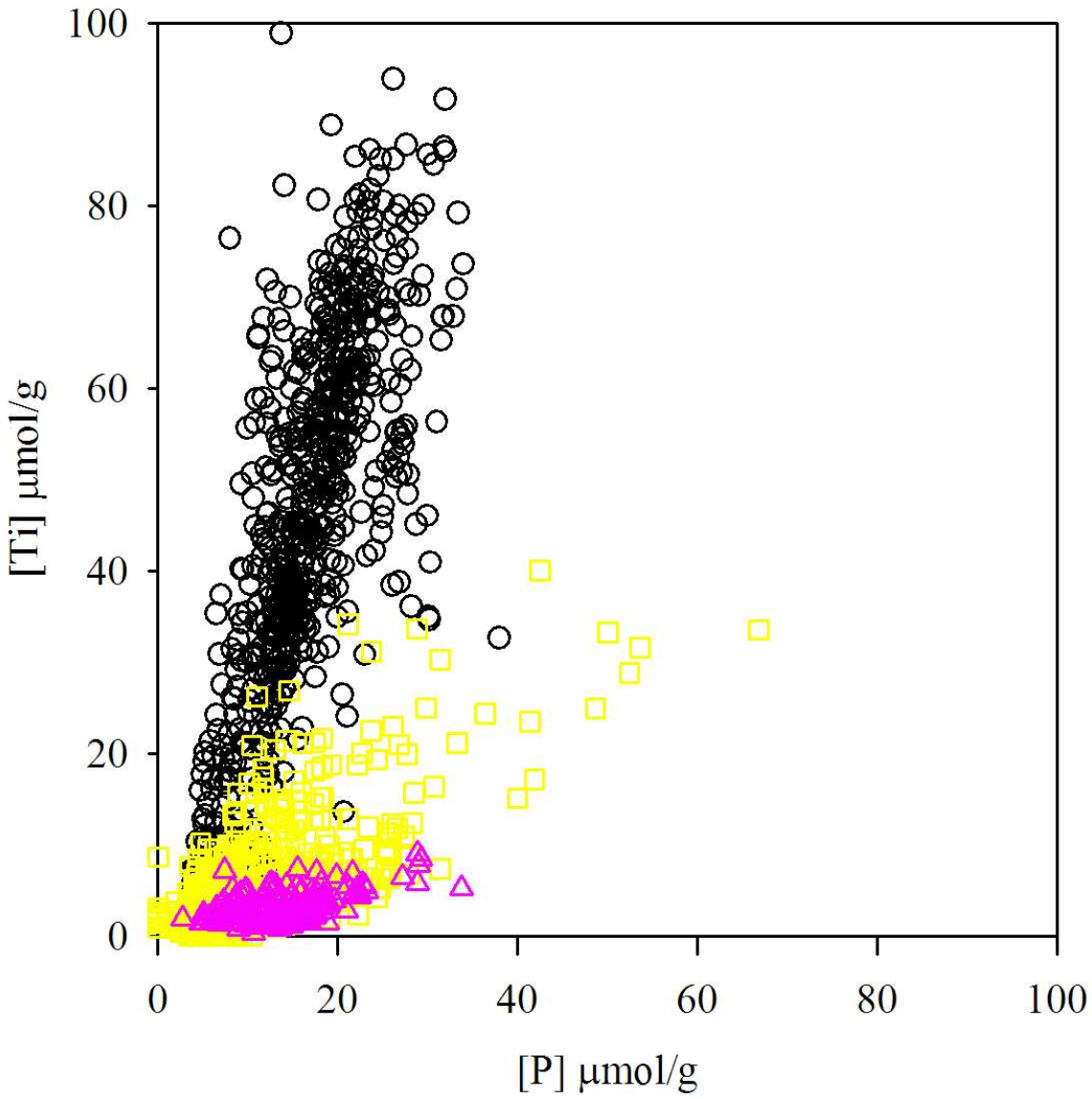

Figure 29. Ti concentration versus P concentration comparison plot for RR0603-03 (pink triangles), the JGOFS transect (yellow squares) and the Southern Ocean sites (black circles).

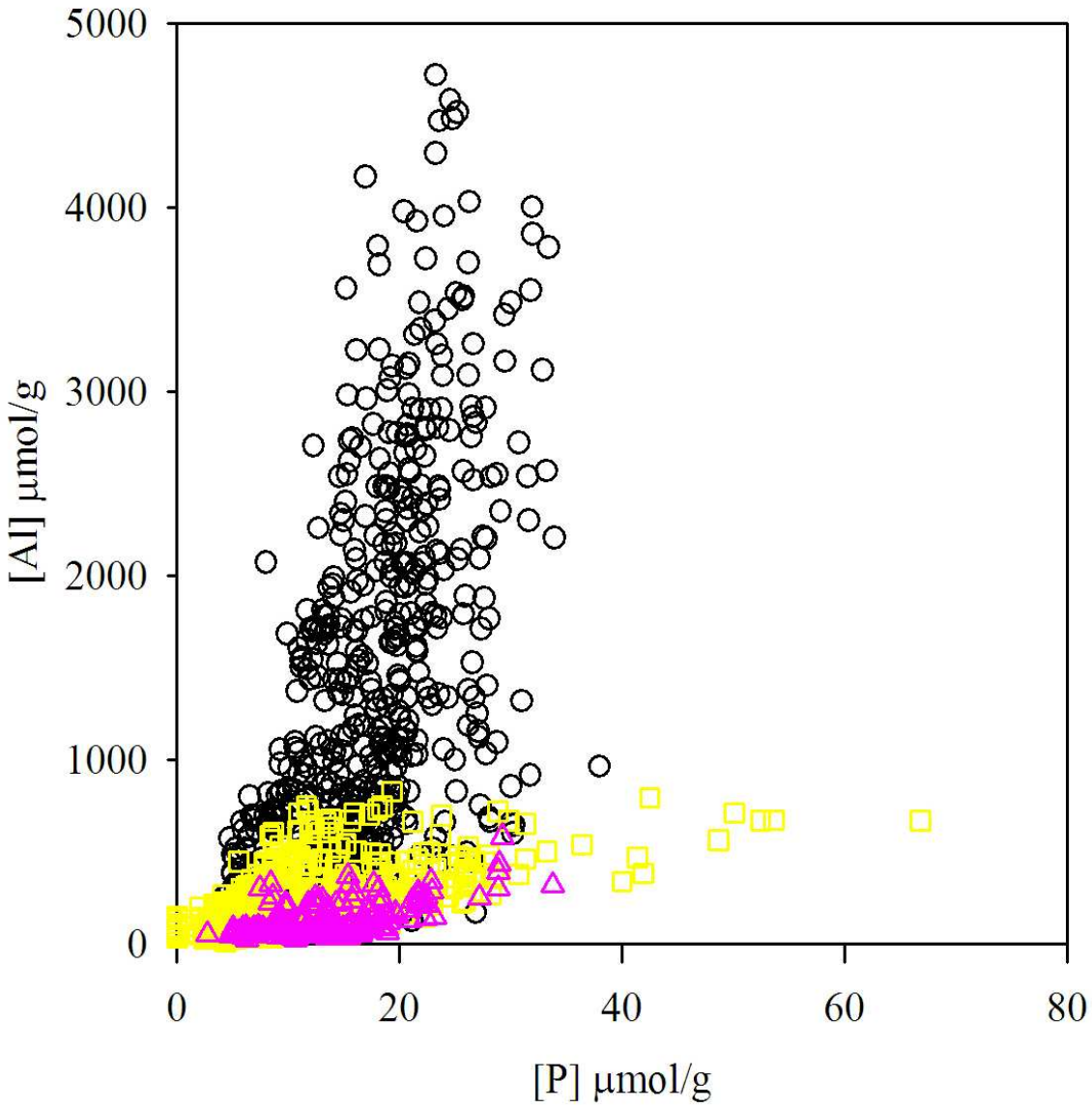

Figure 30. Al concentration versus P concentration comparison plot for RR0603-03 (pink triangles), the JGOFS transect (yellow squares) and the Southern Ocean sites (black circles).

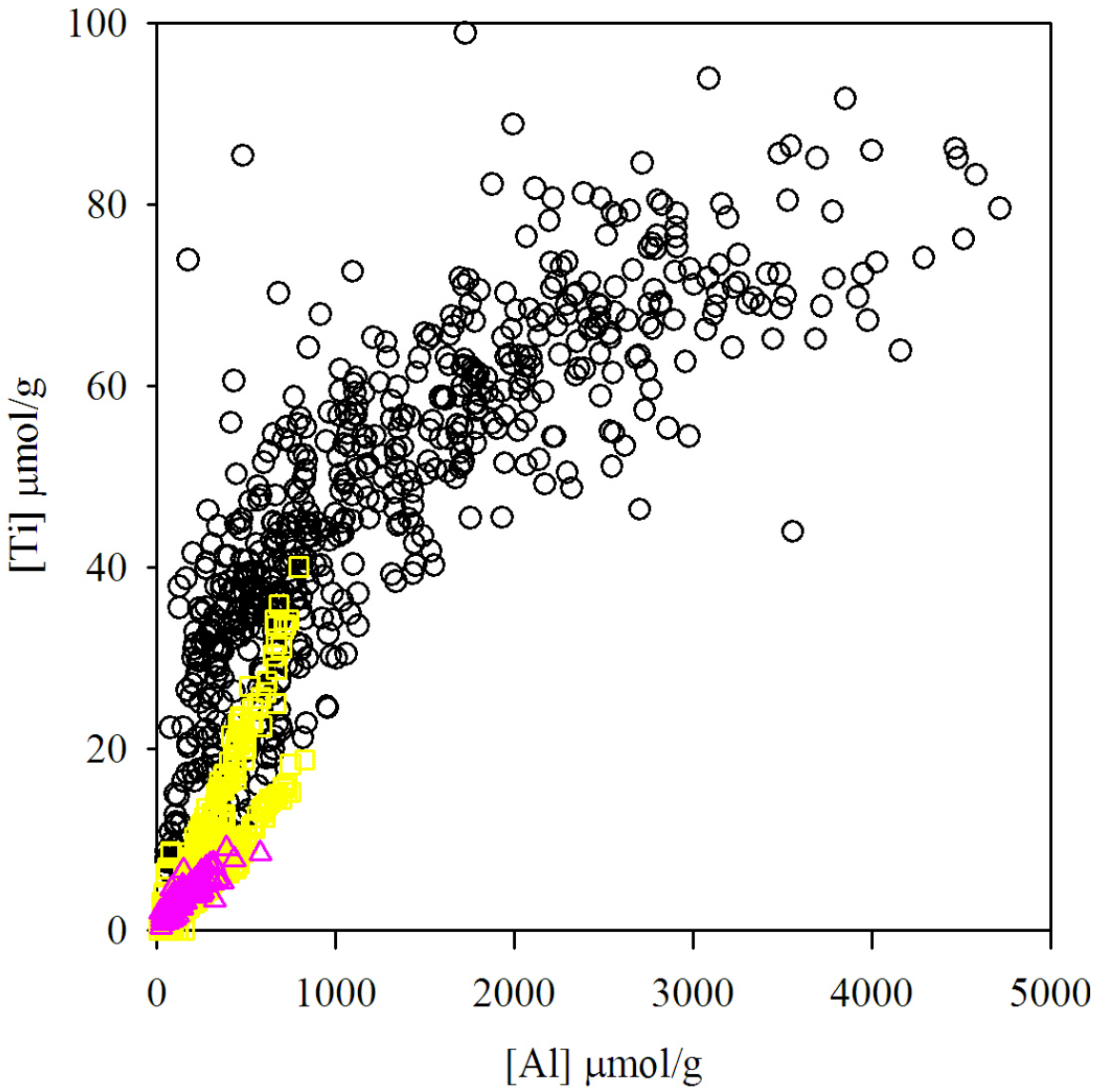

Figure 31. Ti concentration versus Al concentration comparison plot for RR0603-03 (pink triangles), the JGOFS transect (yellow squares) and the Southern Ocean sites (black circles).

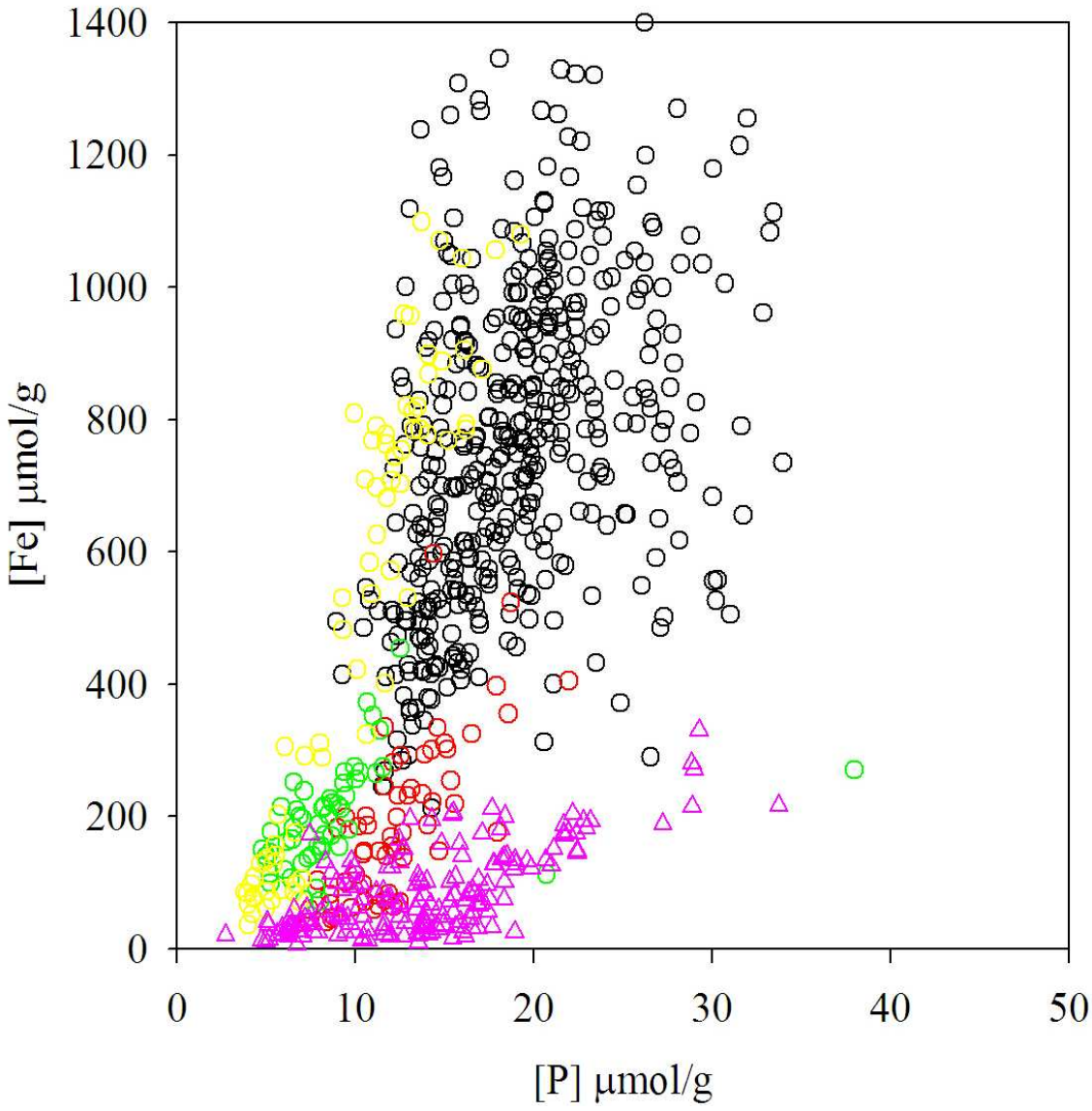

Figure 32. Fe concentration versus P concentration comparison plot for RR0603-03 (pink triangles) and for Southern Ocean sites RC13-259 (yellow circles), RC13-254 (green circles), E45-29 (red circles) and Site 1089 (black circles).

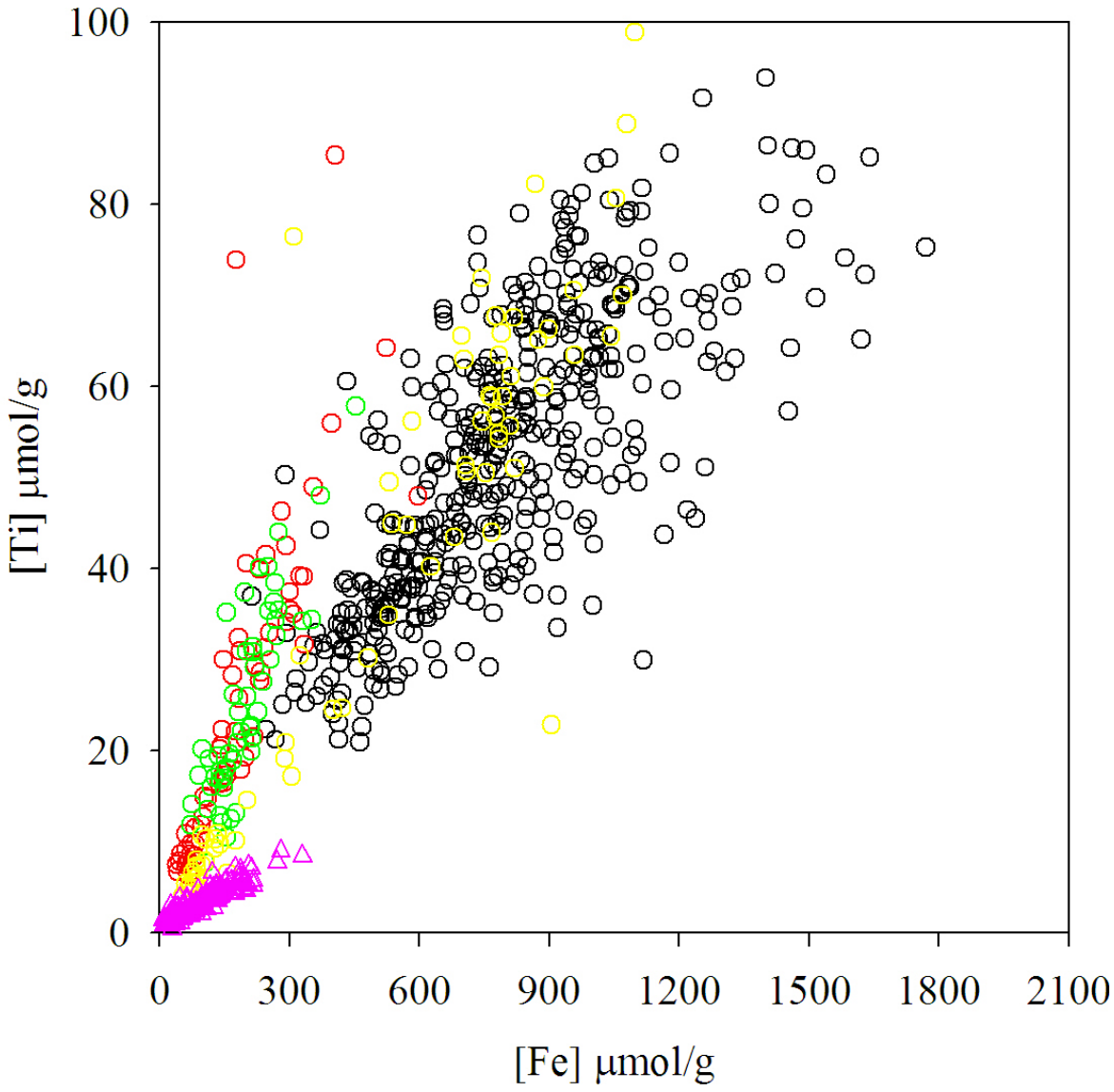

Figure 33. Ti concentration versus Fe concentration comparison plot for RR0603-03 (pink triangles) and for Southern Ocean sites RC13-259 (yellow circles), RC13-254 (green circles), E45-29 (red circles) and Site 1089 (black circles).

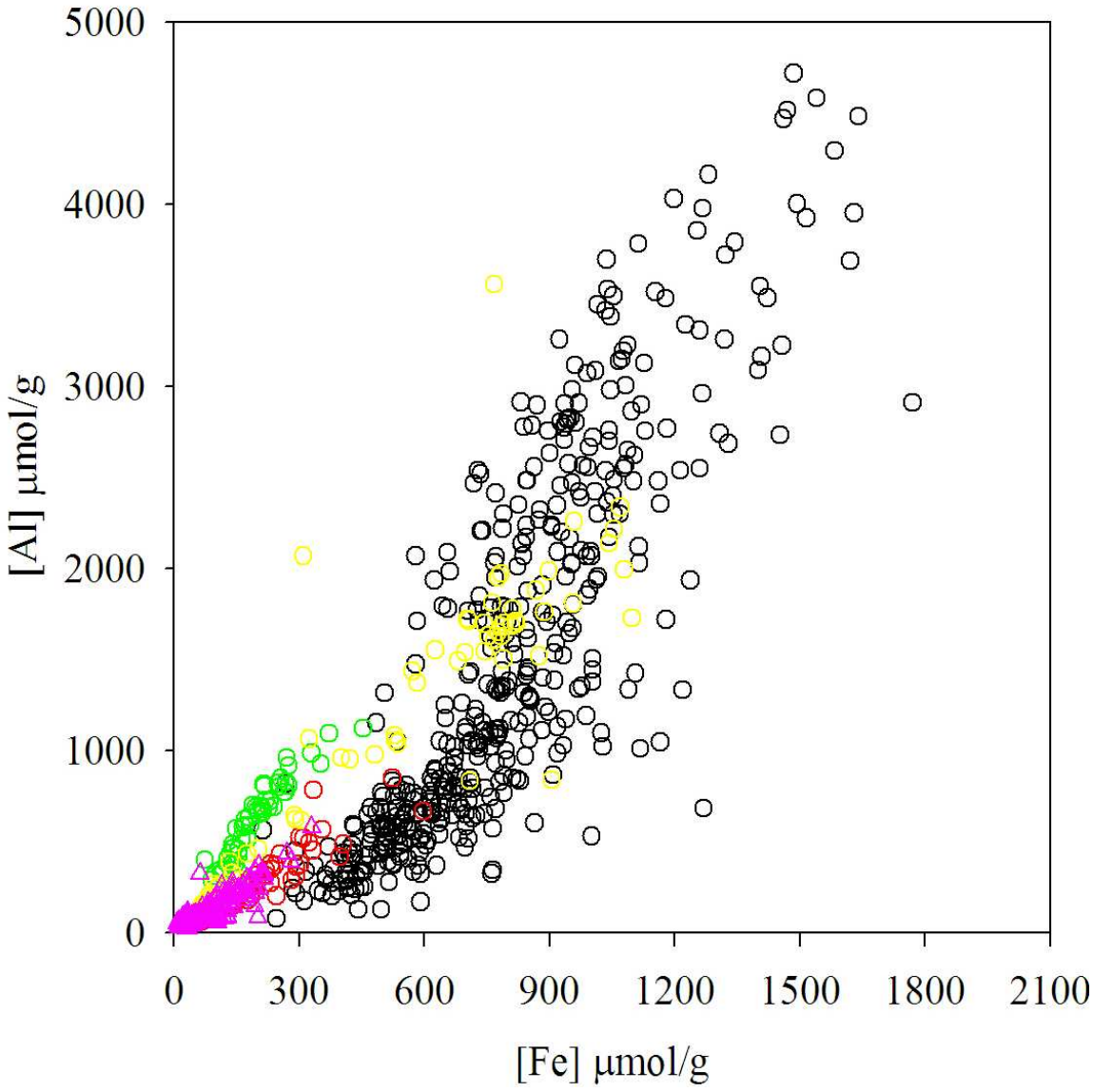

Figure 34. Al concentration versus Fe concentration comparison plot for RR0603-03 (pink triangles) and for Southern Ocean sites RC13-259 (yellow circles), RC13-254 (green circles), E45-29 (red circles) and Site 1089 (black circles).

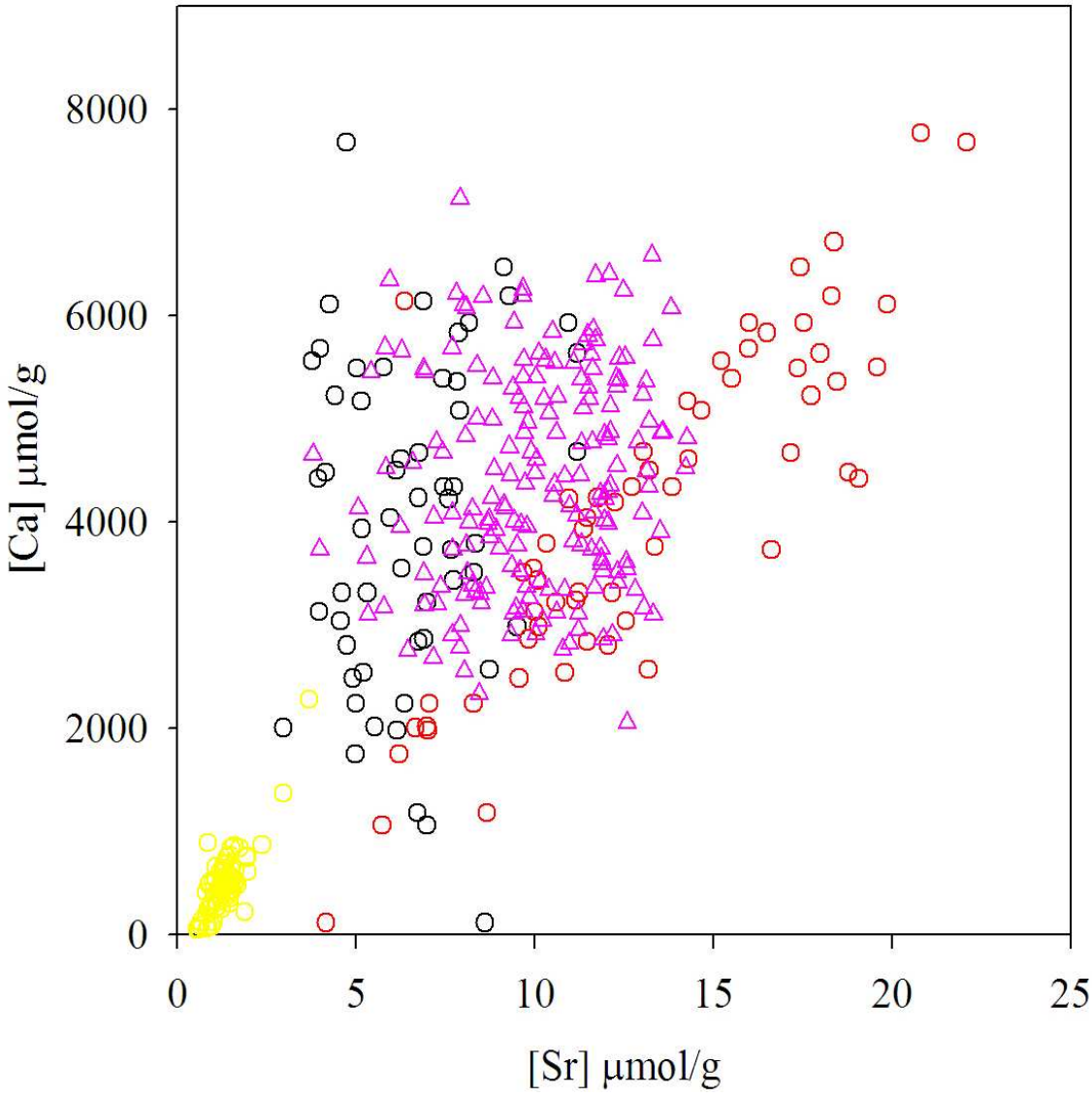

Figure 35. Ca concentration versus Sr concentration comparison plot for RR0603-03 (pink triangles) and for Southern Ocean sites RC13-259 (yellow circles), E45-29 (red circles) and Site 1089 (black circles).

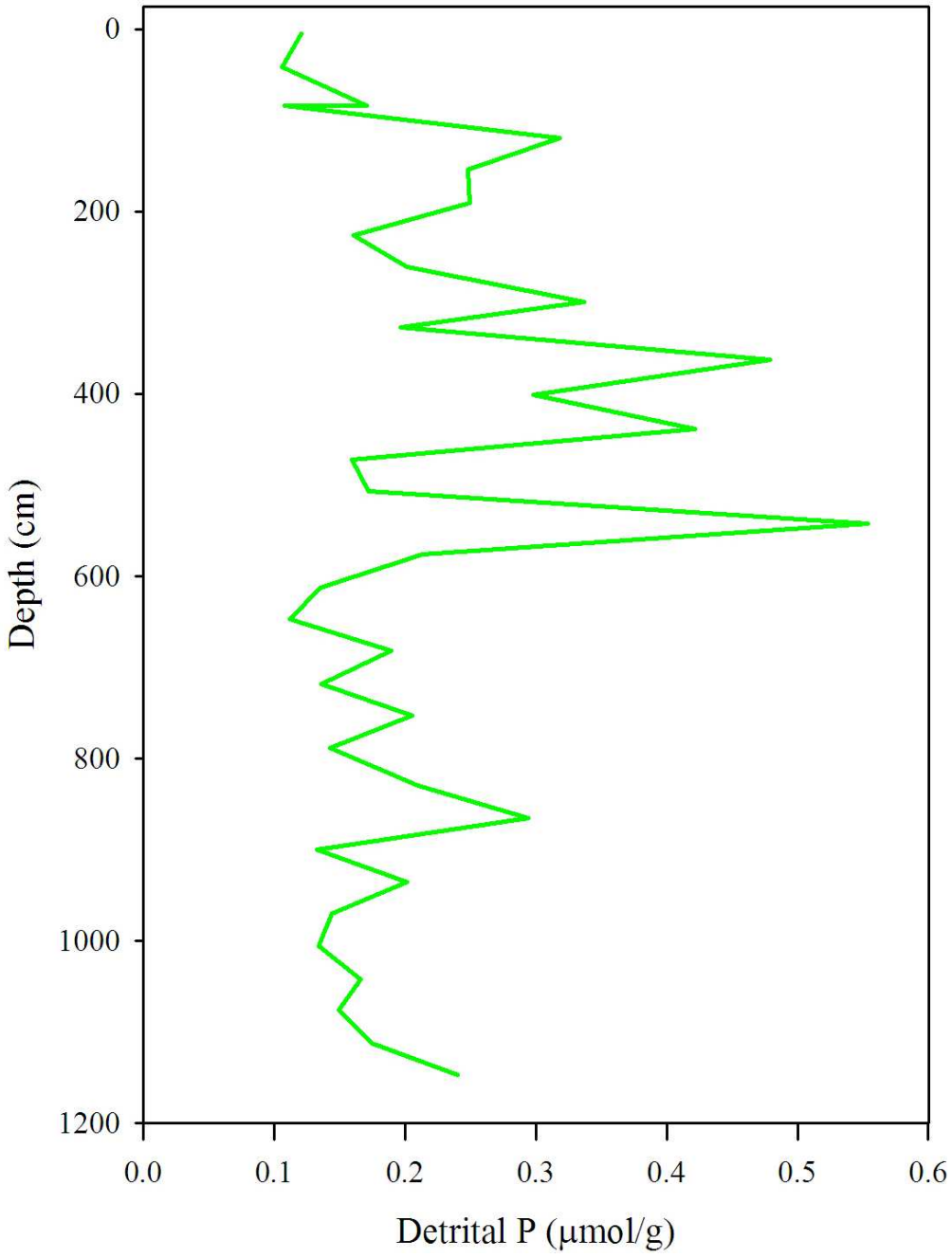

Figure 36. Detrital P concentration with depth for RR0603-03.

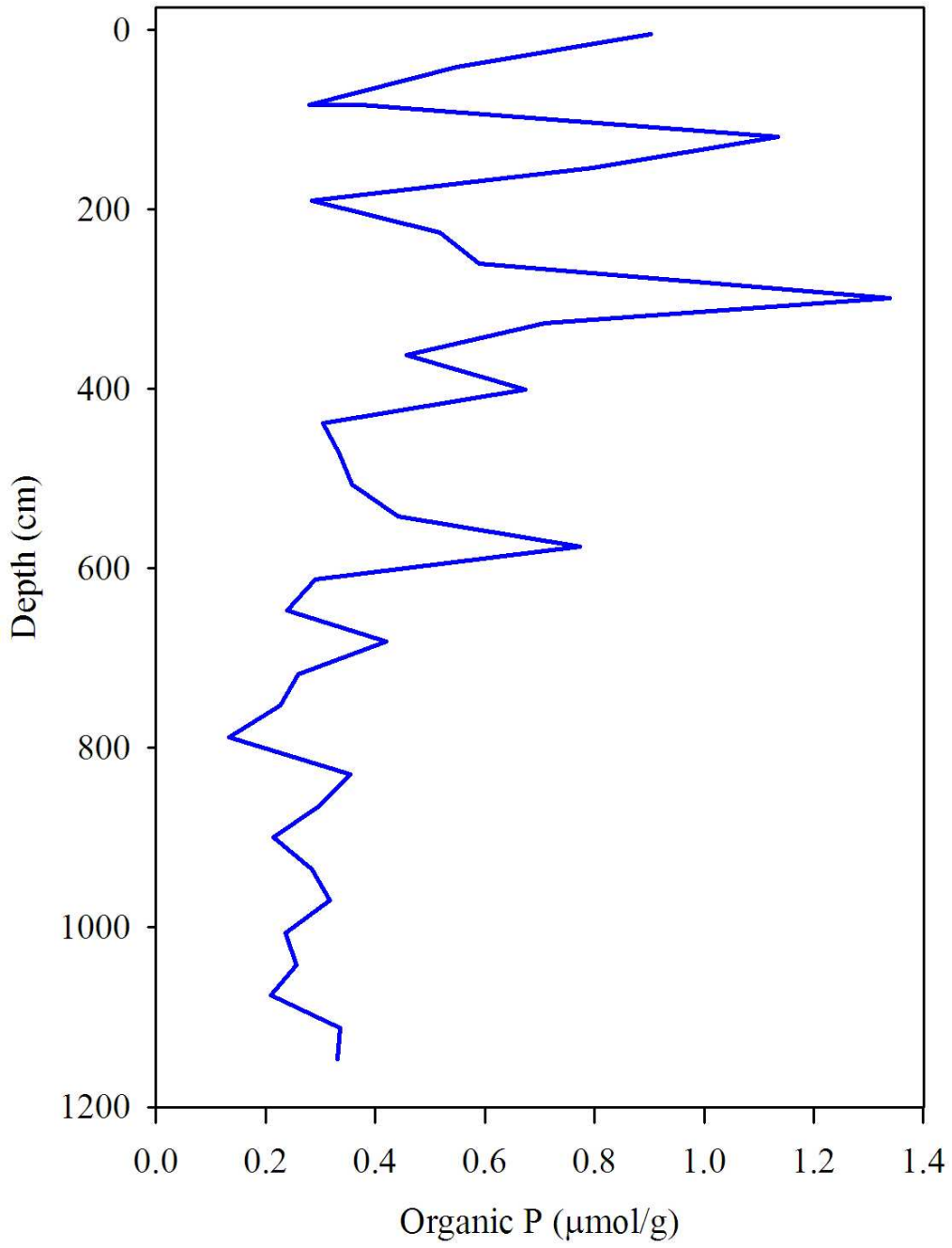

Figure 37. Organic P concentration with depth for RR0603-03.

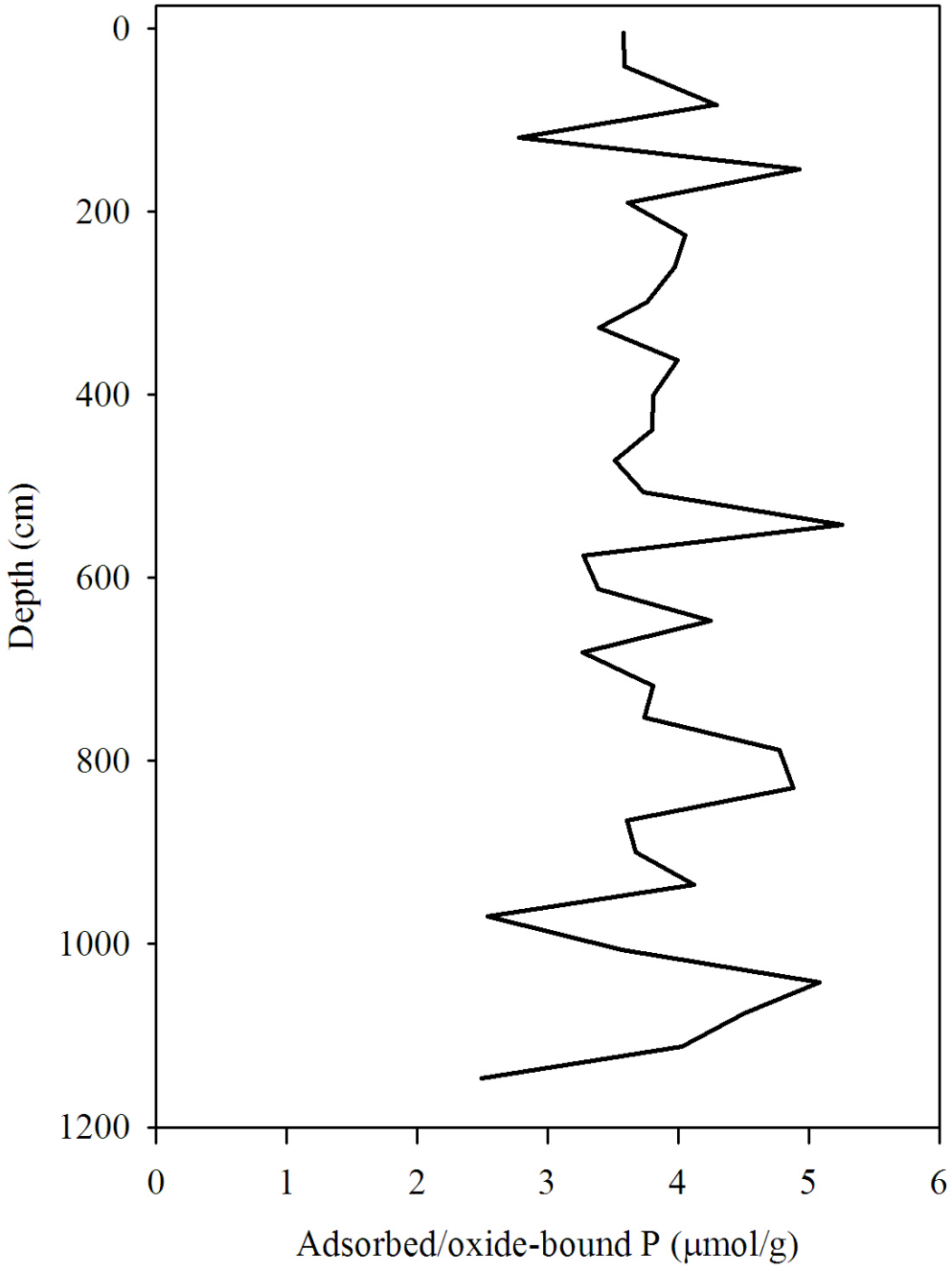

Figure 38. Adsorbed/oxide-bound P concentration with depth for RR0603-03.

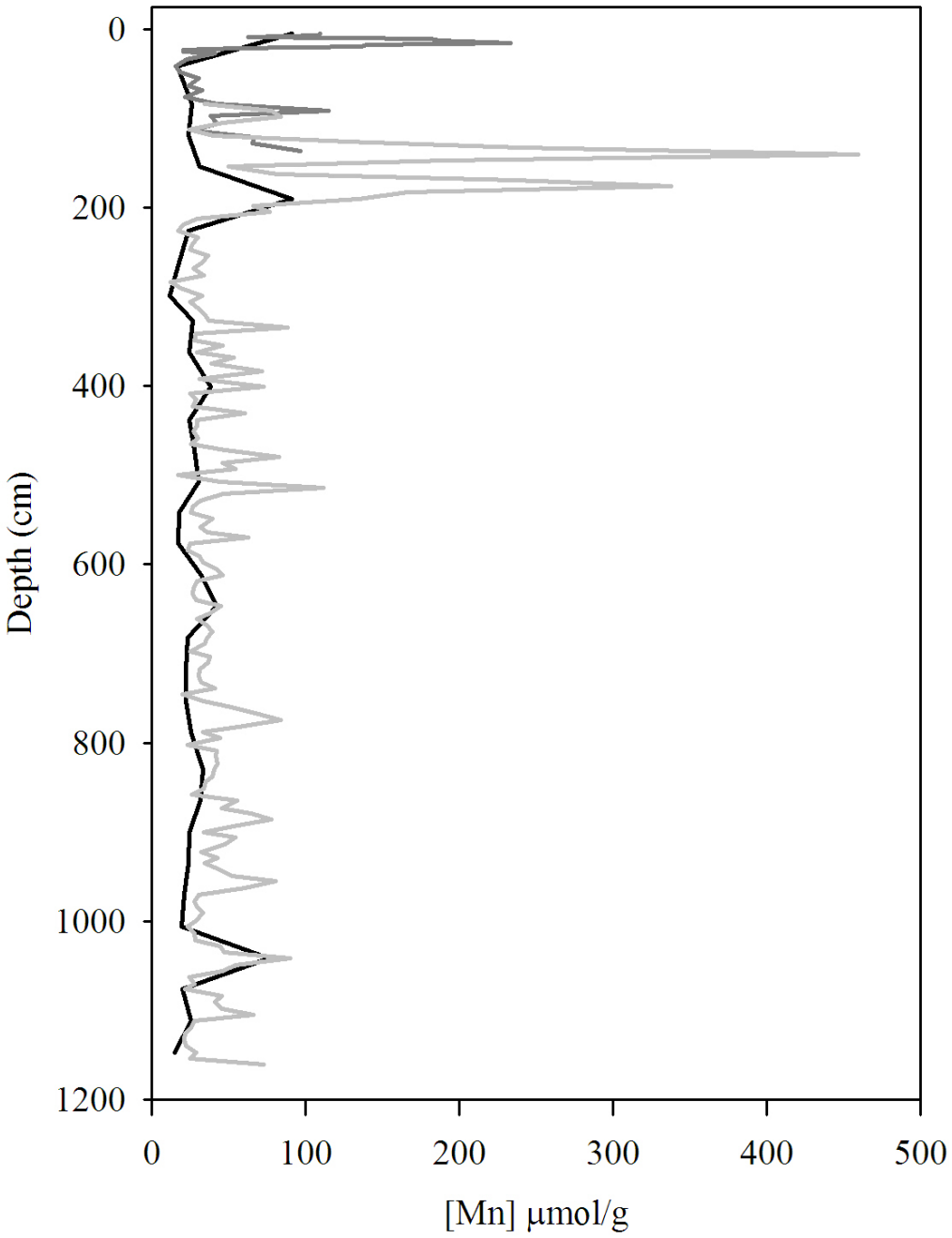

Figure 39. Oxide-bound Mn concentration (black) compared to total Mn concentration (gray) with depth for RR0603-03.

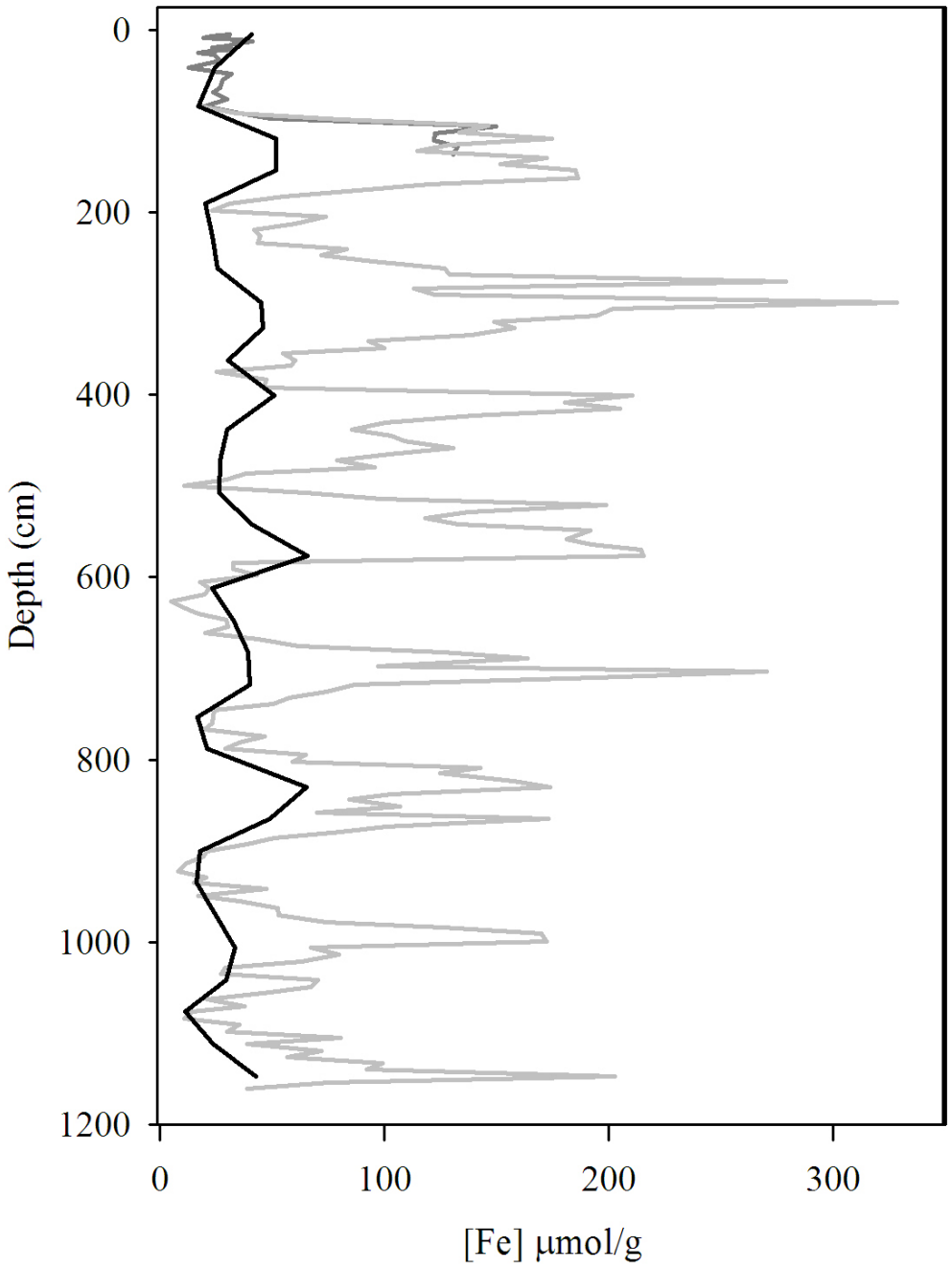

Figure 40. Oxide-bound Fe concentration (black) compared to total Fe concentration (gray) with depth for RR0603-03.

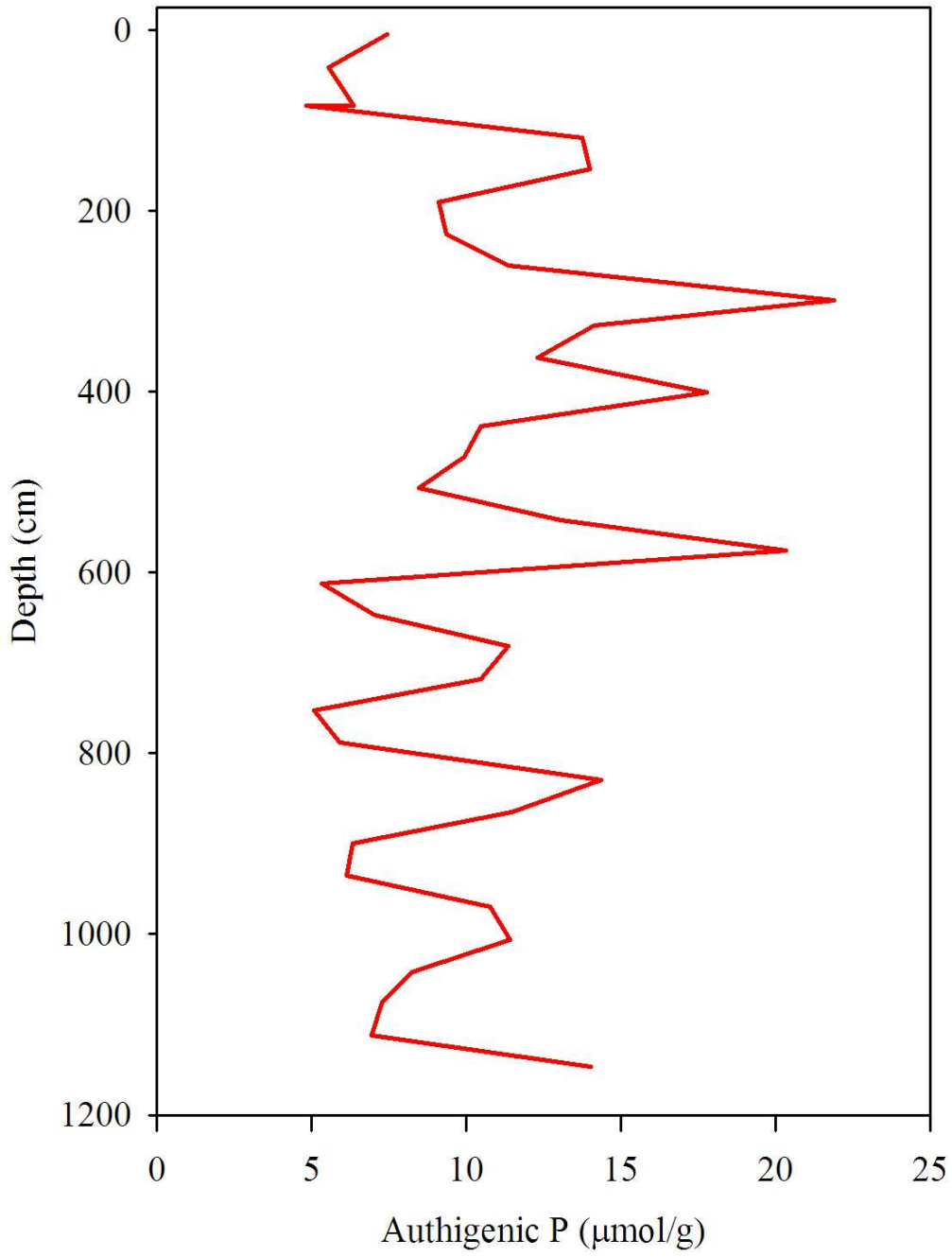

Figure 41. Authigenic P concentration with depth for RR0603-03.

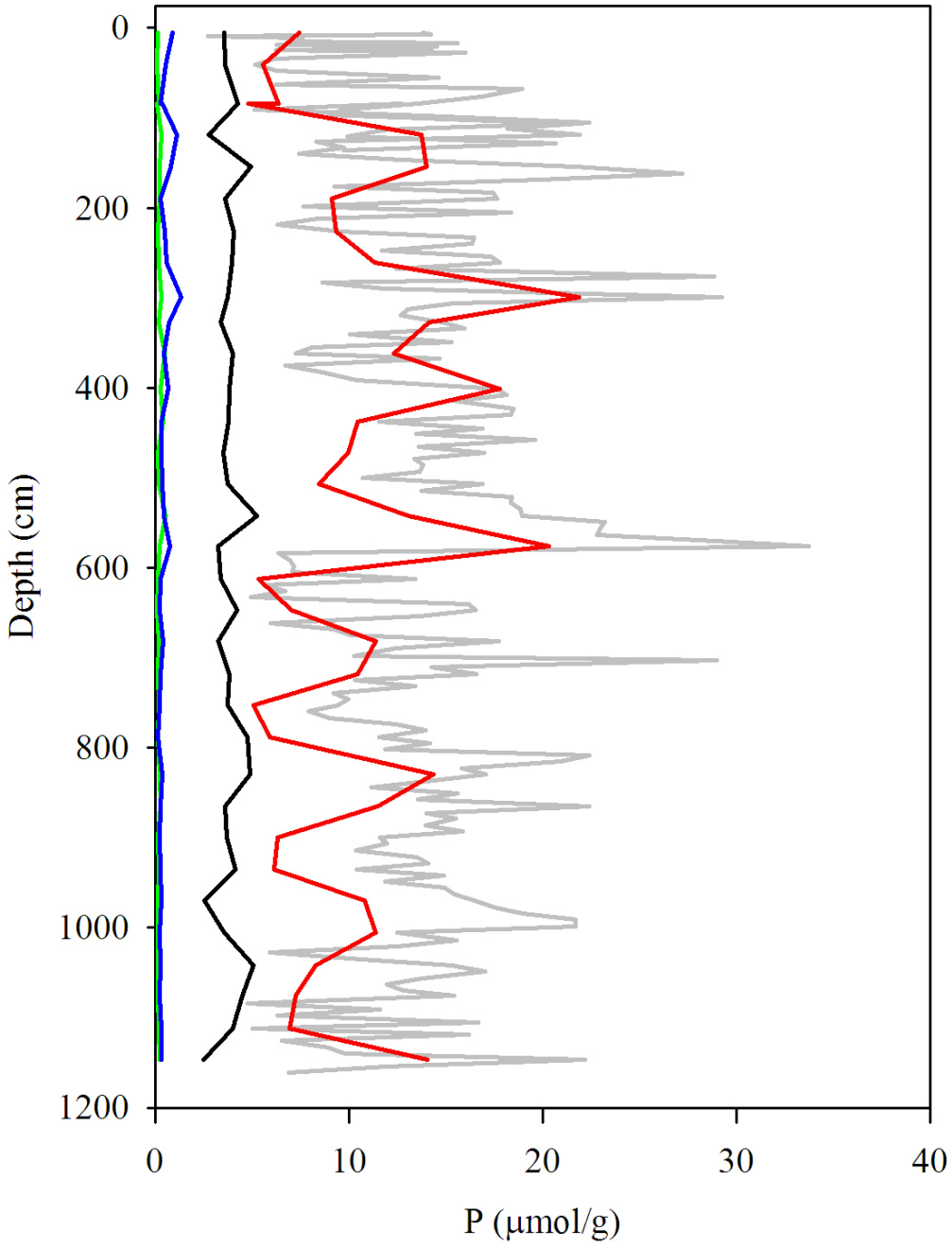

Figure 42. P compilation. Authigenic P (red), oxide-bound P (black), organic P (blue), detrital P (green) and total P concentration (gray) with depth.

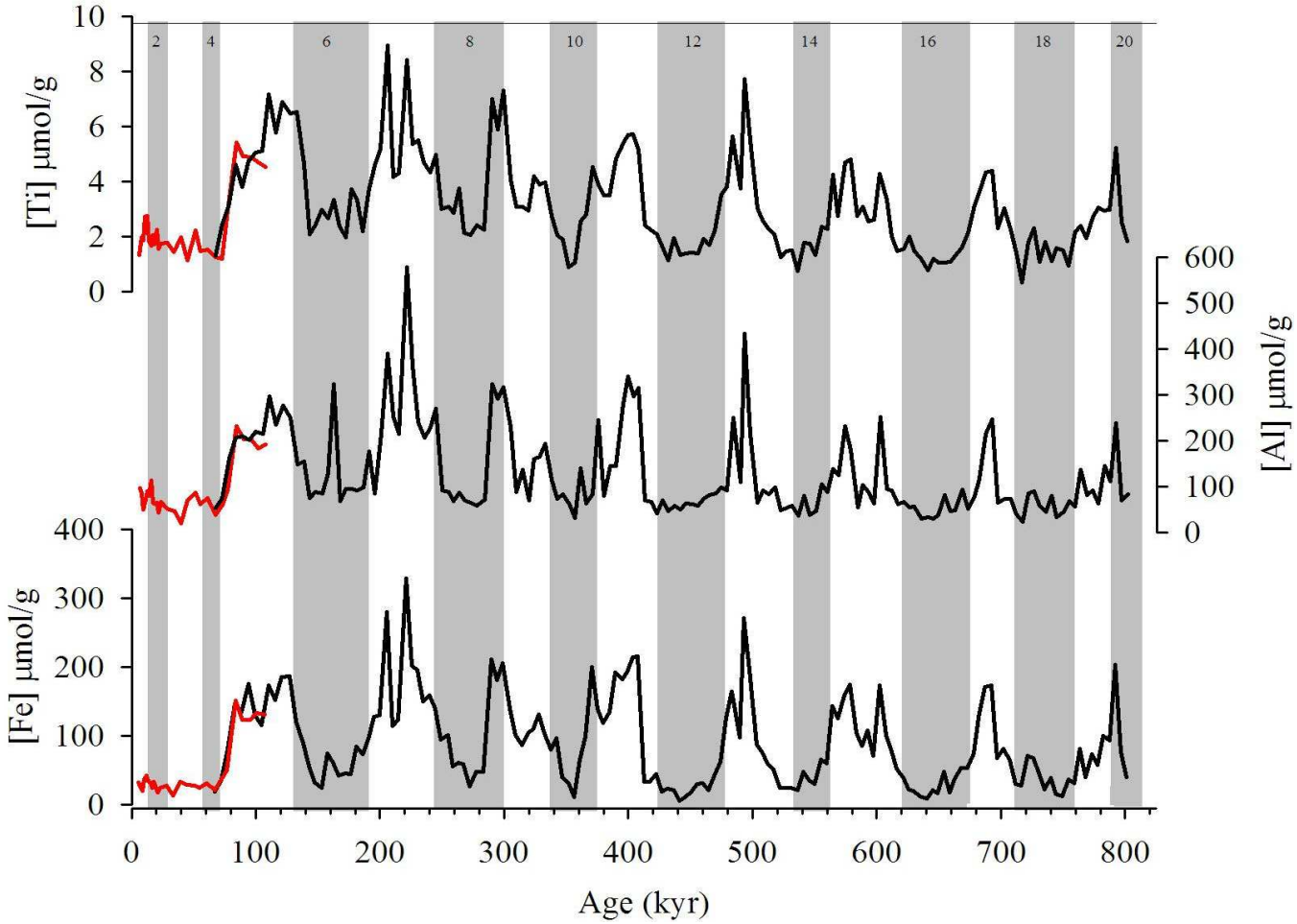

Figure 43. Ti, Al and Fe concentration versus age for RR0603-03. Gray vertical bars represent glacial intervals with their corresponding MIS number labeled at the top. Trigger core data is shown in red.

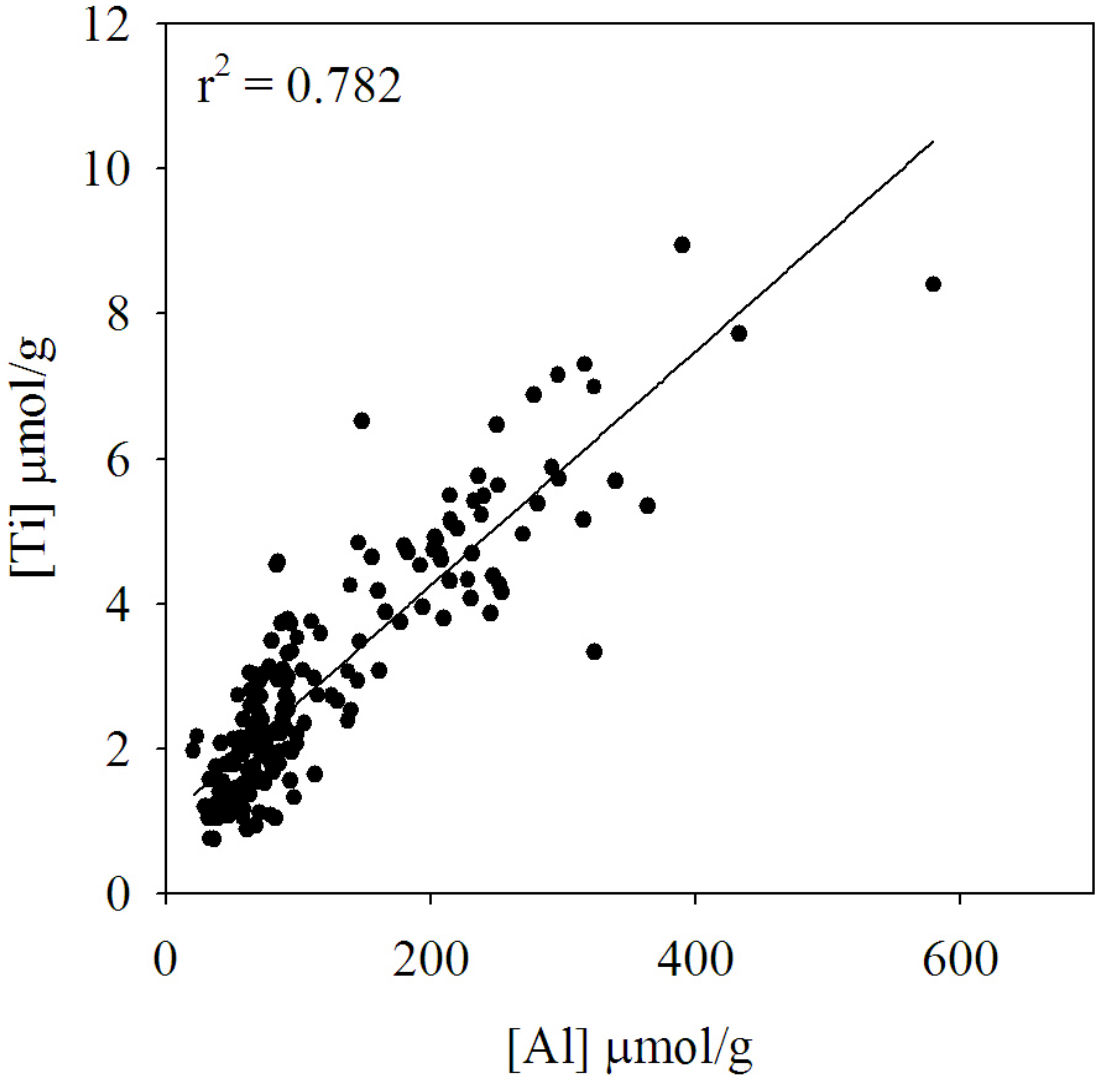

Figure 44. Ti concentration versus Al concentration. The spearman coefficient is provided in the top left corner.

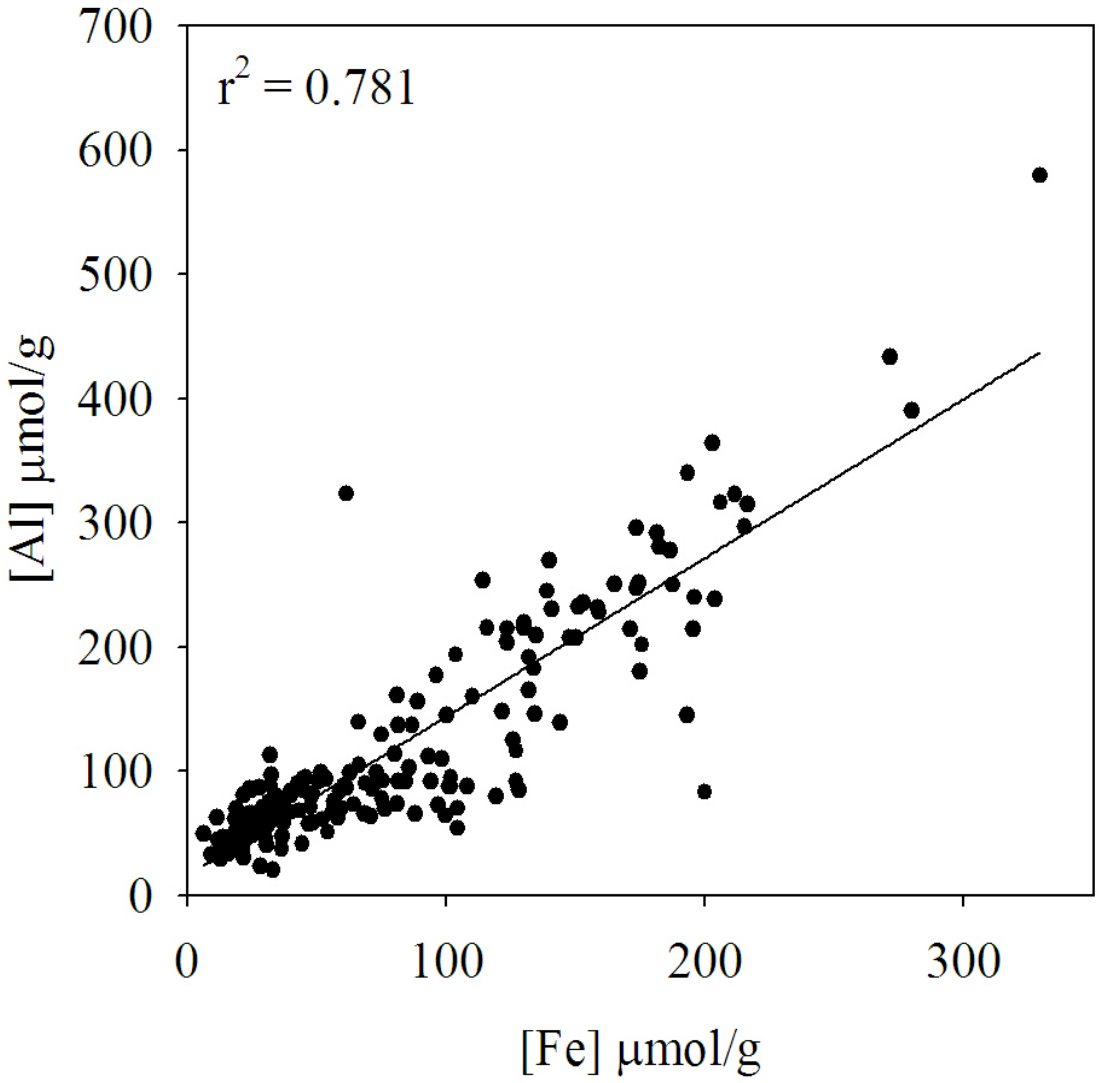

Figure 45. Al concentration versus Fe concentration. The spearman coefficient is provided in the top left corner.

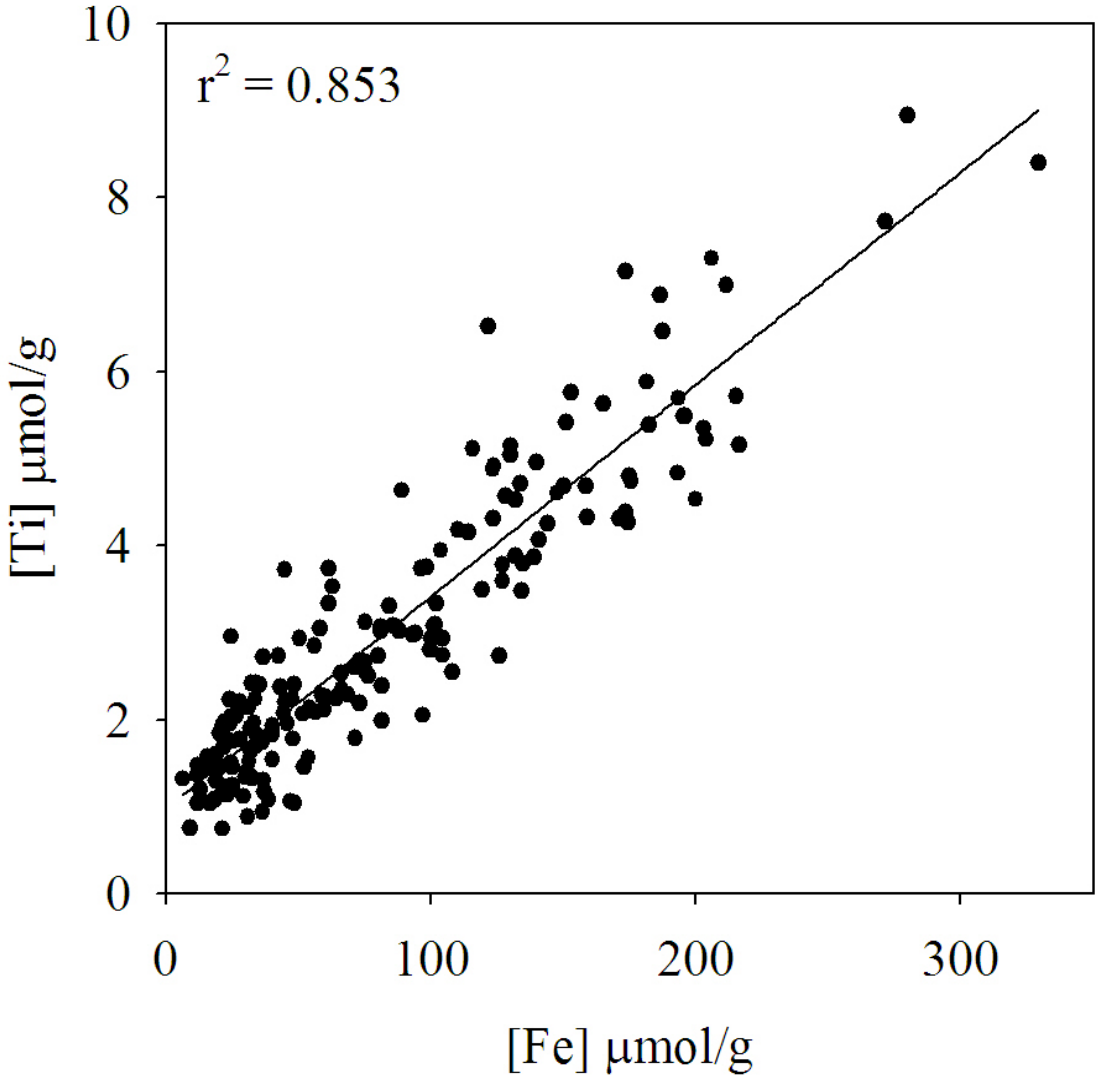

Figure 46. Ti concentration versus Fe concentration. The spearman coefficient is provided in the top left corner.

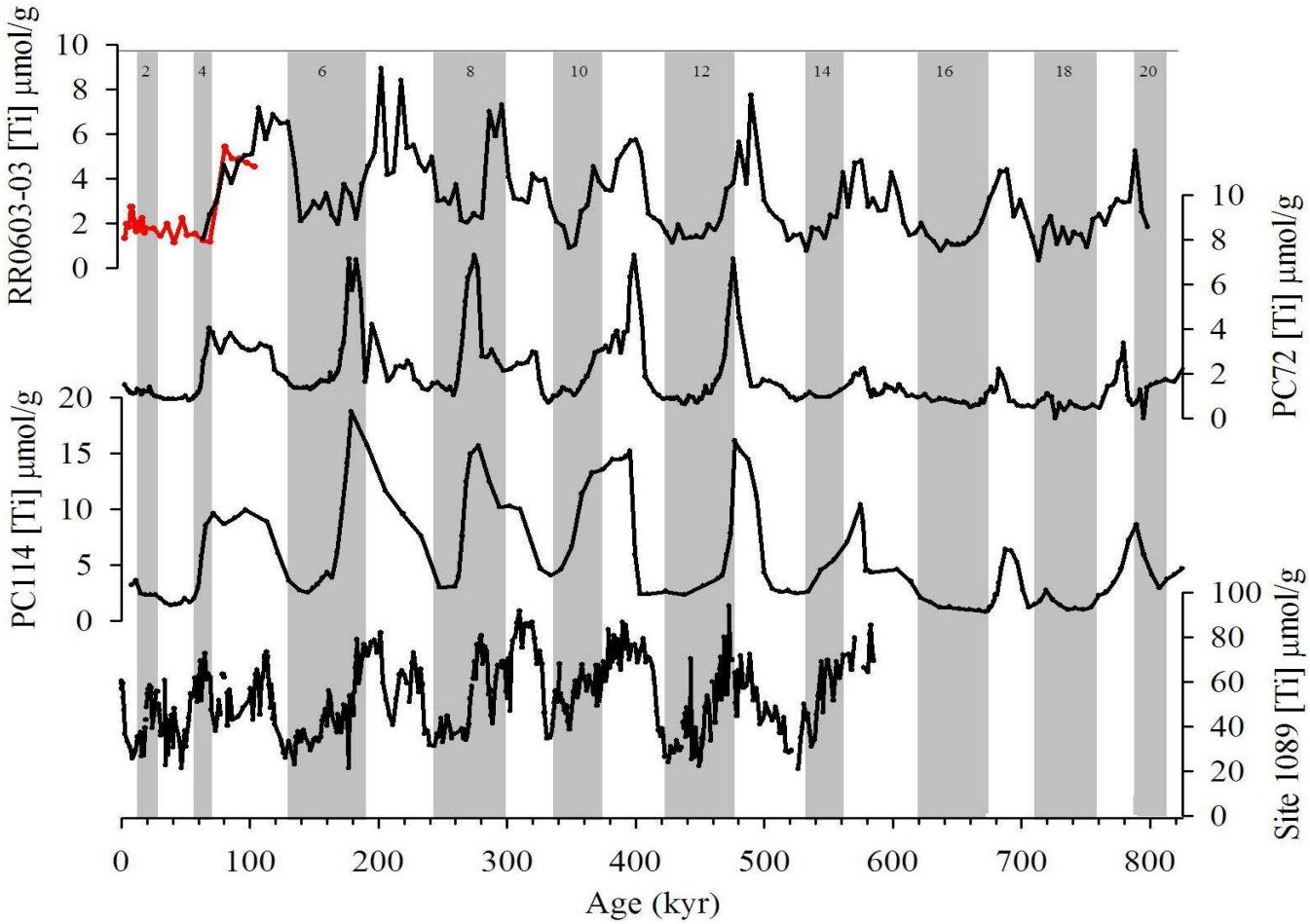

Figure 47. Ti concentration versus age comparison. Ti concentrations versus age for equatorial sites RR0603-03, PC72, PC114, and Southern Ocean Site 1089. Gray vertical bars represent glacial intervals with their corresponding MIS number labeled at the top. Trigger core data for RR0603-03 is shown in red.

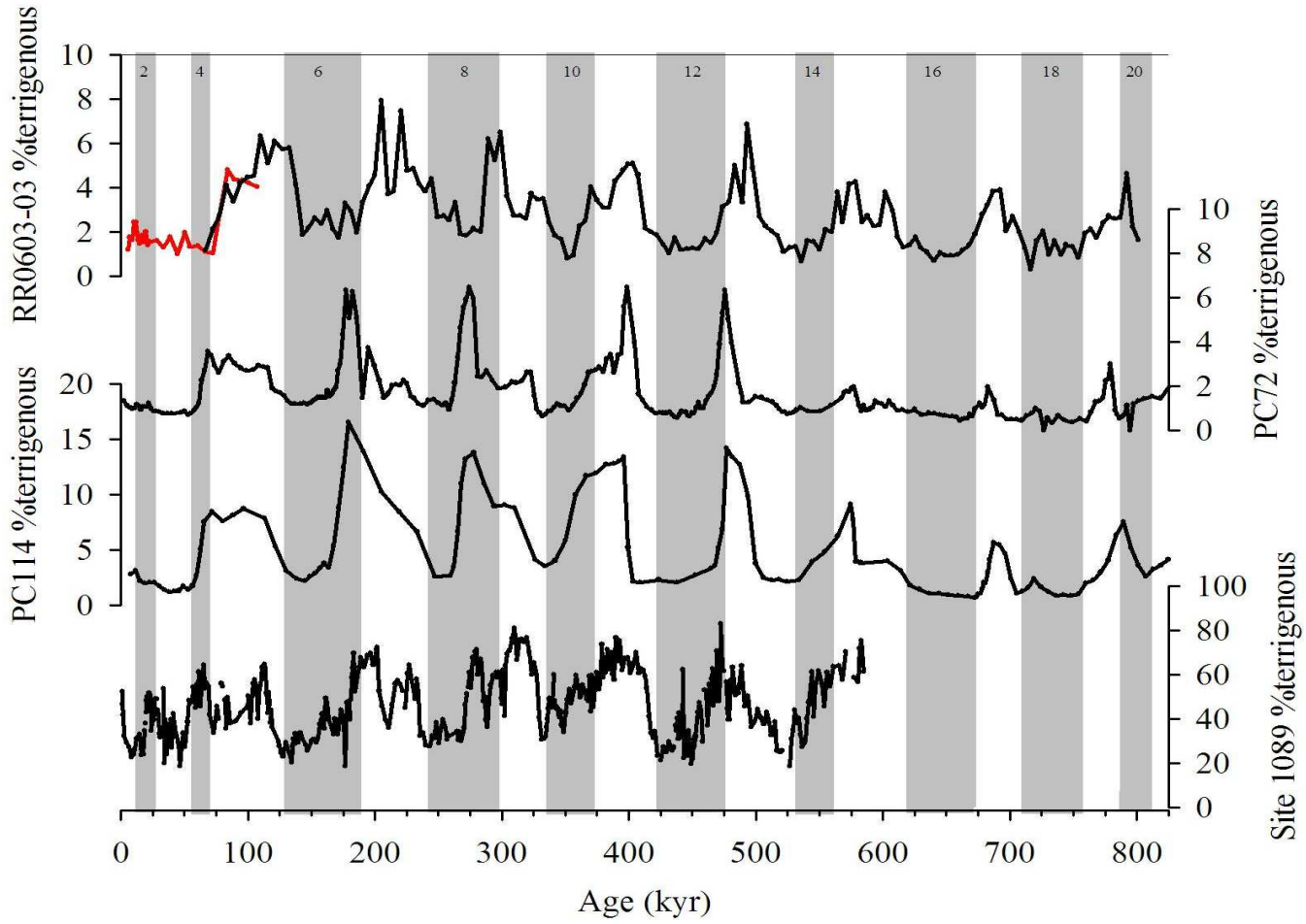

Figure 48. Percent terrigenous versus age comparison. Ti-normalized %terrigenous versus age for equatorial Pacific sites RR0603-03, PC72, PC114 and Southern Ocean Site 1089. Gray vertical bars represent glacial intervals with their corresponding MIS number labeled at the top. Trigger core data for RR0603-03 is shown in red.

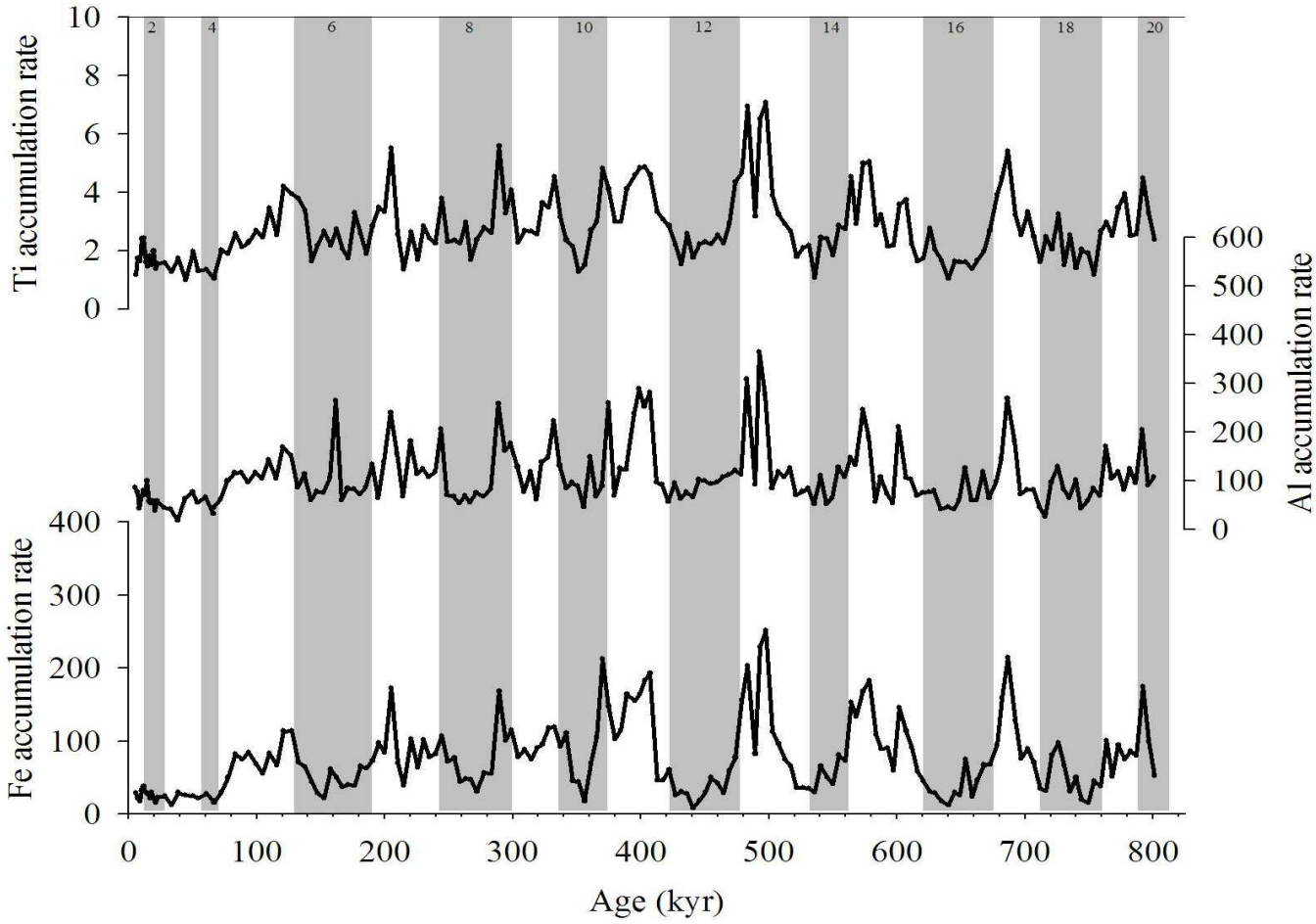

Figure 49. RR0603-03 accumulation rates versus age for Ti, Al and Fe in units of μmol cm^{-2} kyr^{-1}. Accumulation rate calculations for this graph are using the DBD closest to the sample and within the same sediment facies. Gray vertical bars represent glacial intervals with their corresponding MIS number labeled at the top.

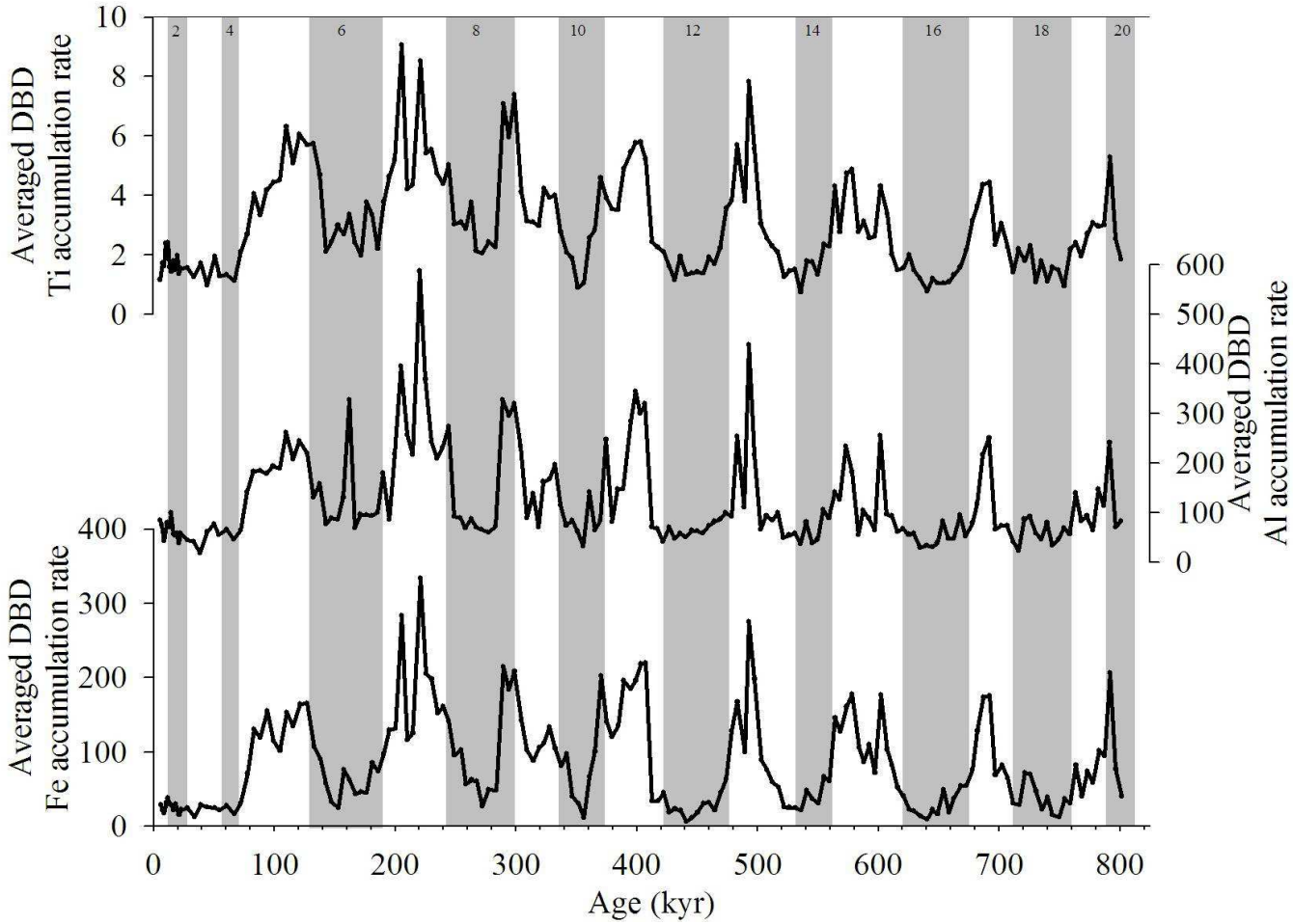

Figure 50. RR0603-03 averaged DBD accumulation rates versus age for Ti, Al and Fe in units of μmol cm^{-2} kyr^{-1}. Accumulation rate calculations for this graph are using the averaged DBD for the site. Gray vertical bars represent glacial intervals with their corresponding MIS number labeled at the top.

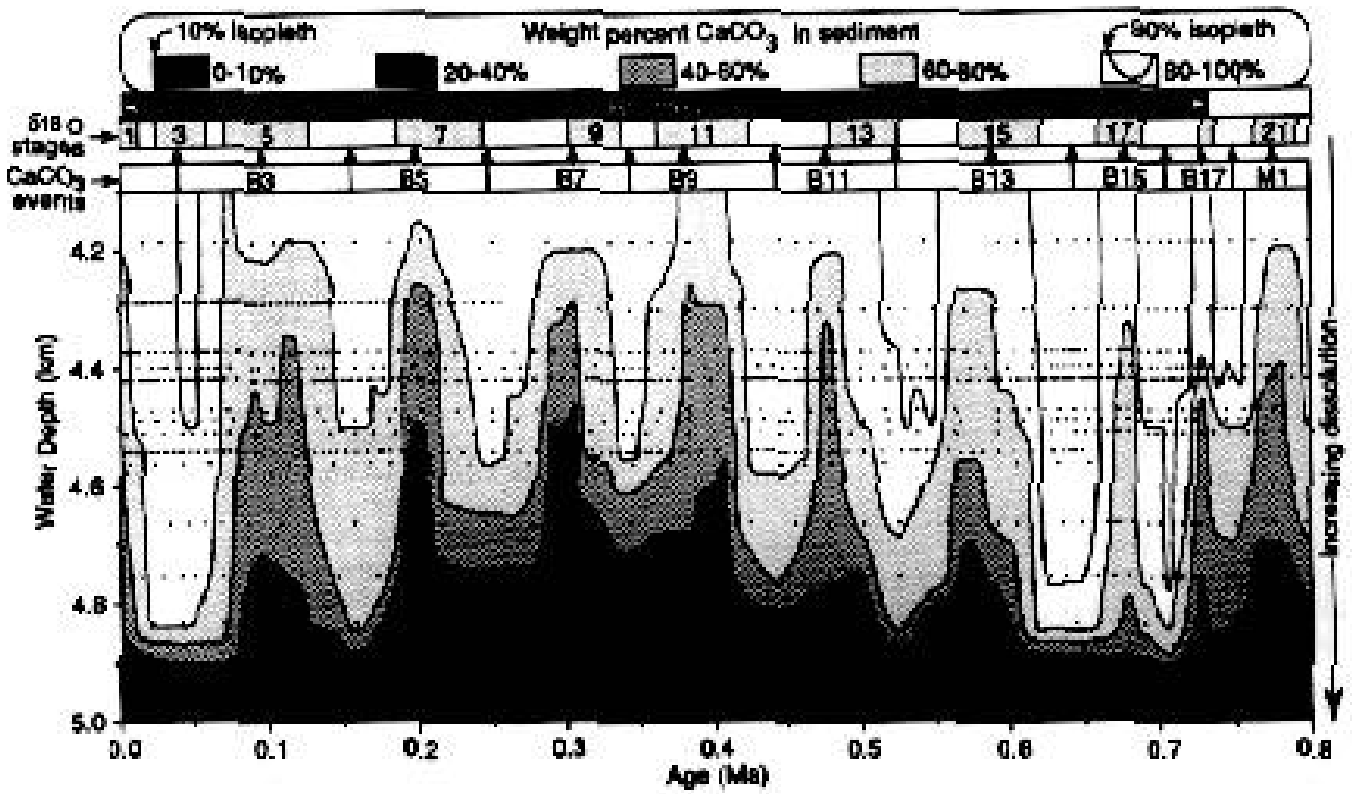

Figure 51. Equatorial Pacific $CaCO_3$ preservation. A cross-sectional diagram of the equatorial Pacific seafloor illustrating $CaCO_3$ preservation over the past 800 kyr. RR0603-03 was recovered at a depth of 4195 m. The diagram shows carbonate preservation at or above 80% for this depth over time (from Farrell and Prell, 1989).

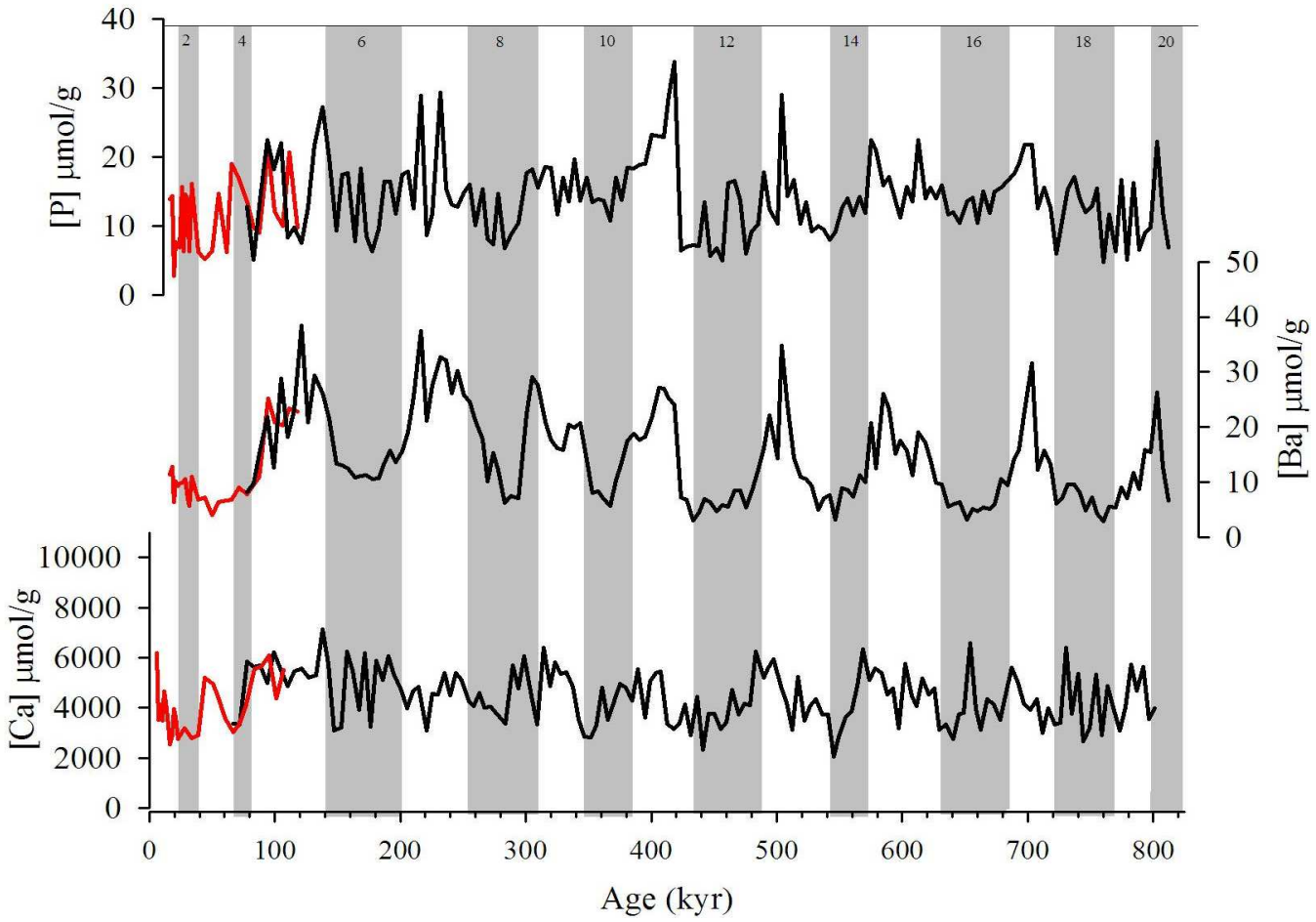

Figure 52. P, Ba and Ca concentrations versus age for RR0603-03. Gray vertical bars represent glacial intervals with their corresponding MIS number labeled at the top. Trigger core data for RR0603-03 is shown in red.

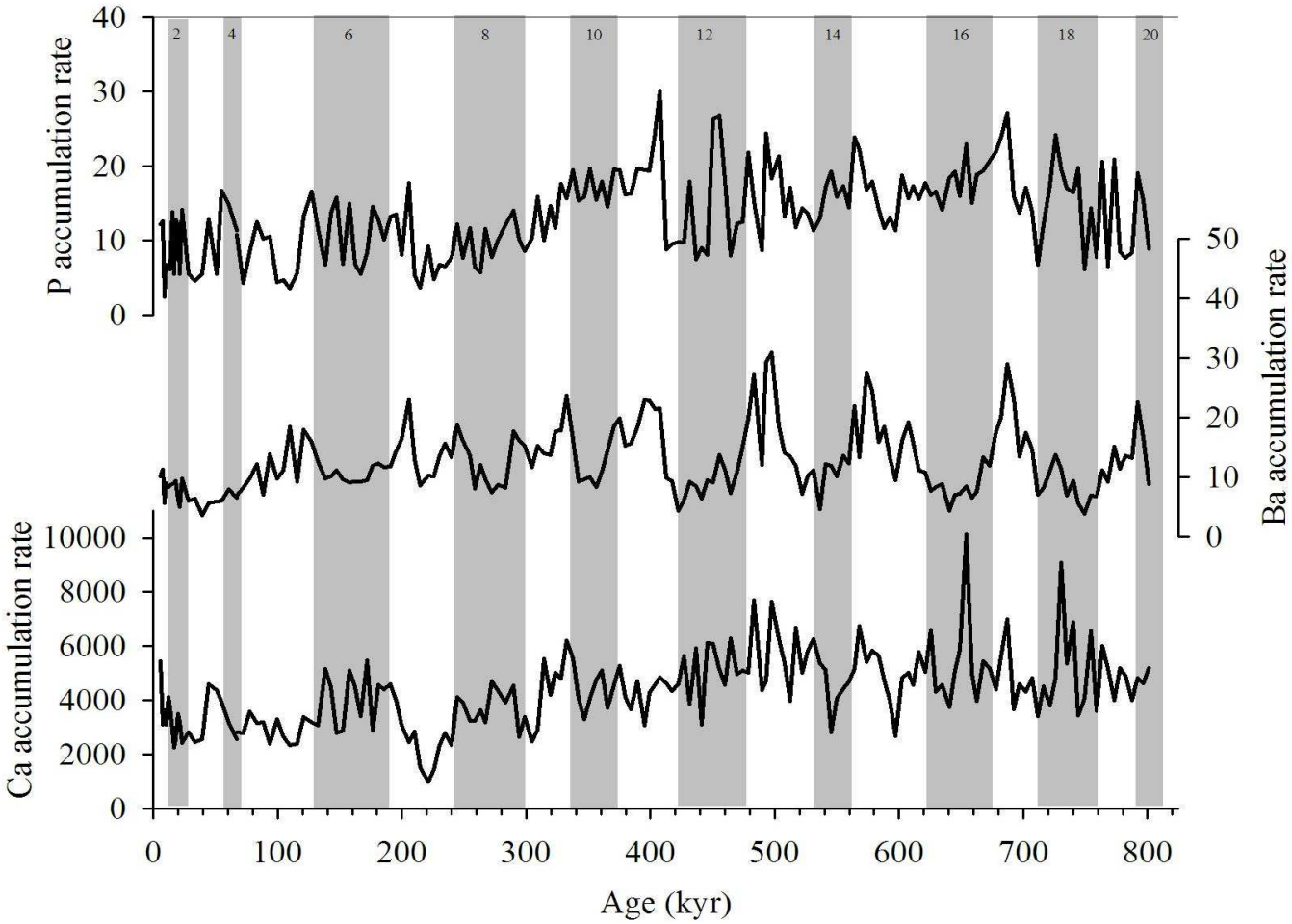

Figure 53. RR0603-03 accumulation rates versus age for P, Ba and Ca in units of μmol cm^{-2} kyr^{-1}. Accumulation rate calculations for this graph are using the DBD closest to the sample and within the same sediment facies. Gray vertical bars represent glacial intervals with their corresponding MIS number labeled at the top.

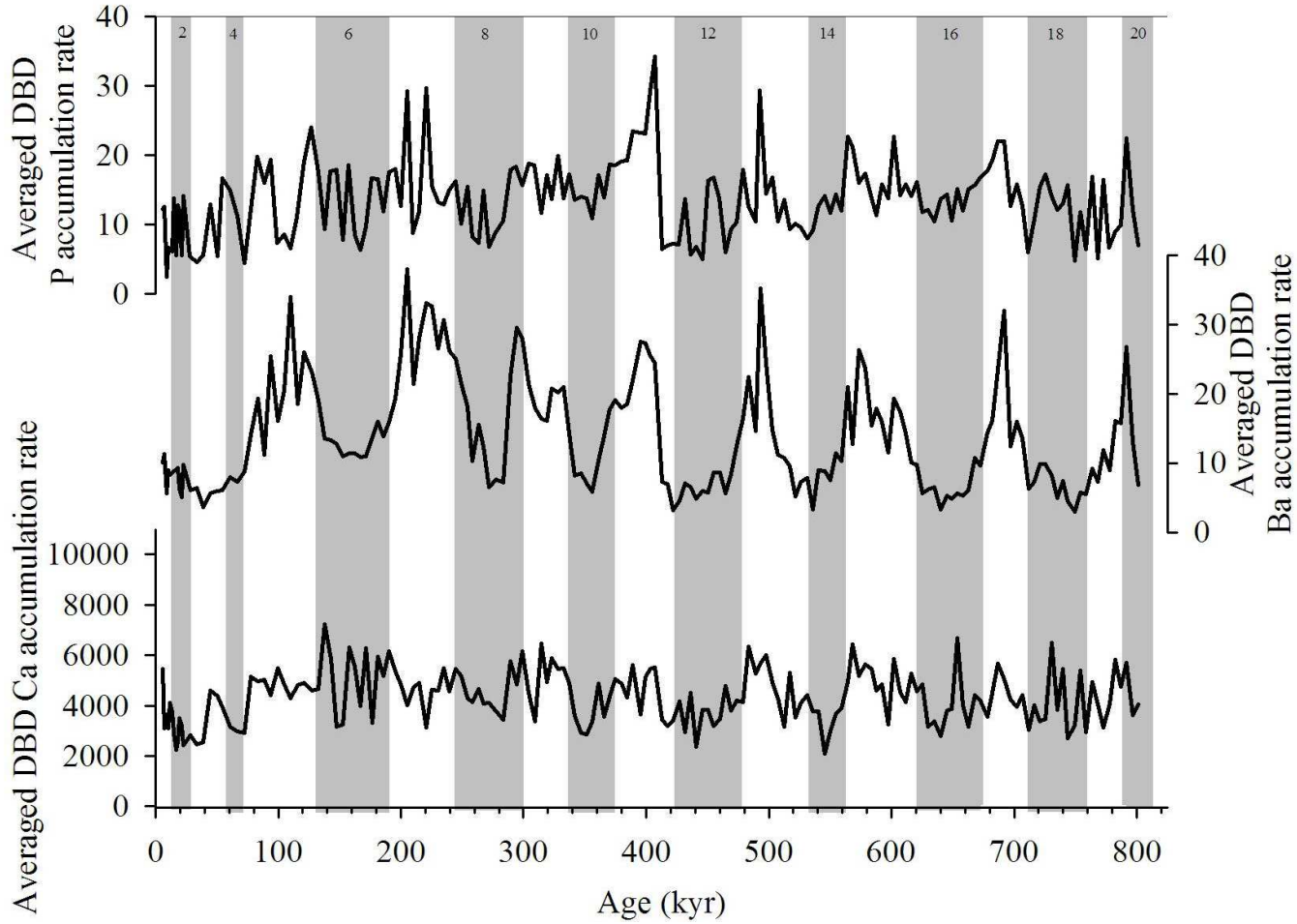

Figure 54. RR0603-03 averaged DBD accumulation rates versus age for P, Ba and Ca in units of μmol cm^{-2} kyr^{-1}. Accumulation rate calculations for this graph are using the averaged DBD for the site. Gray vertical bars represent glacial intervals with their corresponding MIS number labeled at the top.

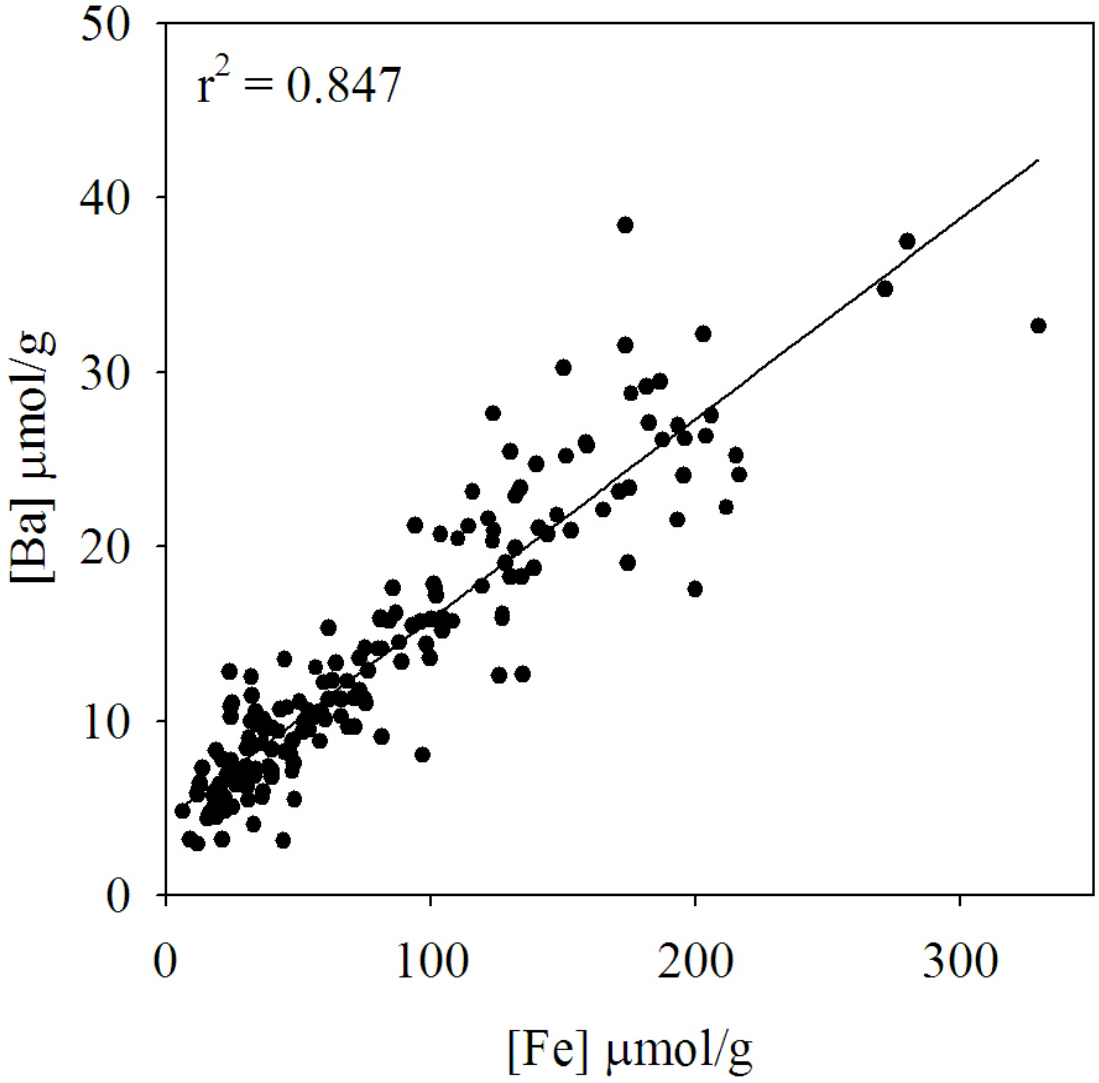

Figure 55. Ba versus Fe concentration. The spearman coefficient is provided in the top left corner.

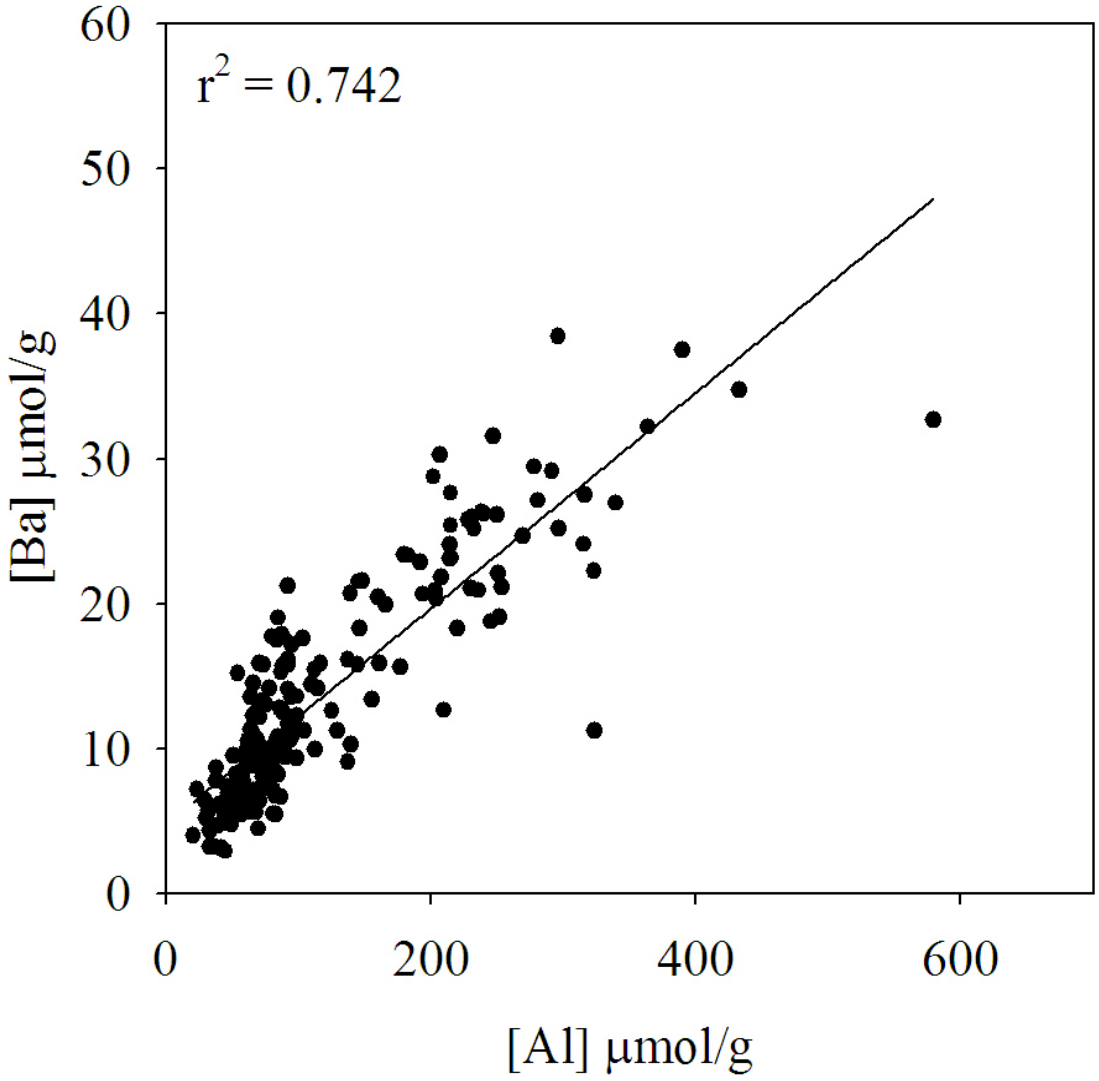

Figure 56. Ba versus Al concentration. The spearman coefficient is provided in the top left corner.

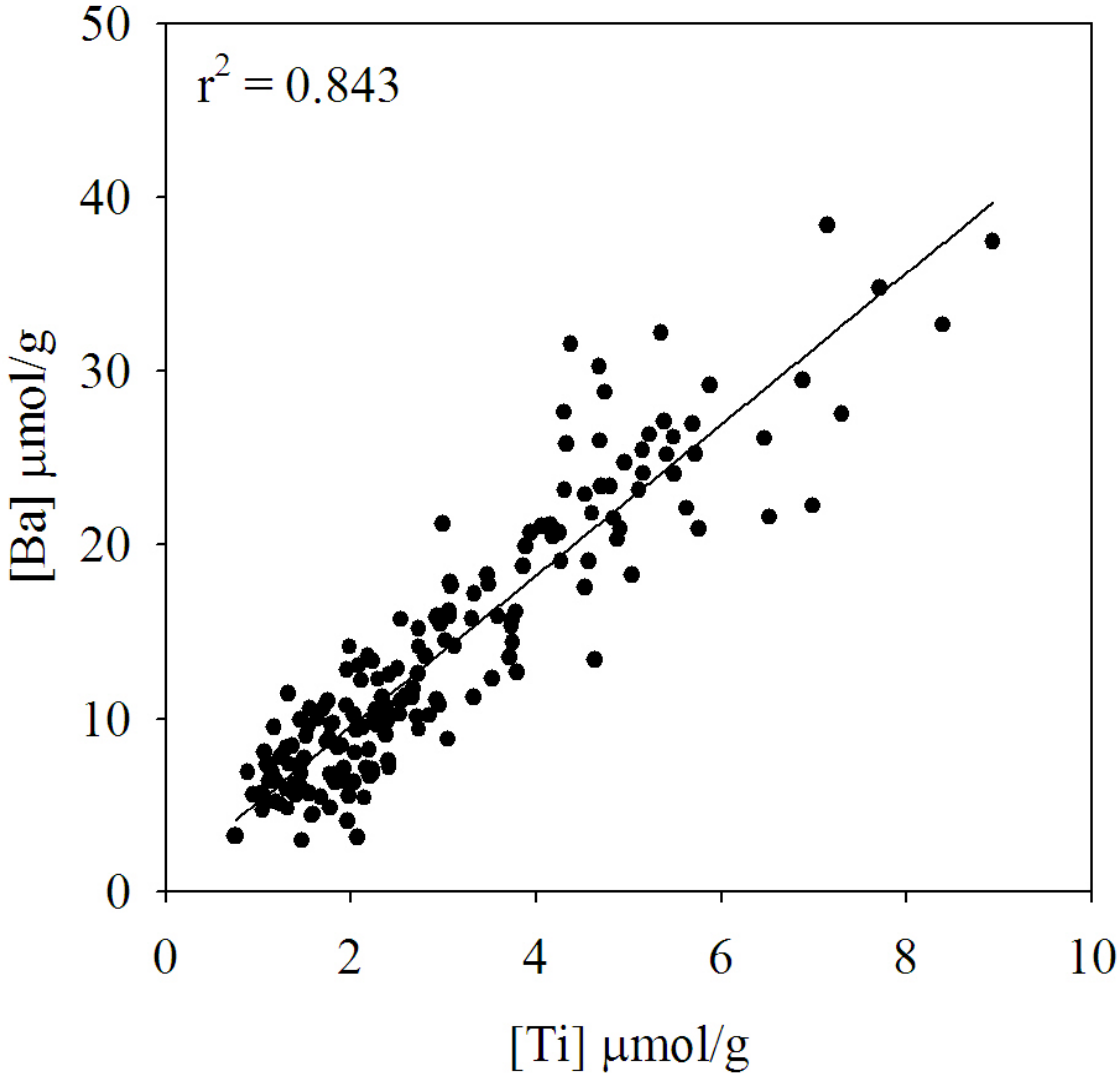

Figure 57. Ba versus Ti concentration. The spearman coefficient is provided in the top left corner.

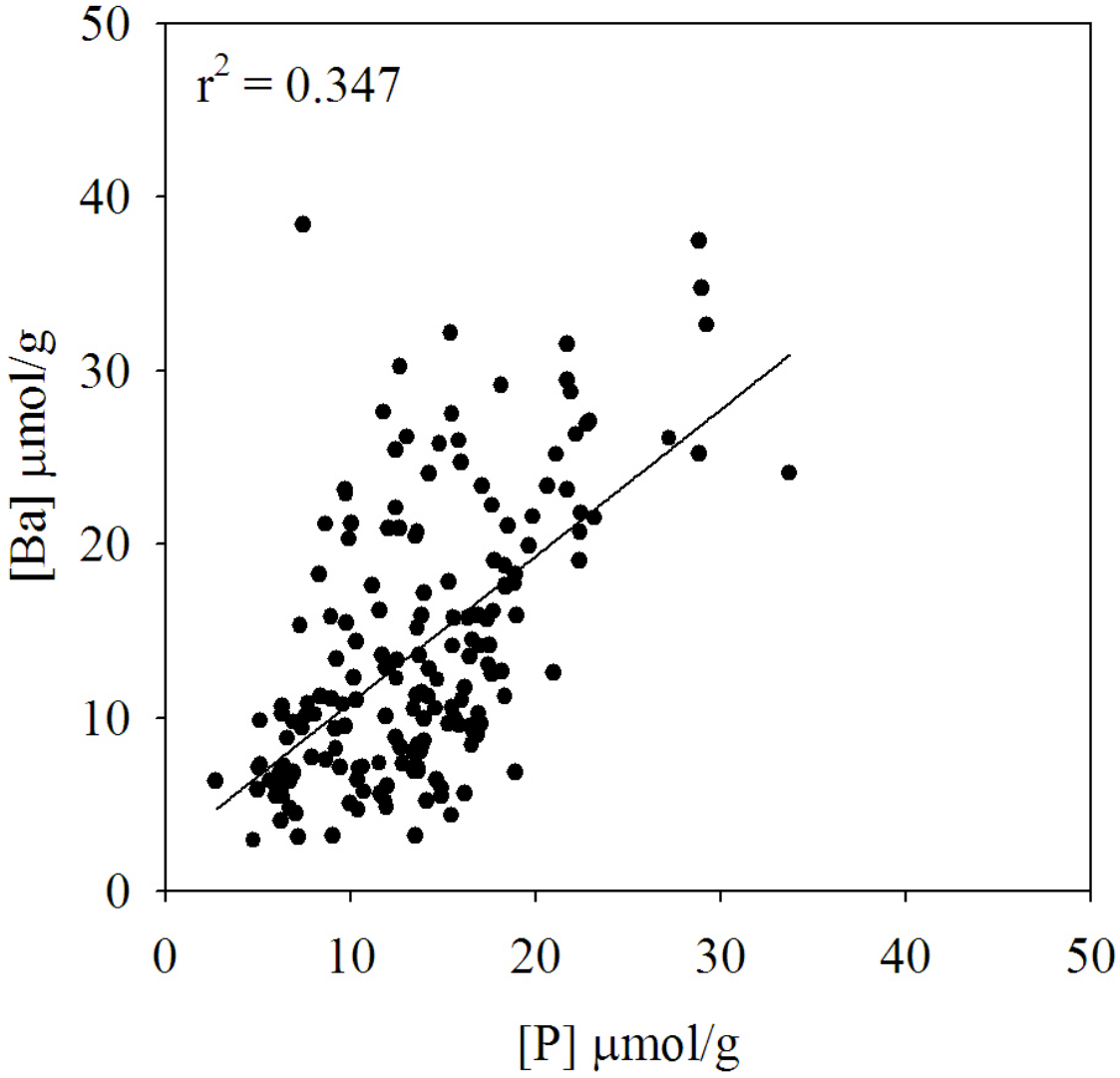

Figure 58. Ba versus P concentration. The spearman coefficient is provided in the top left corner.

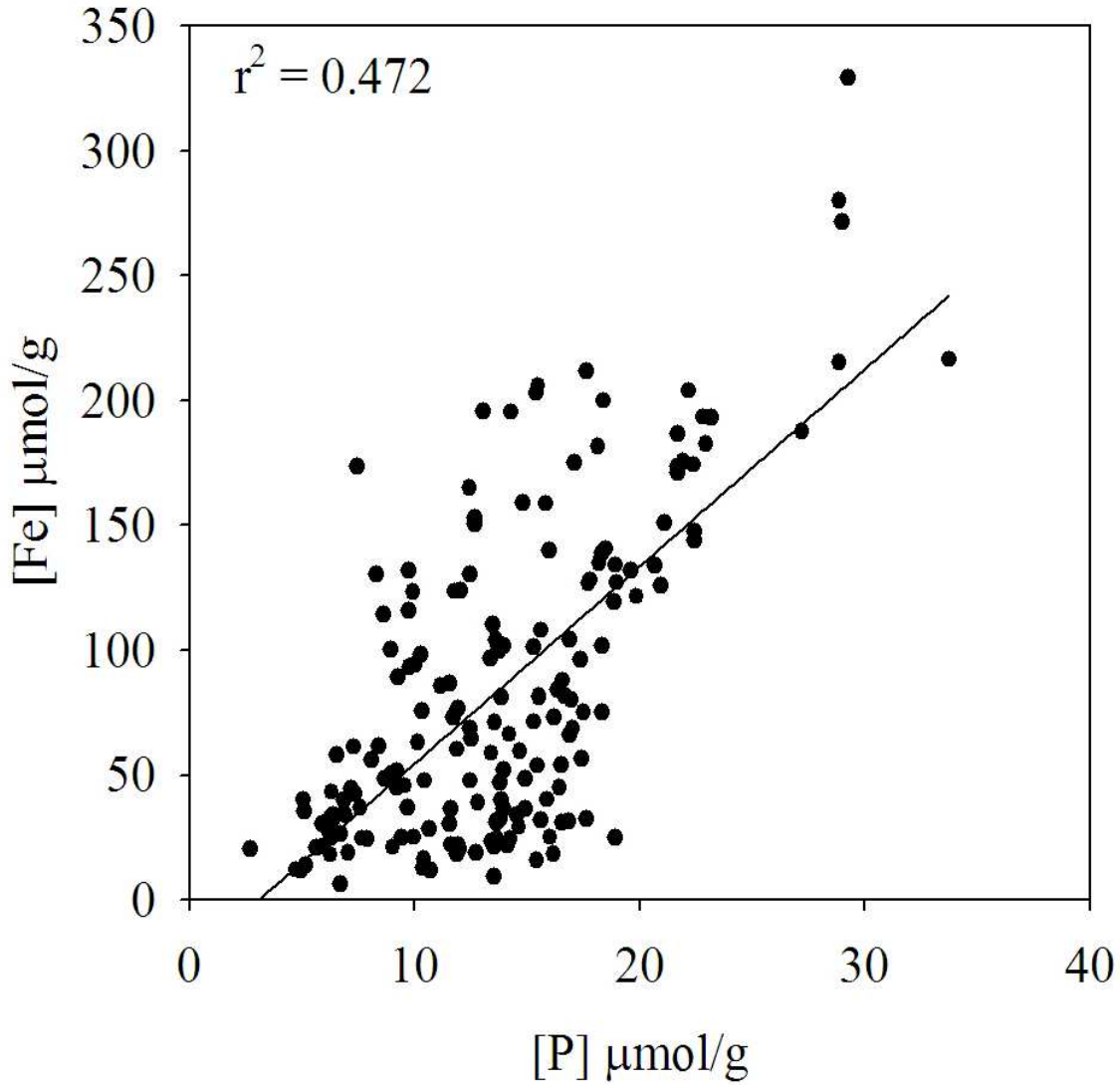

Figure 59. Fe versus P concentration. The spearman coefficient is provided in the top left corner.

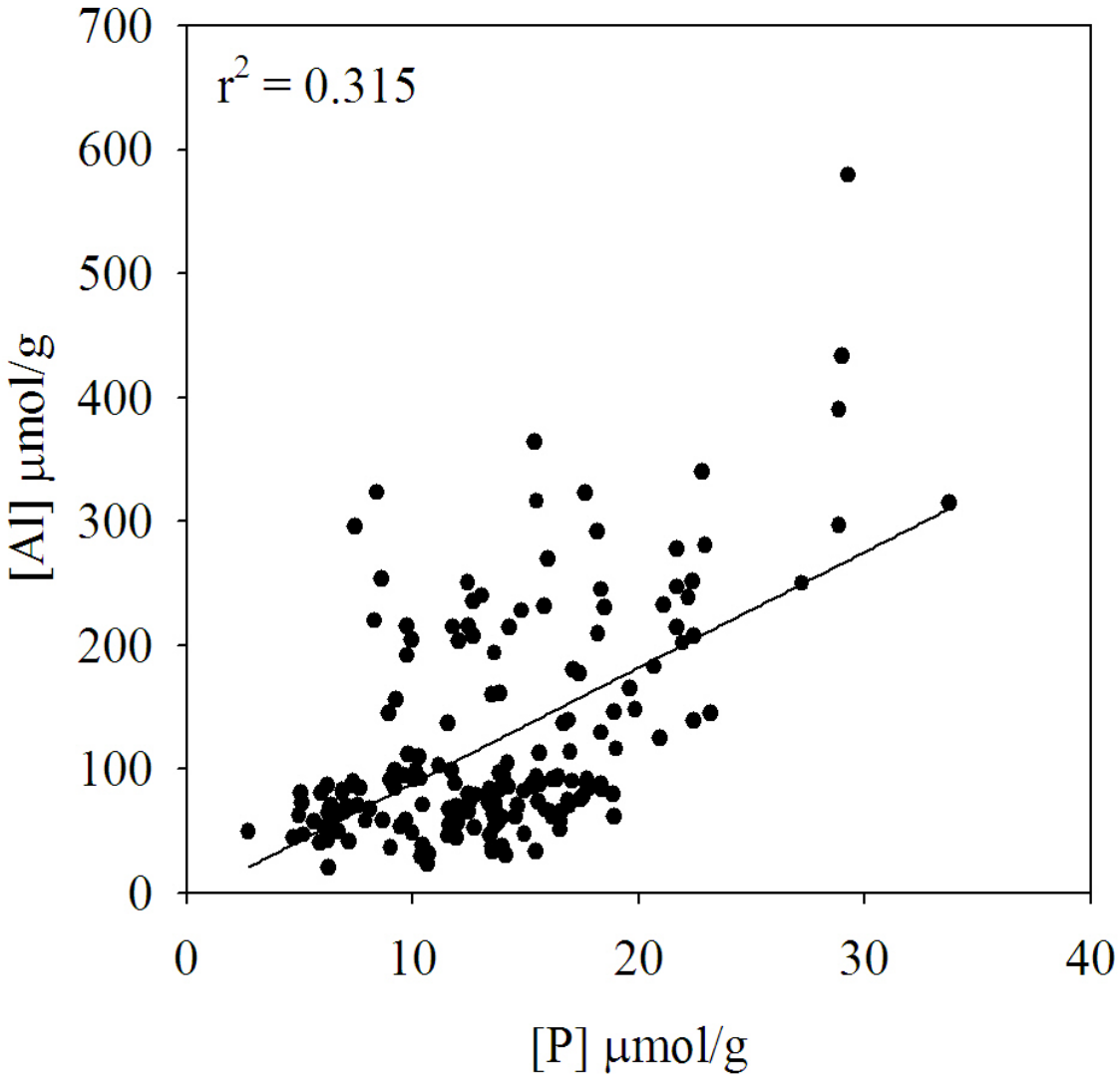

Figure 60. Al versus P concentration. The spearman coefficient is provided in the top left corner.

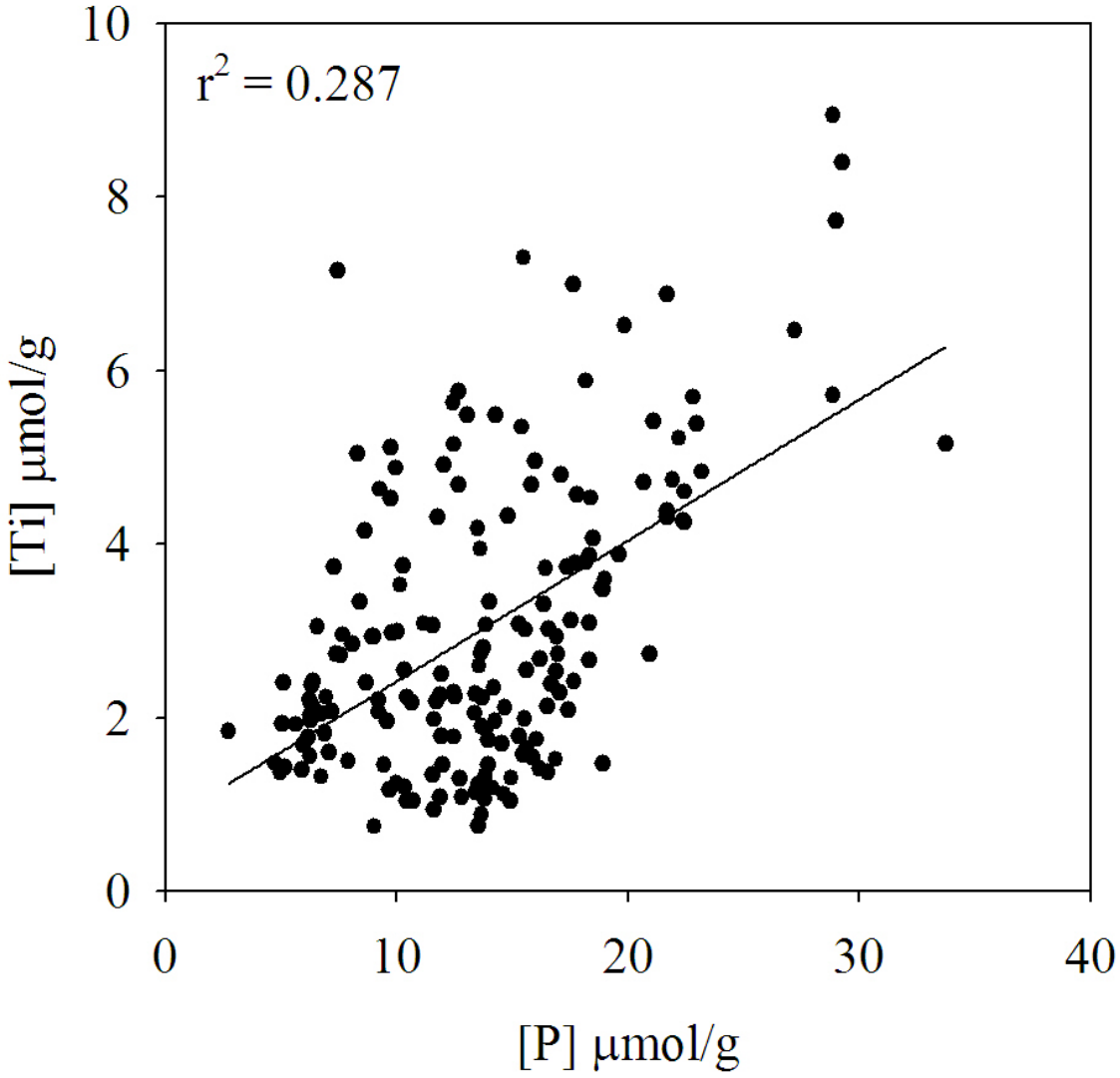

Figure 61. Ti versus P concentration. The spearman coefficient is provided in the top left corner.

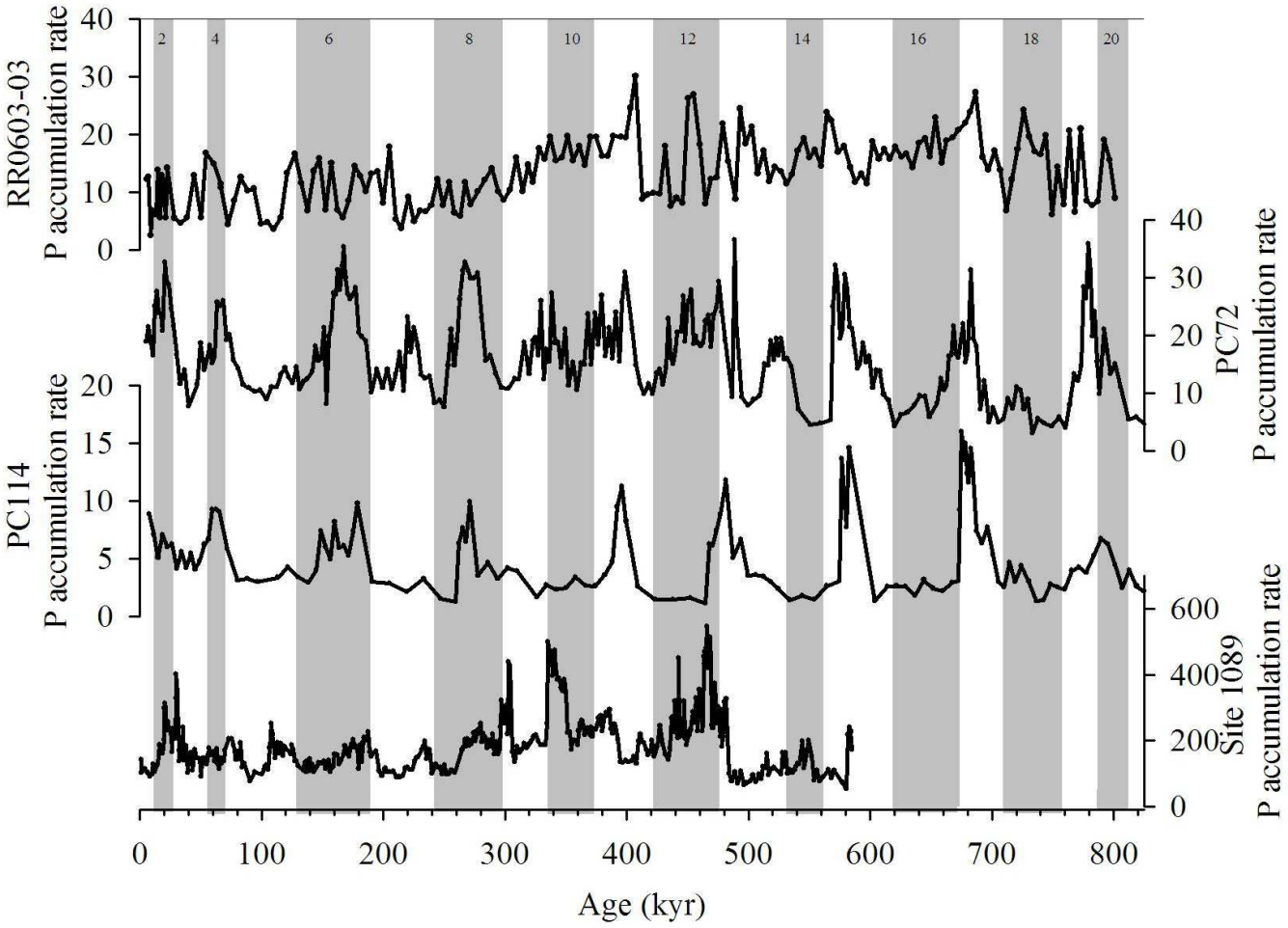

Figure 62. P accumulation rates versus age comparison for equatorial Pacific sites RR0603-03, PC72, PC114 and Southern Ocean Site 1089 in units of μmol cm^{-2} kyr^{-1}. Accumulation rate calculations for RR0603-03 are using the DBD closest to the sample and within the same sediment facies. Gray vertical bars represent glacial intervals with their corresponding MIS number labeled at the top.

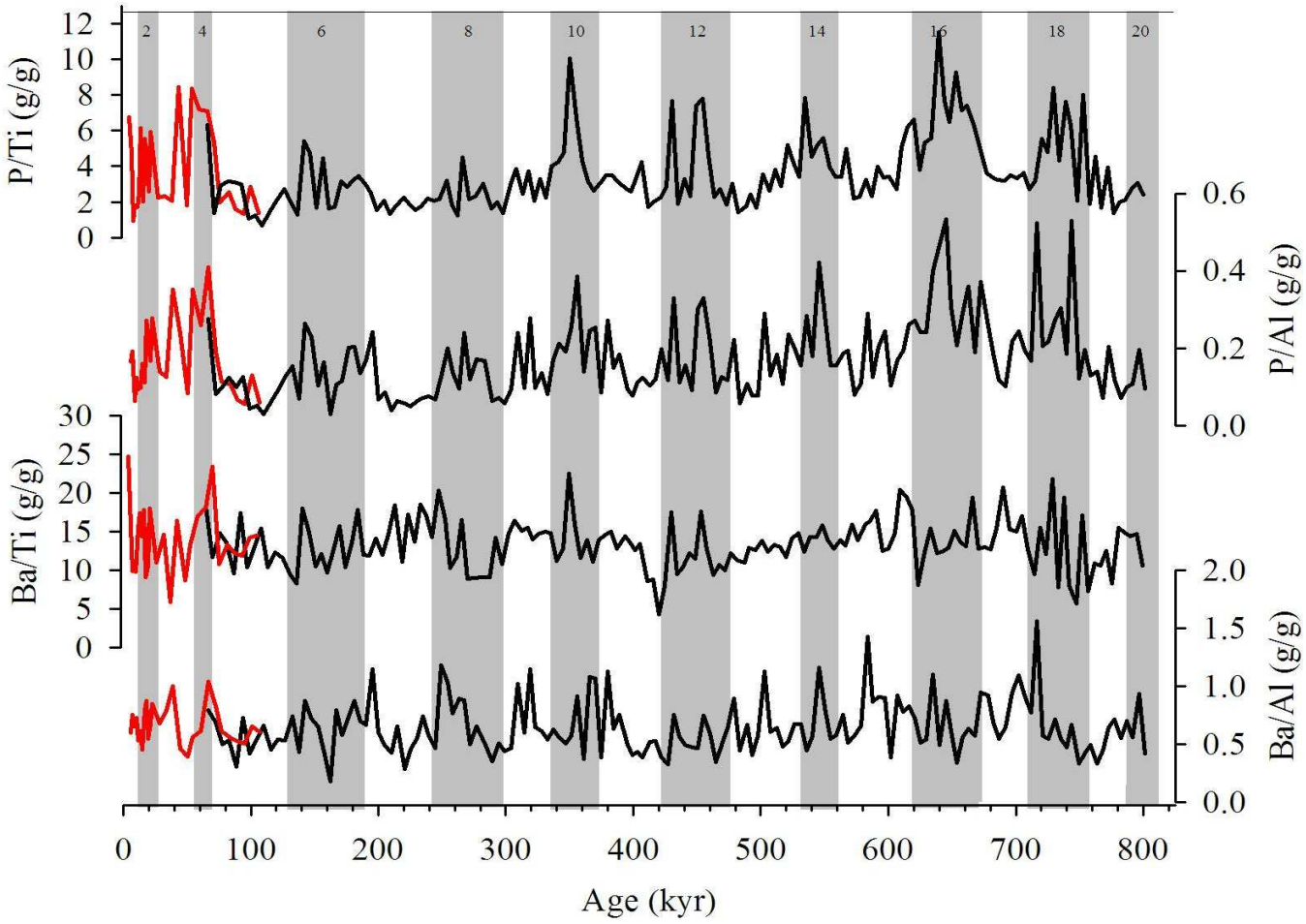

Figure 63. , P/Ti, P/Al, Ba/Ti and Ba/Al ratios versus age for RR0603-03. Gray vertical bars represent glacial intervals with their corresponding MIS number labeled at the top. Trigger core data is shown in red.

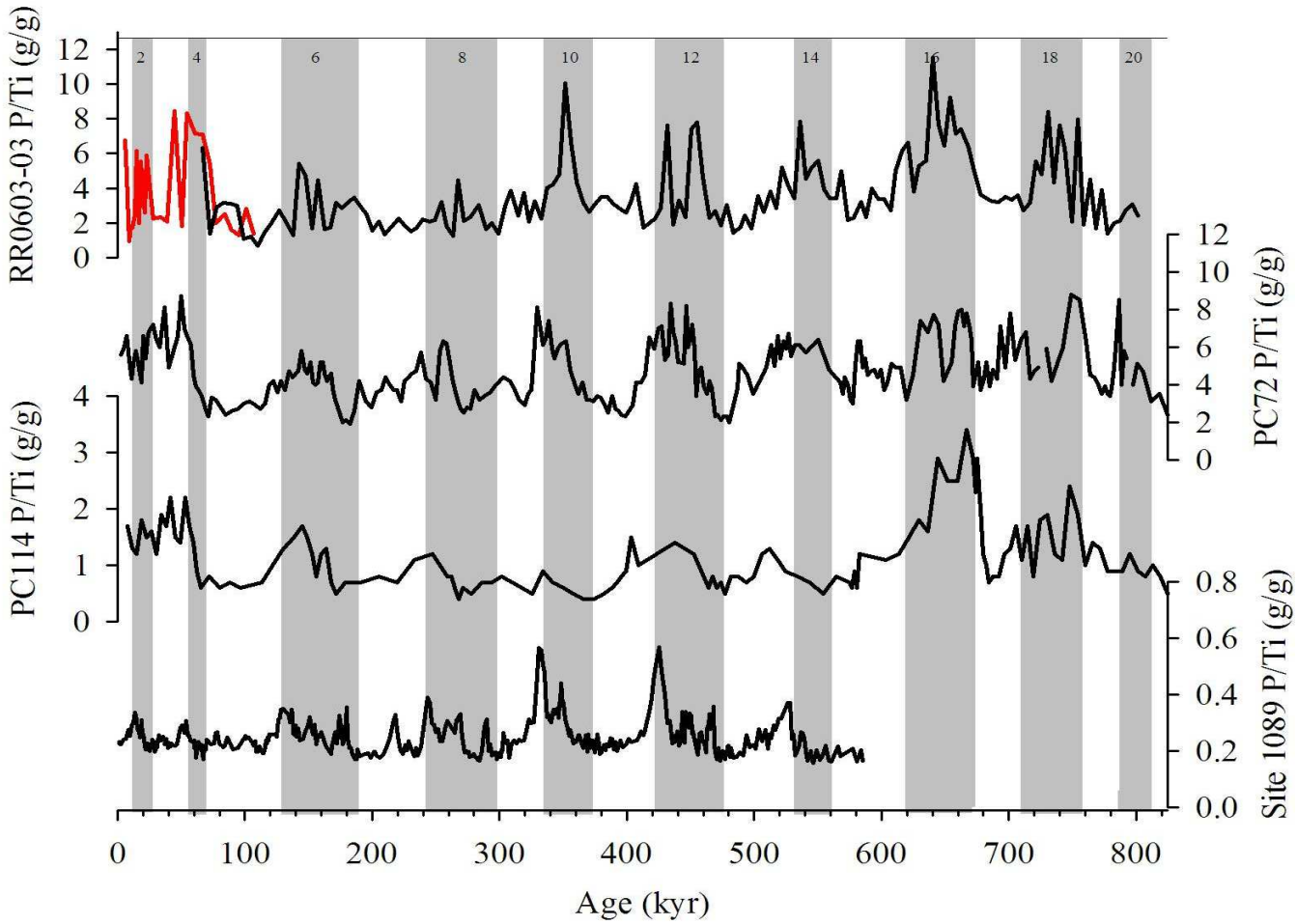

Figure 64. P/Ti ratios versus age comparison for equatorial Pacific sites RR0603-03, PC72, PC114 and Southern Ocean Site 1089. Gray vertical bars represent glacial intervals with their corresponding MIS number labeled at the top. Trigger core data for RR0603-03 is shown in red.

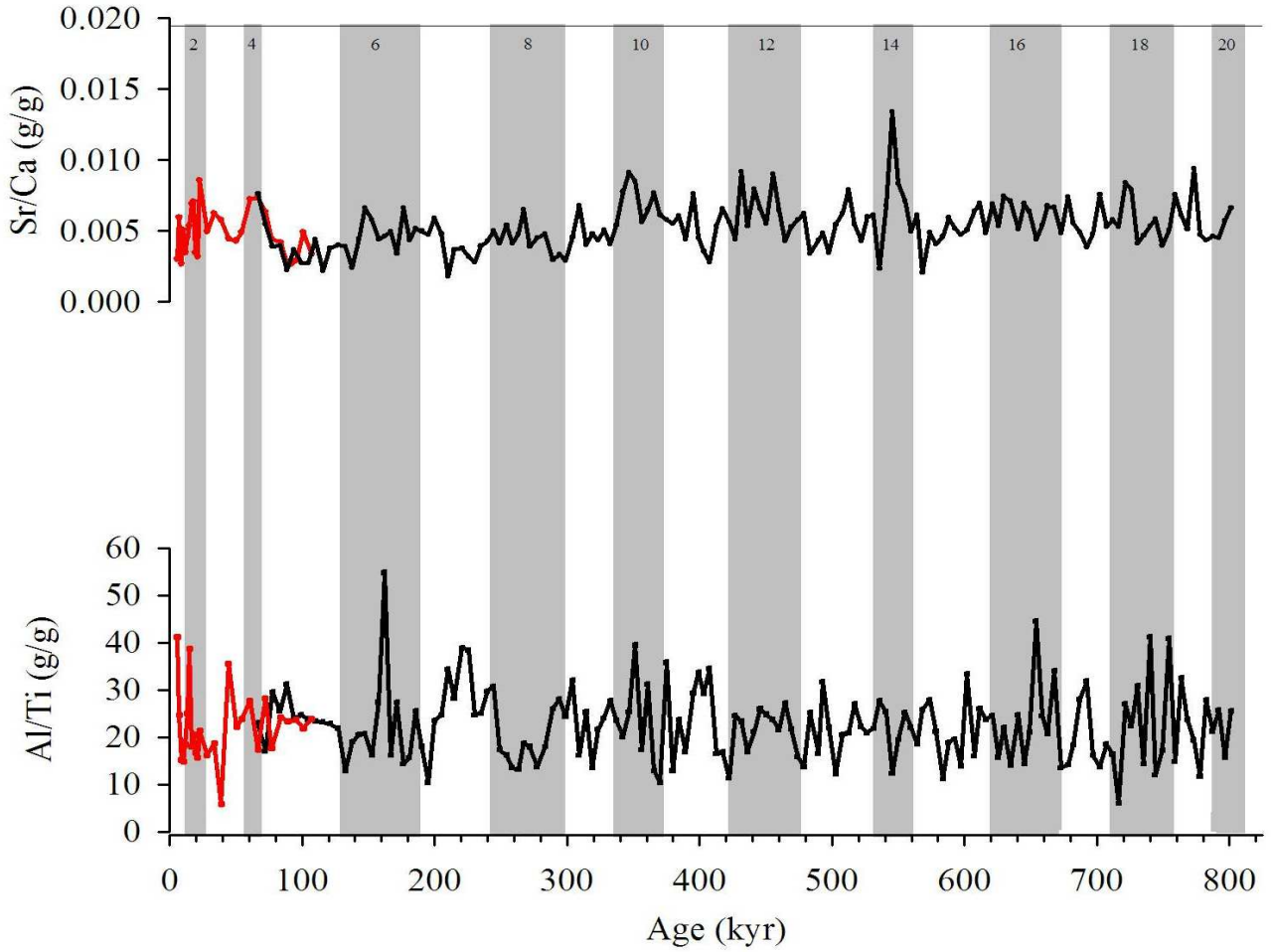

Figure 65. Sr/Ca and Al/Ti ratios for RR0603-03. Gray vertical bars represent glacial intervals with their corresponding MIS number labeled at the top. Trigger core data is shown in red.